Evolution of Morphology: Modifications to Size and Pattern

Evolution of Morphology: Modifications to Size and Pattern

A dissertation presented

by

Aysu N. Uygur

to

The Division of Medical Sciences

in partial fulfillment of the requirements

for the degree of

Doctor of Philosophy

in the subject of

Genetics

Harvard University

Cambridge, Massachusetts

May, 2014

Dissertation Advisor: Dr. Clifford J. Tabin

Aysu N. Uygur

Evolution of Morphology: Modifications to Size and Pattern

Abstract

A remarkable property of developing organisms is the consistency and robustness within the formation of the body plan. In many animals, morphological pattern formation is orchestrated by conserved signaling pathways, through a process of strict spatio-temporal regulation of cell fate specification. Although morphological patterns have been the focus of both classical and recent studies, little is known about how this robust process is modified throughout evolution to accomodate different morphological adaptations.

In this dissertation, I first examine how morphological patterns are conserved throughout the enourmous diversity of size in animal kingdom. We explore scaling of patterning to variations in embryonic size, and focus on the patterning of ventral neurons in the neural tube dorso-ventral axis in three avian species that are drastically different in size: Zebra Finch, Chick and Emu. We find that although the three species end up with comparable proportions of neuronal domains, the dynamics of patterning are very different due to differential response to the morphogen Sonic hedgehog, which mediates cell fate induction along the D-V axis. This difference in response to morphogen across species is intrinsic to cells, and downstream of the pathway receptor Smoothened.

In the second part of this work, I explore developmental mechanisms involved in modifying conserved morphological patterns in order to adapt to a new function throughout evolution. Loss of digits in the tetrapod limbs is one such adaptation that has arose repeatedly as tetrapods occupied and adapted to different habitats. We focus on comparisons between mouse, the three-toed desert rodent Jerboa, and three species of hooved ungulates. We find that digit loss occurs early during limb development prior to chondrogenesis, either during patterning with down regulation of Ptc1 expression, or post-patterning through expansive cell death in the limb. Our findings demonstrate that mechanisms to alter pattern are flexible, and can either happen at time of patterning or subsequently.

Taken together, this dissertation explores evolution of modifications to morphological patterns. The first part focuses on how alterations to size can evolve while conserving pattern, and the second part explores how strictly conserved patterns are modified to accomodate adaptations to function.

Table of Contents

List of Figures and Tables

Chapter One: Introduction

Chapter Two: Scaling Pattern to Variations in Size during Vertebrate Neural Tube Development

Chapter Three: Patterning and Post-patterning Modes of Evolutionary Digit Loss in Mammals

Appendix

Part I. Supplementary Figures for Chapter Two

Part II. Supplementary Figures for Chapter Three

Acknowledgments

My family has a long tradition of storytelling. My grandmother, Pakize, has made my childhood a much more lively and adventurous world with her stories and tales. I could not wait to grow up and explore the world she told so many stories on, and this exploration has turned out to be a scientific one. This work could not have been possible without the support of several very influential people in my life.

First and foremost, I'd like to thank my mentor Dr. Cliff Tabin, whose guidance and supervision has helped conceive, carry on, and complete my graduate work. I knew I wanted to be a part of the Tabin lab the moment I read about Cliff's work, before starting graduate school. Cliff is the most adventurous scientist I have ever known, and I feel very lucky to have worked with him. What we study in the Tabin lab is exactly why I loved and got excited about science, and this lab has been a playground for me for the past 5 years. Yet, despite all the cool science is the lab, Cliff cares more about people than projects, which is what made the Tabin lab feel like home. I am so happy to have been a part of this team.

It scares me to think about leaving the Tabin lab, where I've known amazing people who have influenced me scientifically and non-scientifically. Our tradition of strong post-doc ladies, including Jessica L., Jessica W., Abby, Jenna, Yana, Eddy and Kim, gives me strength. Jessica L. and Abby make it look so easy: they are smart, they juggle multiple things at a time and among all the mayhem they are easy going and caring. During my collaboration with Kim, I've learned a lot on how to approach scientific problems, and how to drive scientific stories home. My rotation mentor, Jessica W., has been a role model in many ways: she is caring for others, passionate about her work,

and very brave scientifically. I am very glad I will be seeing her more often in the near future. Then there is the boys club, Nandan, Patrick T., Akinori and Nick who are always so much fun to be around. I am glad to know they are passing on the spirit to the young post-docs in the lab, Changhee and John Young, who are great additions to the team because they are also very witty and nice, and of course, because they are boys.

My work area, Bay 6, has been a legendary house of Tabin graduate students. I have to especially acknowledge two previous residents of Bay 6, Jimmy and Amy, with whom I shared some of my best Tabin lab moments. Jimmy's presence as a bench neighbour was a privilege, for every science or non-science question, and for every silly joke, there was Jimmy and his soothing motto 'Should be okay'. The lineage of Tabin graduate students has brought in some amazing members, with whom I shared great times in and out of the lab, and even on the west coast! Amy, Alan, Matt, Jessica Chen, Johanna, Tyler and Ariel, you have raised the bar high for what it means to carry the Tabin spirit. Special thanks should also go to Patrick Allard, who has been a great friend to me both in and outside the lab. I already miss his laughter, sense of humor and sincerity and I am confident and we will meet on one of the coasts.

I also feel lucky to share the lab space with all past and present Cepko lab members. Didem joining the Cepko lab had made me really happy even before I met her, and I can tell I wasn't mistaken. Her calm and kind presence in the lab is a haven, she is one of the most elegant and kind people I have known, and I am happy that I will be seeing her often in Boston. Wenjia, Veda and Susana have also been some of my nearby Cepko-neighbors who made the lab a better place.

It is not possible to fit everyone in, but I cannot skip Terri Broderick, Kim Burman, Hongyun Li, Brian Martineau, James deMelo, Vonda Shannon and Ella Sexton, who basically run the show and make sure the hell does not break lose around here. I would also like to thank past and present Dissertation Committee members, Drs. Connie Cepko, Spyros Artavanis-Tsakonas, Alex Schier, Andy McMahon, Jenna Galloway and Dick Maas for their valuable input and advice.

Our collaborator Dr. James Briscoe's intellectual input has also been instrumental for my project and my training, I'd like to thank him for all the discussions we had and the time he set aside, including time I spent in his lab learning techniques. Dr. Vanessa Ribes from Briscoe lab is an amazing mentor, with all her energy and kindness.

I will have to rewind to my undergraduate days and acknowledge some of the people who have helped me take my first steps into the world of science. I worked in Dr. Bruce Goode's lab for several years, and cannot imagine a better lab for my initial exposure to science. I will never forget the 'bring your notebook' meetings, and I hope to keep his advice on impeccable note-taking, along with many other science skills I inherited from him. Bruce's enthusiasm for science, his overall energy and generosity with his time has left a mark on me. I would also like to acknowledge Dr. Karen Daugherty for mentoring me at the bench side. Now that I am in her shoes as a graduate student, I can finally truly appreciate how much time she invested on me.

My life outside of lab has been surrounded by a group of people that I care for very deeply. Boston would not have been home without them, and we may have

overdone the expat lifestyle. Members of our band Boston Meyhanesi may not know how therapeutic our weekly rehearsal and concerts have been. Podcast recordings with Alp and İlker were some of the most memorable and fun events of my time in graduate school. Extended lunches in Longwood were worth every three hours/day.

My past and current roommates, Balım, Burak and Eylül have a special place in my heart and in my life. They have practically been my siblings away from home. It has always been soothing to come home to apartment 615 and joke around the scandalous Turkish political scene, argue on Settlers of Catan, prepare Boston 'shame lists' and 'fame lists', organize theme parties or enter the breakfast universe. Balım's caring heart and hardcore skills at getting things done, Burak's thorough analysis of any situation, and Eylül's witty sense of humor are the reasons why at the end of the day, everything has to be okay. Özge, Kıvanç, Semir, Doruk, Sarim, Şölen and Kerim, with you I am ready to stay in Boston for another 10 years.

My best friend, partner in crime, İlker Öztop deserves more than a paragraph, but this will have to make do. İlker, you've been a seminal part of my time in graduate school, sticking with me through the thickest and thinnest. Giving the pohpoh at the appropriate dose, you and I have shown the world why a little folly always comes in handy. Starting projects with you has been what made science meaningful, and it will continue to be so. We have a long way to go in conquering the world, Padi. It's a true privilige to be your friend and queen.

Cem, who I stumbled into towards the end of my degree, has shared with me every step of the last mile in grad school. I cannot think of any moment we spent

together where I wasn't smiling or laughing. You have been a true comrade and a real champi, supporting me, literally carrying me, cheering me up (sometimes at the expense of entering the abyss) and introducing me to a long list of guilty pleasures. I'm very happy you are by my side, you made the finish line seem like piece of cake.

Finally, I'd like to acknowledge my family away from Boston, scattered around the world and in Turkey. Aybike, Derya, Talya, Yalçınkalp, Koray, İdil, I am so lucky to have you amazing people as friends. Zeyno, I carry you everywhere I go, and it would all be meaningless without you. Sena, all the science experiments started with you! Semala, your presence brings our family the calmness it needs. My brother Cengo has grown up to be an adult during the years I was away from home, my time with him has taught me perhaps the most valuable thing in life: strength comes with loving and caring. My sister, Gülçin, is the strongest person I know! Our lifelong companionship gives me courage.

Growing up, I thought all fathers were as amazing as mine. My dad got me my first telescope, my first map of the solar system, my first microscope, my first science books and told me stories of all the 'adventures' he's been through. Both my thirst for adventure and interest in science stems from his influence on me. Thank you for being the most resourceful, fun and selfless person I know.

Everyone is still a kid around their mothers, I am no exception. My mom has fully supported me with everything that was important to me, and some day I can only hope to be as hardworking, caring and dedicated as she is.

Chapter One

Introduction

“But for what purpose was the earth formed?" asked Candide. "To drive us mad," replied Martin.”

from Candide

On Growth and Pattern

In morphogenesis, a pattern is defined as the complex organization of cells in space and time. Pattern formation is a crucial feature of all developing animals and occurs at many levels of biological organization from cells to organs to organisms. Mechanisms that generate patterns can vary in detail, they share the common feature of a ‘signal’ that carries information and varies in space or time.

Morphological pattern formation is orchestrated by several highly conserved signaling pathways in animals, and in all developing organisms patterning dynamics are closely related to growth dynamics. In his seminal work ‘On Growth and Form’, D’Arcy Wentworth Thompson writes ‘Like any other aspect of form, pattern is correlated with growth, and even determined by it’. How, then, can we explain the enormous diversity of size in the animal kingdom, whose members share homologous structures with common templates or patterns that appear to be perfectly scaled to their size? The first part of this thesis deals with this problem, which is interesting in both developmental and evolutionary perspectives.

The second part of this thesis deals with evolutionary modifications to not size, but the conserved patterns in morphology. Homologous structures are known to be patterned by the same toolkit, or common signaling events, in different animals. Yet we see adaptive modifications to patterns, as animals alter conserved morphologies to accomodate their specific niche. The tetrapod limb is one such example, where the diversity of function produces a deviation from the highly conserved pentadactyl ground state in digit number. Vertebrates from a diverse range of taxa have reduced the number of their digits in order to meet specific locomotion or other functional

adaptations, and it remains to be explored which developmental mechanisms are employed.

This work aims to investigate morphology from an evolutionary perspective, and explore mechanisms involved in adapting morphogenesis to variations in size or pattern.

Part 1. Scaling Morphogen Mediated Patterns to Variations in Size

Morphogen Mediated Pattern Formation

A fundamental property of developing organisms is the remarkable consistency within the formation of the body plan. The plasticity of embryonic development was first explored through a set of classical experiments by Hans Spemann and Hilda Mangold at the beginning of the 20th century, where they demonstrated that the vertebrate embryo is able to adjust to extreme perturbations in size, and thereby scale its morphology to size with surprising accuracy(Spemann H 1924; Spemann 1938; Morgan 1895).

In many species ranging from cnidarians to humans, morphological patterning is guided by a spatial gradient of morphogens, long-range extracellular effectors that induce different cell fates in a concentration dependent manner. During embryonic development, morphogen gradients are launched by evolutionarily conserved molecular networks, and correct morphological patterning is established proportional to the embryonic size, within or across species. The scale and effect of the morphogen gradient is thought to be determined by intrinsic properties (such as degradation rate or diffusivity of the morphogen protein) which are extracellular to the target cells. However,

the gradient of morphogen *response* is what ultimately generates pattern, and can be modulated both by extracellular components and intracellular components.

The morphogen gradient model dates back to the theoretical work of Lewis Wolpert (Wolpert 2011). The 'French Flag Model' he proposed is accepted as the conventional view of morphogen mediated pattern formation. According to this model, a morphogen signal is secreted from a localized source, spreads through the tissue, and subdivides the tissue into domains of differential gene expression. Patterning by a morphogen gradient has three distinguishing principles. First, the secreted morphogen can act on cells at a distance from the source. Second, cells within the morphogen's signaling range respond to a threshold concentration and are induced to different cell fates. Finally, the morphogen concentration should act as the major positional cue for cell fate specification(Gurdon & Bourillot 2001).

Our improved understanding of the morphogen gradient and function has led to elaborations on the conventional model, and further questions need to be addressed in order to fully grasp the mechanism of signal interpretation by target cells. One important insight that was recently gained is that duration of morphogen signaling is as important to cellular response as concentration of morphogen(Dessaud et al. 2007). It appears that in the chick neural tube, progenitors convert to specific cell fates upon exposure to either different concentrations or durations of the morphogen Sonic hedgehog, revealing a new strategy for morphogen interpretation where the concentration and duration of a signal are integrated to control differential gene expression in responding cells. Similarly, in the vertebrate limb patterning, previous studies have reported that it is not just the concentration of the Shh morphogen, but

also duration of exposure that determines digit identity and pattern in the autopod(Harfe et al. 2004).

Pattern and Size

Establishment of a particular morphological pattern by morphogen activity along varying signaling ranges is a fundamental process. Classical examples are the variations in size of the embryos in avian and amphibian species, wherein even 2-fold size differences yield invariant body plans(Cooke 1981).

The amphibian embryo has been an established classical model for studying pattern scaling since the classical Spemann experiments, where dorsal half of newt embryos grow to be proportionately patterned tadpoles, albeit smaller. These experiments from the early 20th century have been repeated in Xenopus embryos, and mainly focus on the early dorsal-ventral gradient of BMP signaling in the Xenopus blastula (De Robertis 2009). In early vertebrate embryos, dorso-ventral patterning is guided by four different BMP ligands that are secreted uniformly but eventually form a gradient across the D-V axis. Such a gradient is established and is resistant to perturbations in size due to a proposed Expander-repressor mechanism. First, a BMP ligand inhibitor (chordin) is expressed at the dorsal pole and forms a concentration gradient that peaks dorsally. Chordin functions to inhibit BMP ligands on the dorsal pole and shuttle BMP ligands towards the ventral pole, such that a BMP activity gradient that peaks in the ventral side is effectively established. Second, an expander protein (Admp) is expressed at the dorsal pole. Admp is a BMP ligand that eventually expands the BMP gradient by competing with other BMP ligands over the ventral shuttling by repressor chordin. Third, auto-repression of Admp stabilizes the spread and amplitude of the gradient according to the total size of the target field of tissue, thereby fine-tuning the

activity gradient to the size of the embryo. This model of expander-repressor mechanism is proposed to contribute to the scaling of patterning in size variations of early vertebrate embryos (Ben-Zvi et al. 2014; Barkai & Ben-Zvi 2009).

Scaling to size is not a unique property of vertebrate embryos and the Xenopus blastula is certainly not the only case. Studies on the Drosophila wing have provided direct evidence that scaling of developmental patterning to variations in size can also be achieved at the *level of morphogen activity gradient itself* (Teleman & Cohen 2000). In this study, Teleman et al. show that in mutant flies with variations in size of wing compartment, shape of *Dpp* gradient is adjusted proportionately, as reflected by expression domain of target gene *Spalt*. This size accommodation occurs at the level of *Dpp* activity gradient (and not at level of target gene regulation), because phosphorylation status of MAD proteins, the *Dpp* signal transducers, is reflective of *Spalt* expression.

Ultimately, development of all multicellular organisms is challenged by changes in size and morphology and robustness and flexibility of pattern formation lies at the core of this challenge. Coordination of growth and patterning can be achieved if pattern itself dictates size, or same mechanism governs both processes. When size is different at time of patterning, external physical factors may alter shape of a gradient. Another possibility is that scaling is inherent to the the patterning process itself, as is the case in establishing the BMP activity in early Xenopus embryo.

Sonic hedgehog signaling cascade in the neural tube

This thesis focuses on pattern and scaling in the vertebrate neural tube dorso-ventral axis, where morphogen Sonic hedgehog (SHH) acts to specify 5 distinct neuronal subtype domains at a distance from the ventral midline. The strength of using the vertebrate neural tube dorso ventral axis is that each progenitor domain expresses a specific set of transcription factors, thereby providing a molecular read-out for mophogen response.

Sonic hedgehog activity has been well studied in the neural tube and other systems. The secreted molecule sonic hedgehog (SHH) is a ligand of the hedgehog signaling cascade and acts as a morphogen. It plays a key role in vertebrate organogenesis, including limb patterning, organization of the brain, and neuronal subtype specification in the vertebrate neural tube(Ingham & McMahon 2001). When this evolutionarily conserved pathway is impaired in vertebrates, birth defects and tumorigenesis result(Jiang & Hui 2008).

As with other morphogens, the SHH signaling cascade starts with the release of the SHH protein from a localized population of cells (**Outlined in Figure 1.1**). Production and release of Sonic hedgehog involves a series of post-translational modifications, in which the precursor protein is cholesterol modified at the C terminus and palmitoylated at the N terminus(Chen et al. 2004). The active SHH protein (ShhNp) is then released from producing cells through a multi-pass transmembrane protein dispatched 1 (DISP1). The formation of this high molecular weight, cholesterol-modified ShhNp complex appears to influence the ligand's diffusion abilities(Zeng et al. 2001; Guerrero & Chiang 2007; Y Li et al. 2006).

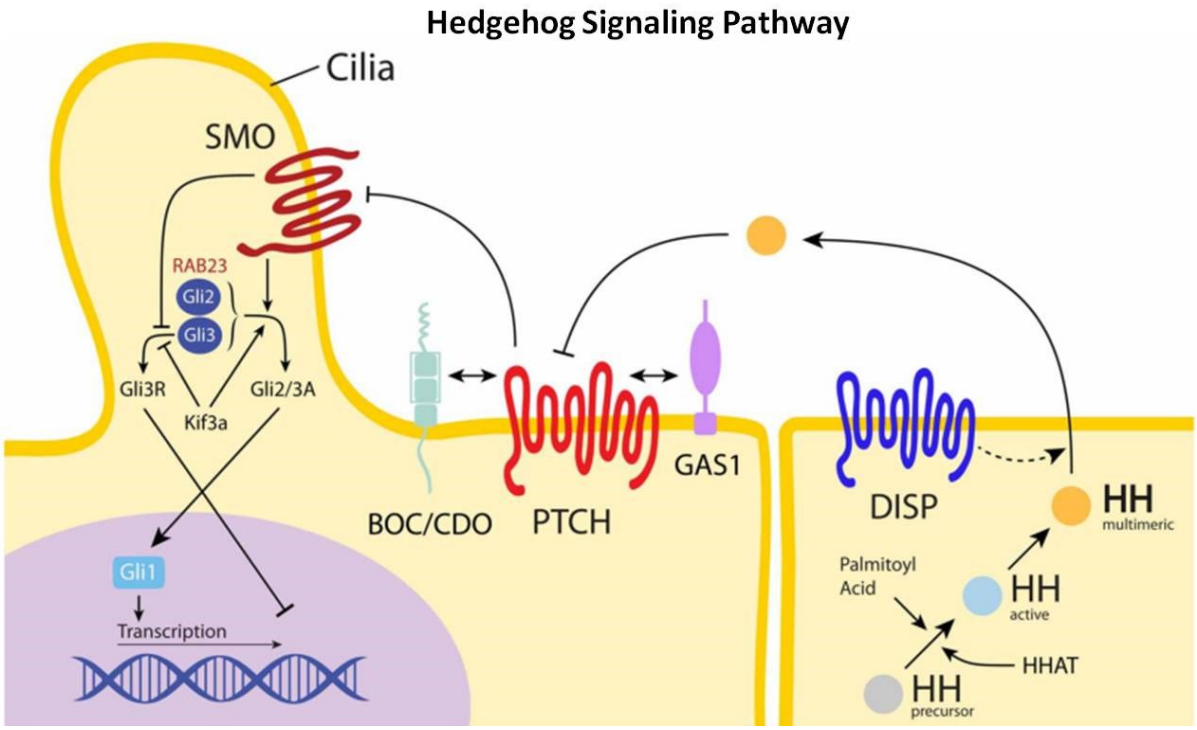

Figure 1.1 : **Sonic Hedgehog Signaling Pathway**: Figure adapted from Pan et al. (Pan et al. 2013). The vertebrate sonic hedgehog signaling pathway, with the SHH secreting cell (right) and receiving cell (left) represented. SHH pathway receptor PTCH1 inhibits Smoothened in the off-state. When morphogen SHH binds PTCH1, this inhibition is relieved, and signaling cascade starts with downstream proteins interacting with Smoothened.

Spread of Sonic hedgehog in its target field is influenced by the expression of transmembrane proteins that bind SHH, such as ECM heparin sulfate proteoglycans (HSPGs) and cell surface proteins PTC1, PTC2, HIP1, GAS1, CDO and BOC (Martinelli & Fan 2007; The et al. 1999; Chuang & McMahon 1999; Tenzen et al. 2006; Holtz et al. 2013). In the absence of Sonic hedgehog, receptor PTC1 represses the activity of a seven-pass transmembrane protein Smoothened (Smo)(Chen et al. 2002). As a result, three zinc finger transcriptional factors (GLI1, GLI2, and GLI3) that are downstream of SMO in the signaling cascade are proteolytically processed and lose their ability to function as transcriptional activators. GLI3 has been shown to be a transcriptional repressors in its proteolytically processed form. The binding of SHH to its target receptor Patched1 (PTC1) starts the hedgehog signaling cascade and leads to the internalization of the morphogen(Incardona et al. 2002). Receptor PTC1 releases its repression on SMO, and an accumulation of SMO in the cilium leads to the inhibition of GLI processing. GLI3 loses its ability to function as a repressor, whereas the full length activator forms of GLI1 and GLI2 activate downstream transcriptional targets(Corbit, KA, Singla, V, Norman, A.R., Stainier, D.Y., Reiter 2005).

The *GLI* transcription factors are the vertebrate orthologs of Drosophila *Ci*, which is the main effector of hedgehog signaling in flies(Aza-Blanc & Kornberg 1999). The regulation of *Ci/GLI* processing is a key step in the pathway, and determines activator/repressor activity for the downstream targets. As shown in vertebrates, SHH gradient is translated into a GLI activator gradient in the developing limb bud and the neural tube, two tissues where SHH patterning has been extensively studied(Despina Stamataki et al. 2005; Hill et al. 2009). GLI3 function is mostly associated with its

repressor form, GLI3R, which is the processed form of GLI3 when SHH ligand is absent(Meyer & Roelink 2003; Wang et al. 2000). Conversely, Gli1 and Gli2 mainly function in their full-length activator form in presence of SHH signal, most notably during the patterning of the neural tube. Recent findings show that ratio of the GLI activator form to repressor form (GliA/GliR) is the main effector of the SHH cascade(Despina Stamataki et al. 2005), leading to either repression or activation of many transcriptional targets that GLI factors regulate.

One of the downstream transcriptional targets of GLI activation is *PTC1*, the Hedgehog receptor(Goodrich et al. 1996; Marigo et al. 1996). This is an important regulatory strategy used in many morphogen systems, wherein activation of signal transduction cascade leads to upregulation of pathway inhibitors in order to tone down signaling(Perrimon & McMahon 1999). PTC1 is a negative regulator of the hedgehog signaling in two ways: First, it inhibits the activity of SMO in the absence of ligand SHH. Additionally, it sequesters the ligand SHH, thus limiting the range over which the morphogen can diffuse(Chen & Struhl 1996).

Patterning of the neural tube by a gradient of SHH

The activity of SHH in the development of the spinal cord represents an example where progress has been made in understanding the dynamics of morphogen action. During the dorso-ventral patterning of the vertebrate neural tube, distinct neuronal subtype progenitors emerge in precise spatial order upon the long-range graded SHH signal that emanates from the ventrally positioned notochord and the floor plate(Yamada et al. 1993; Ericson et al. 1995). Genetic evidence in mice shows requirement for Shh signaling during specification of most ventral cell types(Chiang et al. 1996).*In vitro* assays indicate that a range of SHH concentrations can induce specific

combinations of transcription factors, which result in five distinct progenitor cell fates in the ventral half, as outlined in **Figure 1.2** (Briscoe et al. 2000). These transcription

Figure 1.2: Sonic hedgehog mediated patterning in the vertebrate neural tube

a and b adapted from (Jessell 2000) **a.** SHH is produced in the notochord underlying the neural tube and sequentially in the floor plate at the ventral midline of the neural tube. **b.**It emanates from the source and diffuses into the tissue**. c.** The morphogen concentration gradient induces specific cell types along the ventral half of the neural tube, each progenitor domain has a distinct set of transcription factors expressed.

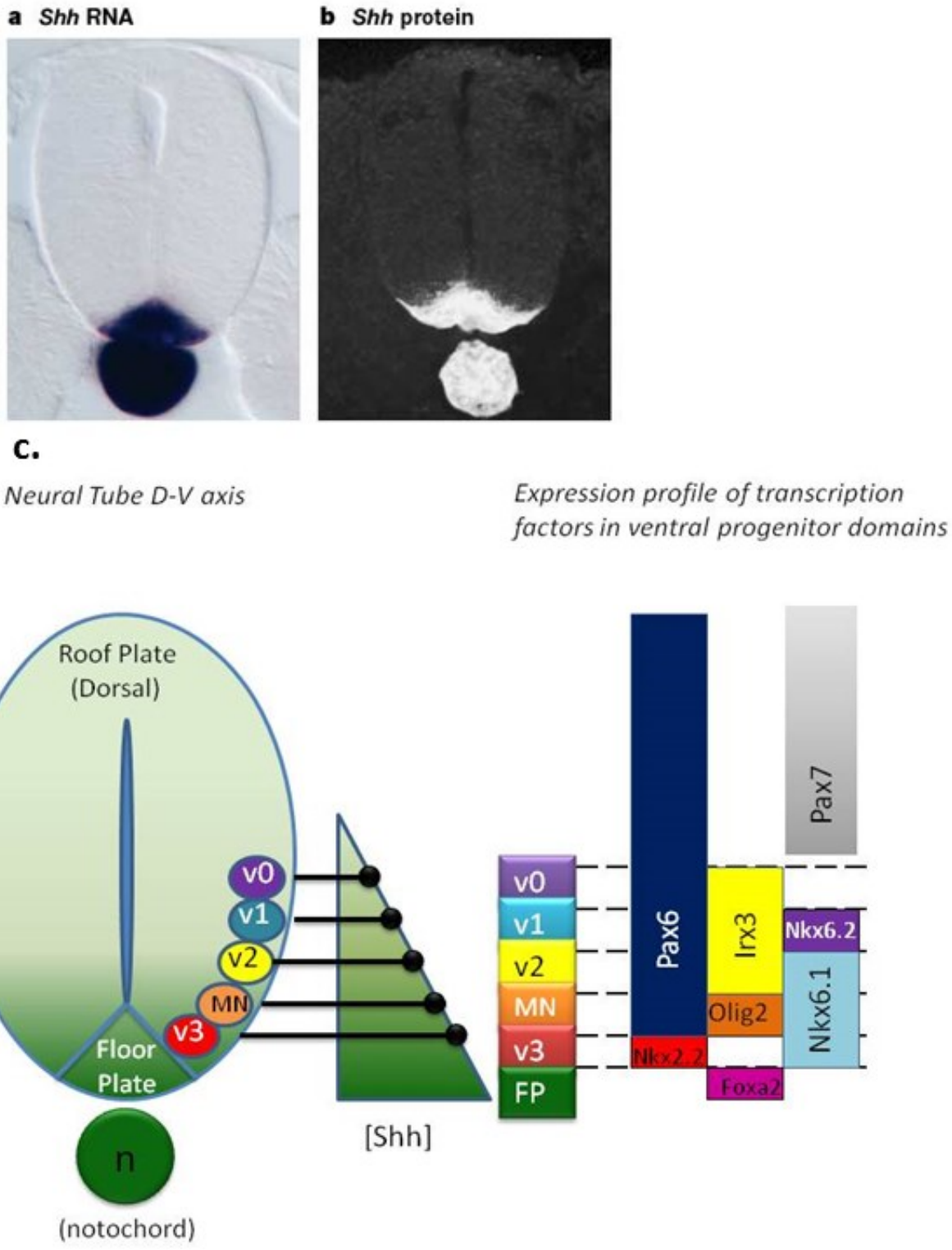

Figure 1.2 (continued)

factors, which include members of the homeodomain and basic helix-loop-helix families, are subdivided into two groups based on their regulation by the Shh pathway(Briscoe et al. 2000; Ericson et al. 1997). Expression of class I transcription factors is repressed by Shh signaling, while expression of class II factors is activated upon Shh exposure. Cross-repression of these factors serves to sharpen the boundaries between the distinct progenitor domains(Dessaud et al. 2008).

The induced pattern of expression is determined by both time and level of exposure to SHH concentration(Harfe et al. 2004; Dessaud et al. 2007). The SHH target transcription factor NKX2.2 is expressed in the ventral-most progenitor domain, pV3, which is closest to the SHH ligand source *in vivo. In vitro*, the induction of this gene requires the highest and longest exposure to recombinant SHH-N. Studies show that all transcription factors regulated by SHH follow this pattern. **Figure1.2** summarizes some of the transcription factors that mark the ventral progenitor domains, induced by a gradient of SHH concentration. Both concentration and time of exposure of cells to SHH are critical for cell type specification, and recent findings suggest that any absolute SHH concentration is converted into duration of hedgehog signaling in the responding cell(Nishi et al. 2009; Kutejova et al. 2009).

One important regulation in many morphogen systems is negative feedback. In SHH pathway, signal transduction by SHH ligand binding to receptor PTC1 leads to the upregulation of pathway inhibitors and attenuation of signaling(Perrimon & McMahon 1999). PTC1 exerts its negative feedback effect in two ways: First, by inhibiting SMO activity in the absence of SHH, and second, by sequestering SHH ligand and thereby affecting morphogen diffusivity across its field of range(Chen & Struhl 1996). Theoretical

work on SHH morphogen diffusivity suggests mechanisms that promote intracellular degradation of the SHH ligand decrease the spatial SHH concentration profile(Saha & Schaffer 2006). Therefore, cell-autonomous and non-cell autonomous effects of ligand-dependent antagonism together can decrease the magnitude and range of morphogen signaling gradient.

Recent experimental data also supports a model in this direction. Jeong et al. 2004 have demonstrated that in mouse embryos that lack PTC1 and HIP1 feedback activities (in genetic backgrounds a)*Ptc1+/-* b) *Hip-/-* and c) *Ptc+/-;Hip-/-*) moderate patterning defects are observed, consistent with increased magnitude and range of SHH signaling(Jeong & McMahon 2005). Most recent work from Ben Allen's lab defines PTCH2 as an additional Hedgehog pathway agonist with a role in ligand-dependent feedback inhibition (LDA), a process that they conclude to be governed by PTCH1, PTCH2 and HHIP1 collectively in vertebrate embryos (Holtz et al. 2013). They employ a combination of mouse and chick *in vivo* studies in the neural tube, as well as cell-based assays to (1) confirm PTCH2 to be a HH antagonist (this has only been shown in cell based assays previously) and (2) show that when HH feedback up-regulation function is abrogated altogether in *MT-Ptch1;Ptc1-/-;HHip1-/-;Ptc2-/-* mice, ectopic ventral cell fates are observed even in dorsal-most regions of the neural tube, mimicking a constitutive Hh activation. This finally reconciles vertebrate data with what was previously observed in *Drosophila*: that PTC1 feedback up-regulation is indispensable for restricting the range of pathway activity away from the morphogen source.

After onset of cell fate specification, the second phase of neural tube patterning starts: differentiation. A critical step in the progression of progenitors into differentiated

neurons is the expression of distinct proneural bHLH genes in the progenitor domains, such as Neurogenin 1 (*Ngn1*), Neurogenin 2 (*Ngn2*) and *Mash1*. These proteins have regulatory roles or progenitors to exit cell cycle, move into the mantle zone and induce pan-neural characteristics(Hatakeyama et al. 2004; Fior & Henrique 2005). Notably, Notch signaling activates the expression of Hes family of bHLH repressors, which prevent the expression of proneural bHLH proteins. Misexpression of Notch pathway components have been shown to disrupts differentiation dynamics in the neural tube(Ohtsuka et al. 2001; Ohtsuka et al. 1999; Handler et al. 2000; Hatakeyama et al. 2004). Thus, opponent activities of several different families of transcription factors may account for how distinct neuronal cell types are organized. In fact, recent studies (Kicheva et al., unpublished) show that differentiation rate is unique for each progenitor cell type, and therefore, differentiation dynamics may contribute to the ultimate pattern in the neural tube. **Figure 1.3** represents distinct phases of cell type induction (phase 1) and differentiation (phase 2) in the chick neural tube.

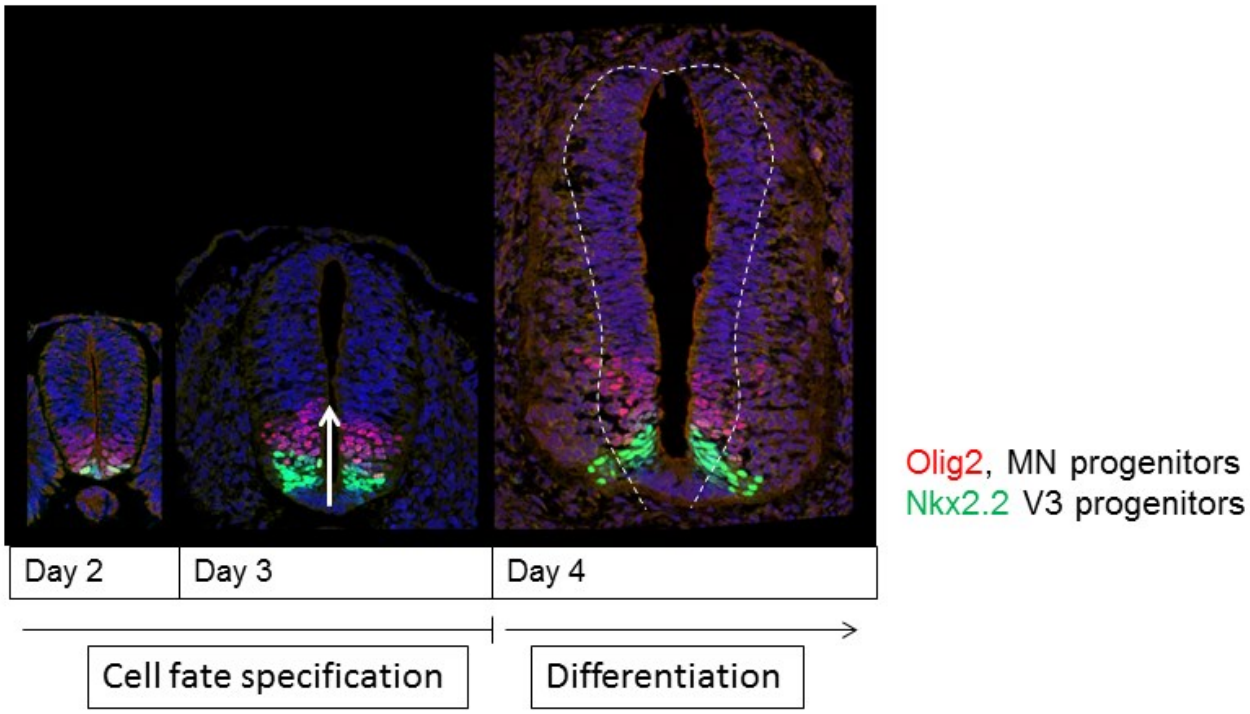

Figure 1.3: Two phases of neural tube development in chick Neural tube development and patterning can be separated into two distinct phases. The first one is the induction of distinct cell types and formation of progenitor domains across the dorso-ventral axis. Once all domains are distinctly specified, progenitor exit cell cycle, move into the mantle zone (outside the area outlined in dashed white lines) and start differentiation. Rate of differentiation is distinct for different cell types and is known to contribute to patterning dynamics.

Chick, Zebra finch and Emu as model species for comparative studies of Shh morphogen gradient

In chick and mouse neural tube, despite significant data on how patterning is formed along the D-V axis by Shh morphogen activity, little is known about the relationship between patterning, size and scaling of the morphogen gradient over different distances. In 2005, it was shown that a gradient of GLI transcriptional activity is sufficient to orchestrate patterning of the ventral neural tube, even in the absence of SHH morphogen(D Stamataki et al. 2005a). This makes the ventral neural tube an ideal system to study morphogen activity, as expression profiles of GLI proteins and target transcription factors can be used as a read-out for patterning. Zebra finches (*Taeniopygia guttata*) have the smallest egg size of all avian species (Paganelli , Ar 1974), while the Emu eggs (*Dromaius novaehollandiae*) are among of the largest. Exploring patterning dynamics in two ends of the size spectrum, along with the commonly used model organism chick (*Gallus gallus*), provides an opportunity to gain insights on how animals retain proportionate patterns while at the same time altering tissue size at time of patterning **(Supplementary Figure S1.1)**. In summary, Zebra Finch, Chick, and Emu embryonic neural tube development is one example where cross-species size differences entail adjusting the morphogen activity gradient. The strength of using avian species is that among members of the same class, we can expect signaling pathways to be highly conserved, while at the same time egg size diversity in bird species is expected to provide a range of embryonic sizes.

Conclusion

The implications of this study is to further extend our understanding of evolutionary processes by identifying mechanisms through which conserved morphogen function is adjusted to different embryonic sizes.

We use the ventral neural tube as the model system, where morphogen Sonic hedgehog patterns 5 different distinct cell types. The advantages of this well-studied system are multi-faceted. Firstly, induction of a distinct set of transcription factors provides a robust molecular read out for morphogen response. Second, availability of an *in-vitro* explant technique enables the study of morphogen dynamics in a controlled environment. Finally, this is a well-conserved structure that is critical to the development and survival of all vertebrate species, and exploring the mechanistic of how it adapts to size can be universally insightful for animal evolution.

Part 2. Modifications to Pattern: An Introduction to Evolution of Pentadactyly and a Reduction to Digit Number

> "The Vertebrated animals enjoy as extensive and diversified a sphere of active existence as the Invertebrated. They people the seas and can move swiftly both beneath and upon the surface of water: they can course over the dry land, and traverse the substance of the earth: they can rise above that surface and soar in the lofty regions of aerial space. The instruments for effecting these different kinds of locomotion – diving and swimming, burrowing and running, climbing and flying – are accordingly very different in their configuration and proportions." – Sir Richard Owen, *On the Nature of Limbs,* 1849.

Extending from seminal work and theories of Charles Darwin and his contemporaries, mid-19th century marks a Renaissance in comparative vertebrate anatomy. Many great morphologists of the time draw attention to homology between limbs of different species and the deviations from conserved the archetypal pattern that

arise in each vertebrate lineage. One such deviation is the variation to the number of digits deriving from the pentadactyl count of ancestral tetrapods. In is work 'On the Nature of Limbs', Sir Richard Owen compares limb elements in a multitude of species and notes the homology between the hoof of the horse and the middle digit of man. Today, experimental embryology and modern molecular biology confirm this observation and aim to build on these findings to further explore evolutionary mechanisms that result in variation to digit count.

Origins of Limbs and Autopoda

To revisit the evolutionary origins of limb, one needs to look at the appearance of paired appendages in *Agnatha*, the jawless fish, 560 million years ago(Kumar & Hedges 1998). Serially duplicated paired appendages (pectoral and pelvic fins) are homologous to the forelimbs and hindlimbs in tetrapods, evidence of which lies in the shared morphology and mechanisms of induction for these elements during embryonic development. Indeed, both fins and limbs start out as mesenchymal buds, surrounded by a layer of ectoderm. Expression of *Tbx5* in the forelimb and pectoral fin, and the expression of *Tbx4* in the hind limb and pelvic fin is required for the bud induction(Garrity et al. 2002). Expression of genes that govern bud outgrowth and formation are also comparable (such as *Fgf8* and *Wnt7a*). Additionally, both the limb skeleton of tetrapods and proximal fin skeleton of fish forms through endochondral ossification, whereby bone mineralization is laid down on a cartilage scaffold. Interestingly, homology stops at the distal-most elements, and the distal fin rays in fish form by direct ossification in the dermal apical fold. On the other hand, digits in the vertebrate autopod are a continuation of the endochondral skeleton.

The jawed vertebrates (*Gnathostomata*) are divided into two branches: the cartilaginous fish (*Chondrichthyes*) and the bony fish (*Osteichthyes*). Within the bony fish, a further subdivision separates the ray-finned (*Actinopterygii*: the vast majority of modern fish) from the lobe-finned fish (*Sarcopterygii*: lungfish, coelocanths, and all modern tetrapods). It is thought that the origin of digits in distal-most part of the paired appendages lies early within this branch of *Sarcopterygii*. Ancestral *Sarcopterygians*, as represented by the species *Eusthenopteron* that arose about 385 million years ago, appear to have a forelimb-like elements with a short and fat basal bone homologous to the humerus and a more elongated radial bone that was positioned anteriorly much like the radius. The remaining elements, while indicative of a complex endochondral skeleton, are difficult to assign homology to modern tetrapods, and none appear similar to the serially reiterated jointed digits. Soon after, around 365 myo, a structure homologues to the autopod appears in early tetrapods with emergence of *Acanthostega* and *Ichthyostega,* although it should be noted that these species were still aquatic and polydactylous.(Shubin 2002)

Investigations into the genetic control of digit formation have given us some insight into the putative evolutionary mechanisms that gave rise to the autopod. Expression analysis and functional studies have uncovered signaling pathways and molecular markers that direct the outgrowth and patterning of the limb elements, and comparisons between modern limbs, fins, and fossils have revealed homologies between these elements(Coates 1994; Butterfield et al. 2010). As the expression patterns of certain genes that govern limb growth and patterning, such as *Tbx4/5, Fgf8, Fgf10* and *Wnt7a* are spatiotemporally comparable in teleost fins and tetrapod limbs,

studies have focused on more downstream patterning events for tackling the mechanism responsible for the formation of autopod as a novel structure. One such candidate has been the Hox gene cluster, the expression of which can be divided into two distinct phases of activity.

Hox genes are transcriptional regulator genes that play key roles in segmental patterning of axial and skeletal elements in vertebrates. The four Hox clusters (a, b, c and d) found in vertebrates are highly conserved among species, which suggests that the distinct clusters and their relative organization are essential for function. It is now well established that HoxA and HoxD genes play a pivotal role during limb development and patterning, most notably in allocation of prechondrogenic condensations(Zakany & Duboule 1996) and the proliferation of skeletal progenitors(Goff & Tabin 1997). In the context of paired appendage development, there are two distinct phases to Hox gene expression. The early phase (phase I) governs stylopod and zeugopod formation, and is initiated by onset of *Hox9* expression in the lateral mesoderm prior to the formation of the limb/fin bud. Later, the *Hox9* expression is maintained and other Hox genes (*Hox9-13*) are expressed sequentially along the proximodistal axis of the limb, with the more 5' Hox genes expressed more distally(Tarchini & Duboule 2006; Sordino et al. 1995; Nelson et al. 1996). This first wave of expression is transcriptionally regulated by the opposing activity of regulatory modules located downstream of the Hoxd cluster, orchestrating the process of sequential Hox gene activation from 3' to 5' end of the complex(Tarchini & Duboule 2006; Spitz et al. 2003). The later phase (phase II) of Hox expression is implicated to have a role in autopod patterning, and is extensively studied the tetrapod limb. During this phase, the tetrapod limb exhibits sustained proximodistal

outgrowth and anterior extension Hox gene expression. The more posterior (5') Hox genes (*Hoxd11-13*) are expressed in the digital anlage, which is positioned in the distal margin of the developing bud(Zakany & Duboule 1999). This second phase of Hox expression is regulated by enhancer regions located upstream of the *Hoxd* cluster, in enhancer domains called the Global Control Region (GCR) and Prox region(Spitz et al. 2003; Gonzalez et al. 2007).

Several studies have reported that while the early phase of Hox gene expression is conserved in tetrapod limbs and teleost fins, the second phase of Hox expression is missing in the teleost fin(Sordino et al. 1995; Sordino & Duboule 1996; Sordino et al. 1996). This lead to the hypothesis that the second wave of sustained Hox expression in the distal end of the limb is an evolutionary novelty unique to tetrapods and is associated with appearance of novel enhancer sequences located outside the Hoxd clusters. Fossil record also supported this idea, suggesting that the distal autopod and digits are neomorphic structures, containing wrist/ankle and digit skeletal elements. This model, however, was followed by ambiguity in reports of Hox expression patterns.

A more detailed look into the expression profile of Hox genes in Zebrafish and that of other non-model vertebrates revealed that *Hoxd* genes from homology group 13 are expressed in distal segments of the fin, comparable to their expression pattern in the limb despite some differences in spatio-temporal dynamics(Ahn & Ho 2008; Shubin et al. 2009; Freitas et al. 2007) . The results indicate that tetrapod digit development cannot be associated with a unique distal phase of *Hoxd* expression, since a similar (but not identical) expression pattern is also detected in the shark *Scyliorhinus canicula*, a member of the basal lineage of Gnasthostomes (jawed vertebrates), suggesting that the

second phase of Hox gene expression is a plesiomorphic condition shared by chondricthyans and osteichthyans(Freitas et al. 2007). An alternative scenario, then, for the appearance of the autopod and digits in tetrapods is novel modifications to a deeply conserved Hox regulation in gnasthostomes, extending an already existing Hoxd expression domain(Schneider et al. 2011). Even though distal fins of teleosts and tetrapod limbs are not morphologically homologous, they share deep homology in genetic and regulatory mechanisms that mediate their formation(Shubin et al. 2009). Indeed, a functional homology in Hox gene regulation is supported by conservation of *cis*-regulatory elements between tetrapods, zebrafish and skate, specifically sequences that drive Hoxd expression in distal segments. A recent study by Schneider et al. used an interspecies transgenesis approach to reveal functional conservation between zebrafish, skate and mouse limbs. In this study, Hoxd regulatory element CsB from skate and zebra fish were inserted into a lacZ reporter cassette and shown to promote distal limb expression in transgenic mice(Schneider et al. 2011).

Recently, a *cis*-regulatory element, CsC, has been identified to be tetrapod-specific and shown to activate 5' Hoxd transcription(Gonzalez et al. 2007; Montavon et al. 2011). CsC promotes expression throughout the autopod and recapitulates 5'Hoxd expression domains. Freitas et al. shows that this tetrapod-specific enhancer promotes comparable expression in the developing zebrafish fin. Moreover, ectopic expression of Hox13a in the distal fin enhances proliferation, distal expansion of chondrogenesis and reduction in finfolding(Freitas et al. 2007). These findings, and the identification of a tetrapod specific enhancer, support the idea that additional *cis*-regulatory elements in

the tetrapod lineage served to modify a pre-existing and conserved gene expression and regulatory network in distal the fin/limb bud.

An interesting insight gained from extensive Hox gene studies in mice is that there is a dose-dependent correlation between *Hox11, 12, 13* gene expression and the size and number of distal skeletal elements. As summarized, Hox gene loss-of-function mutations lead to skeletal alterations such as loss of phalanges, reduction in length of elements, or loss of an entire digit. Moreover, targeted expression of *Hox13* gene group in the limb have led to the ectopic formation of autopodal and digit elements in chick embryos(Goff & Tabin 1997; Yokouchi et al. 1995; Gerard et al. 1997; Zakany et al. 1997), suggesting the role of Hox genes during autopod patterning and digit growth is quantitative. *Zákány et al.* have further investigated the regulation of digit size and number through a step-wise reduction of Hox dosage with mice compound mutant for *Hoxd11, Hoxd12, Hoxd13* and *Hoxa13*(Zakany et al. 1997). This study revealed that these four genes are the major determinants of digit morphology, and decreasing Hox dose in the autopod leads to digit size reductions and transition from pentadactyly to polydactyly. An even more dramatic reduction in the Hox dose leads to oligodactyly and finally complete loss of digits. However, it appears that particular Hox complexes can still possess unique roles in patterning, since polydactylous mice were only obtained via disrupting the function of posterior *HoxD* genes specifically, and oligodactylous mice were obtained only by disrupting posterior *HoxA* genes.

Ancestral Polydactyly

Mutations in genes that orchestrate digital patterning in the tetrapod limb show that digit number and identity is specified by an intricate network of signaling molecules

that is tightly regulated. What remains to be explored is how this robust mechanism can be tailored throughout evolution to alter digital pattern to the adaptive needs of different tetrapods. A digit can be defined as consisting of several phalanges and the soft tissue surrounding it. After the establishment of the anteroposterior pre-pattern in the limb, each digit arises as a distinct chondrogenic unit in the autopod. These condensations further grow out to form digital rays, while the inter-digital tissue undergoes apoptotic cell death (in species with webbed toes, the interdigital mesenchyme differentiates into connective tissue). Interdigital cell death has a significant role in sculpting the autopodal plate, as shown in mammals, birds, and non-avian reptiles. This defined digit versus nondigit cell fate is regulated by TGFβ and BMP pathways(Macias et al. 1999).

Each digit is distinct in terms of its morphology and antero-posterior position, but digit identities are roughly conserved between different taxa. What appears to be different in digit development between different taxa is the timing of digital condensation and growth. In amniotes and anurans, for instance, digit condensation starts with the penultimate posterior digit, followed by the posterior-most digit, and subsequently the anterior digits in a posterior-to-anterior order. In contrast, Urodeles develop their digits in an anterior to posterior sequence(Shubin N. 1986; Wake Shubin, N. 1998).

The peculiar shared characteristic of the tetrapod autopodium is the generally conserved pentadactyly that appears to be under an evolutionary constraint. A pattern is considered to be conservative if, despite modifications to its function, it remains unchanged throughout evolution(Wagner Misof, B.Y. 1993). This is also true for the classical definition of homology, defined as the similarity of organs despite differences in form and function, as put forward by Owen in the 19th century(Owen 1848). We know

that while the conserved five-digit pattern has gone through digit number modifications numerous times in different amniote taxa, it is accepted that they share pentadactylous ancestral states, despite ongoing debates over whether the ancestor of all tetrapods had stabilized to a pentadactylous ground state in the limbs, as fossil records support the idea that amphibians had four digits in their forelimbs(Laurin 1998). Nevertheless, it appears that there is a shared ground state to the number of digits.

Evolution of the Pentadactyl Ground State in Vertebrates

The earliest autopods evolved with the Devonian sarcopterygians, which are now known to be polydactylous. Tetrapod evolution coincides with the origin of autopoda, and early polydactylous state of the limbs is thought to be an adaptation to shallow water habitats. Scavangers in tidal swamps, innovation of limbs provided a novel locomotion and facilitated transition from aquatic to terrestrial life(Wagner & Chiu 2001). Two striking early examples from the fossil record are *Acanthostega*, with eight digits in the forelimb(Coates M.I. 1990), and *Ichthyostega* with 7 digits in the hindlimb. The only other known Devonian tetrapod, *Tulerpeton* from Russia, has six digits(Lebedev 1984). The fossil evidence suggests that the primitive condition for earlier tetrapods is polydactyly. Transition to a pentadactyl ground state is first observed in the post-Devonian, Carboniferous *Pederpes*, the earliest fossil with an at least *functional* pentadactyly in the hindlimbs. It is distinct from paddle-like hindlimbs of the late Devonian tetrapods, appears to be adapted for early terrestrial locomotion and is a firm evidence for pentadactyly in an early tetrapod, along with other later examples from Carboniferous era such as *Greerepeton, Proterogyrinus and Silvanerpeton*(Clack 2002). It seems that while earlier tetrapods with polydactylous limbs are water-dwelling, later

tetrapods with fully terrestrial locomotion exhibit a decrease in number of digits, and the pentadactyl ground state seems to arise as an adaptation to land locomotion.

Although it is now clear that earliest tetrapods were polydactylous, it is still not known exactly when digit number was reduced to five or less digits, and there are theories on both a diphyletic versus a monophyletic origin to pentadactyly. Arguments for a diphyletic origin have been put forward since the 1930s, with works of Holmgren, Save-Söderbergh and Jarvik, and more recently by Coates in the 1990s(Coates 1996). Recent modifications to the diphyletic origin hypothesis relies on the assumption that the Devonian tetrapod with six digits, Tulerpeton, is more closely related to anthracosaurs (amniotes and their extinct relatives) than stem-amphibians, thereby arguing that both amniotes and stem-amphibians underwent reduction to five or less digits convergently. However, reexamination of the phylogeny and the argument that Tulerpeton is positioned near the base of anthracosaurs has revealed new insights. According to Laurin, 1998, new analysis of the phylogeny suggests Tulerpeton to be a stem tetrapod, thereby making it more likely that reduction to five or fewer digits might have occured only once, before the last common ancestor of anthracosaurs and amphibians. It should be noted that broader aspects of fin-limb transition are accepted to have accumulated within the group of stem tetrapods, and it is only the stabilization to pentadactyly where debates remain on the common origin.

An interesting detail to note in transition from fins to polydactyly and finally to pentadactyly is that in contrast to previous theories, appearance of digits and pentadactyly seem to be the last adaptations to occur in transitioning from water to land. Modifications for transition from water to land involved adaptations for air-breathing,

feeding, sensory system, development of a neck, changes to the skeletal structures for more weight bearing support, and finally, stabilization to pentadactyly(J A Clack 2009). This adaptation to pentadactyly may have occurred through a selection for wrists and ankles that are more suited for weight bearing needs of terrestrial life. A refinement or restriction to the action of Hoxd13 may have provided autopodal elements that increase flexibility and stability on land, while at the same time constraining the number of digits to five. For instance, we know that mid-Carboniferous tetrapod Casineria had pentadactylous forelimbs that bore phalanges with ligament grooves and claw-like terminal elements.

Interestingly, after the origin and stabilization of pentadactyly, very few species have evolved more than five digits, while many have reduced digit numbers, with or without modifications to digit identity(Caldwell 2003). Due to the high occurrence rate of polydactyly mutations in human and other mammalian populations, as well as the results of genetic manipulations, it appears to be a relatively easy process for an embryo to increase the number of its digits, through perturbations to the mechanisms of antero-posterior patterning in the autopod. A-P patterning of the tetrapod limb is a tightly regulated process orchestrated by the sonic hedgehog morphogen, conferring position and identity of each digit in the limb primordium. In previous literature, digit identities have been assigned according to their position from anterior to posterior, where the anterior-most digit is digit number I. Secretion of SHH ligand is activated by *Hoxd* genes(Zakany et al. 2004) and restricted to the posterior region of the autopod, historically defined as Zone of Polarizing Activity (ZPA). Classical experiments have shown that when grafted anteriorly, cells of ZPA have the ability to induce

supernumerary digits and alter digit identity(Tickle et al. 1975). It was later discovered that the polarizing agent in ZPA is the secreted Shh molecule, which diffuses to form a concentration gradient along the antero-posterior axis of the limb tissue. Positional information across the tissue is thus conferred through exposure of undifferentiated mesenchymal cells to different local concentrations of the diffused Shh molecule, and distinct threshold concentrations induce distinct cell fates(Gritli-Linde et al. 2001; Zeng et al. 2001). Previous studies have reported that digits 3 through 5 arise specifically from mesenchymal cells that have expressed Shh as part of ZPA, whereas digit 2 and parts of digit 3 are specified by paracrine long-range Shh exposure. This lead to the conclusion that digit identities are determined by a combination of: 1) A temporal gradient of autocrine activity (digits 3-5), and 2) A spatial gradient of paracrine activity (digit 2 and 3). Therefore, it is not just the concentration of the Shh morphogen, but also duration of exposure that determines digit identity and pattern in the autopod(Harfe et al. 2004).

The digit primordia accomodate a network of molecular interactions that fine-tune the patterning process. Mouse mutations can be considered as natural experiments where a gene activity within the tight signaling network in the autopod is disrupted. SHH morphogen signaling acts through its downstream GLI proteins (GLI1, GLI2 and GLI3). In the absence of SHH, GLI proteins are cleaved in the cytoplasm into their repressor forms, and translocated to the nucleus to inhibit transcription of SHH target genes. Upon signaling, full-length GLI proteins activate SHH target genes. In the developing autopod, GLI3 is the most prominent GLI, forming a concentration gradient of active versus repressor forms: posterior region of the limb (close to the SHH source) has

higher levels of GLI3 activator, and the anterior region has higher levels of GLI3 repressor. Mice that are mutant for *Gli3 (Gli3-/-)* display polydactylous limbs(Litingtung et al. 2002), and several mouse lines with defective Gli processing have strong phenotypes in limb patterning(Huangfu et al. 2003; Liu et al. 2005). A known mutation that leads to human polydactyly syndrome GCPS (Greig cephalopolysyndactyly syndrome) was recapitulated in a mouse model, with the name extratoes (*Xt*). This mutation is a 3' deletion of *Gli3* gene and the mouse model has been instrumental in uncovering the function of GLI3 in limb patterning(Hui & Joyner 1993). Indeed, in a subsequent paper, Lopez-Rios et al. investigate the role of GLI3 in cell cycle, and report that GLI3 is a negative regulator of digit progenitor proliferation as well as a promoter of BMP-dependent exit of digit progenitors to chondrogenesis(Lopez-Rios et al. 2012). In cases of mouse polydactyly due to GLI3 malfunction or in human cases of GCP syndrome, it is now evident that there are disruptions in Cdk6 mediated entry to cell cycle and BMP dependent exit to chondrogenic differentiation, rather than cell fate patterning defects. As GLI3 is a target of SHH(Dai et al. 1999), it is not surprising to find misexpression of SHH in extratoes (*Xt*) and many other mouse polydactyly mutants, such as hemimelic extra toes (*Ht*) and *Rim4* in which SHH is found to be expressed anteriorly and polydactyly manifests itself as a mirror image duplication of the skeletal pattern. Such ectopic SHH expression and the resulting mirror image duplication is reminiscent of chick transplant experiments where the ZPA region is grafted anteriorly and polydactyly is observed(Masuya et al. 1995).

Notably, mutations in the AER-specific factors affect digital patterning specifically and not limb outgrowth. In a mouse study where BMP2, BMP4 and BMP7 activity were

removed from the AER specifically, the triple mutants displayed normal stylopod, zeugopod and autopod formation; however, polydactyly, interdigital webbing and split hand foot malformations were observed. These results confirm that BMP activity in the AER is essential for digital patterning and the integrity of AER itself. Other perturbations to the signaling events in the autopod have resulted in many different scenarios of polydactyly. Disruption of BMP4 in the limb mesenchyme leads to anterior and posterior extra digits(Robert 2007). This is suggested to be through the regulation of the AER also, since a sustained FGF8 expression is observed in the mutants.For a summary of signaling events controlling early limb patterning, see **Figure 1.4**)

It should be noted that all cases of polydactyly simply results in a duplicate digit, not a distinct digit. Namely, rather than an extra digit with a novel identity, a duplicate digit is formed without a unique function. This may be why, although commonly occurring in nature, polydactyly is not useful evolutionarily. Instead, changing the morphology of another autopodal element, such as a wrist bone, and giving it a novel function may enhance the functionality and flexibility of the autopodal elements. Panda, mole, and elephant are some examples of animals that are known to alter the identity of the sesamoid wrist bone to create a sixth digit with a distinct identity and function(Tabin 1992).

A classic example of sesamoid modification is the Panda's thumb, or Panda's peculiar thumb, as Stephen J. Gould titles it in his essay from 1978(Gould 1978). What he calls the peculiar thumb is not actually a thumb or a digit at all, in anatomical sense. It is a radial sesamoid bone that is enlarged and lengthened, functional in grasping bamboo and flexible enough to help Panda handle its food at maximum ease and

efficiency. The rest of the five digits remain functional in the autopod and the regular thumb, digit number I, is still not the opposable thumb that has evolved in the human autopod. Instead, panda's solution to digital dexterity comes from modifying a wrist bone and re-organizing the muscles to give it a new form and function.

Similarly, talpid moles (genus *Talpa*) have modified their radial sesamoid bone such that it is a large, sickle-shaped extension anterior to their five digits. The animal uses this extra digit-like extension as a means of increasing the autopodal area and supporting the animal while digging. There are no phalanges or segments to the bone, but it can be moved independently just like an extra digit. As in the case for panda, the modified sesamoid bone is equipped with muscle and tendons. Early development of this structure is correlated with strong Msx2 expression which hints at the recruitment of mechanisms that are normally required for autopodial digital and interdigital sculpting. Msx genes are known to play pivotal roles in the patterning of the autopod, such as regulating the apoptotic programme, controlling bone development and differentiation. However, the extent and integrity of AER does not seem to be affected in the mole autopod, and the basic pentadactyl patterning is not interfered(Mitgutsch et al. 2012).

The elephant's 'sixth toe' is another example of sesamoid bone exaptation (modification of existing structures into new form and function). In this case, the sesamoid bone is employed as a false digit to provide support for the tip-toed posture of the elephant. Similar with the two previous scenarios, musculotendinous structures still accompany the elephant false digit, even though it is used for stabilizing posture, and not necessarily dactile flexibility(Hutchinson et al. 2011).

Mutations in genes that orchestrate digital patterning in the tetrapod limb show that digit number and identity is specified by an intricate network of signaling molecules that is tightly regulated. What remains to be explored is how this robust mechanism can be tailored throughout evolution to alter digital pattern to the adaptive needs of different tetrapods.

Evolutionary History of Digit Loss

Experimental studies on the mechanisms of digit loss date back to 1949, when Bretscher reported that treating early limb buds of *Xenopus laevis* frogs with the mitotic inhibitor colchicine leads to loss of digits, as well as a reduction in the number of primordial limb cells(Bretscher 1949). Follow-up work on this study, as repeated in other model organisms, suggested that patterning of skeletal elements could depend on competition for mesenchymal limb cells during chondrogenesis(Alberch & Gale 1983). Consequently, perturbations in limb size can indirectly lead to loss of phalanges or complete digits. This interpretation has additional implications to evolutionary perspective to digit loss, as discussed in the next section with the case of urodeles. Indeed, the order of digital loss during experimental perturbations to limb size could recapitulate phylogenetic pattern of digit loss, suggesting a possible mechanism for evolutionary mechanism to digit reduction in certain taxa.

Other experimental manipulations that lead to digital loss in model systems have helped dissect out the gene pathways and regulators that orchestrate limb patterning. Gene expression analysis in these mutants has shaped a model wherein BMPs, Ffg4 and gremlin act within a network to temporally and spatially control Shh mediated patterning, a process that regulates number of digital elements. In Shh-/- mice, limb

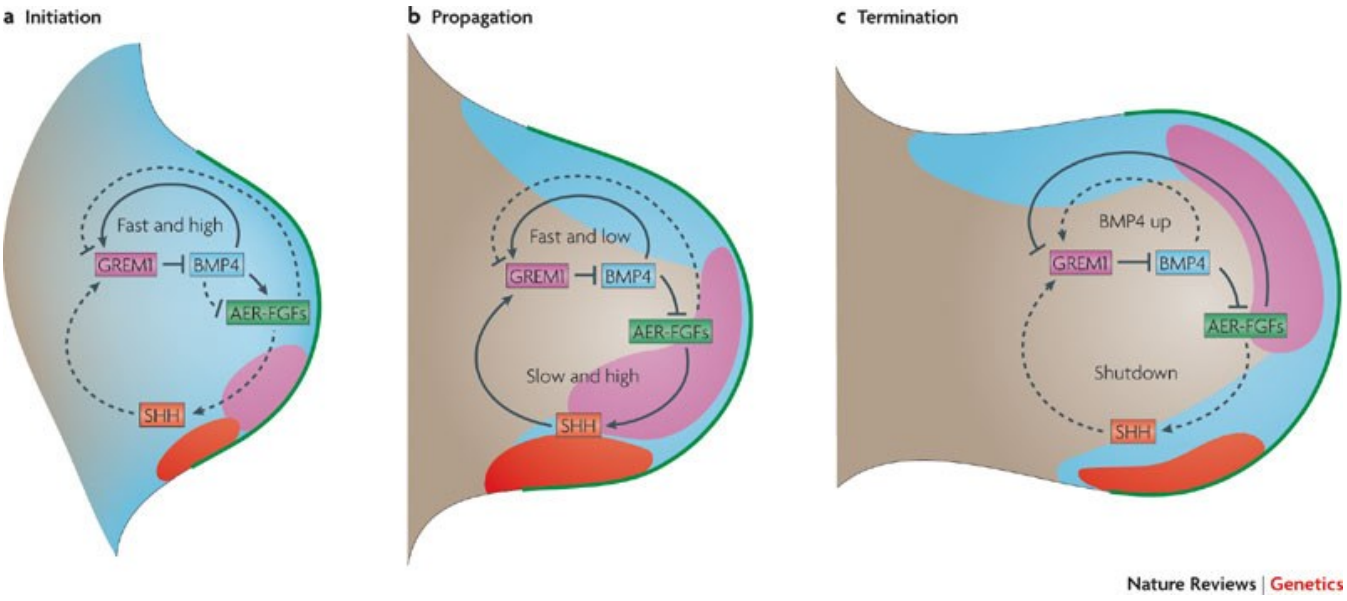

Figure 1.4: Signaling events regulating growh and patterning in the vertebrate limb This figure is adapted from (Zeller et al. 2009), outlines signaling pathways that are spatio-temporally dynamic and regulate growth and pattern during early limb development.

development progresses normally in the proximal end, but the distal structures feature anomalies in the growth and patterning of skeletal structures, including no digits in the forelimb and only one digit (digit I) in the hindlimbs(Chiang et al. 2001; Kraus et al. 2001). The *limb deformity* gene mutant mice are known to have impaired AER signaling function and result in disrupted FGF4-Shh feedback loop, as well as loss of posterior digits(Haramis et al. 1995). In a similar scenario, when Gremlin mediated BMP antagonism on Shh is disrupted in gremlin-/- mutants, reduced digit number and loss of digit identity is observed(Michos et al. 2004).

Although phylogenetic and possibly pleiotropic constraints have stabilized digit number to five, a number of taxa have independently reduced number of digits in form of straightforward digit loss, or in some cases, along with a frame shift in digit identity.

Birds

The tridactyl avian wing is a classic example of digit reduction, having evolved from the pentadactyl hand of early theropod dinosaurs. However, this transformation is of special interest not only due to the reduction in digit number throughout class Aves, but also due to the hypothesized homeotic transformation in digit identity. Indeed, although the three digits of the avian manus are morphologically homologous to digits I, II and III of the theropod dinosaur fossils, embryonic studies show that these digits arise at positions II, III, IV in birds(Bever et al. 2011). Interestingly, as the avian manus develops, it features five mesenchymal condensations as does any other pentadactyl manus. Later in development, the anterior most digit at position I fails to chondrify, and the posterior most digit V develops into a short, cartilaginous metacarpal stunt which fails to further develop. Digits at positions II, III and IV continue to develop into digital

identities I, II and III (Larsson et al. 2010). The fact that tridactyly develops from a transitionary pentadactyl stage suggests that there are strong developmental constraints to the pentadactyl ground state(Galis F Metz JAJ 2001) and that digit loss happens secondary to an establishment of pentadactyl pattern.

There still remains a paradox in digit identity in the avian wing. This has been explained by Frame Shift hypothesis, accepting that both developmental studies determining digital positions and fossil studies identifying homology were valid, and proposing that a homeotic transformation in digit identity occurred in theropod evolution before the origin of Aves, leading to mesenchymal condensations of digits I, II and III in altered positions(Bever et al. 2011). This hypothesis has been opposed by the argument that mechanisms of digital patterning remain too pleiotropic to be adapted(Galis et al. 2002; Galis et al. 2005). However, one should note that homeotic transformations are common thoughout the evolution of body segments in arthropods and vertebrate skeleton. Moreover, comparative expression analysis of Hox genes in mouse versus chick manus shows that in both species, HoxD13, but not HoxD10,11 and 12 are expressed in digit I (Chiang et al. 2001; Vargas AO 2005a; Vargas AO 2005b). A recent study has also done a detailed transcriptome analysis of the tridactyl chick wing, confirming the identities of digits I, II and III, despite the shift in their position(Wang et al. 2011).

Urodeles

Urodeles, an order of class Amphibia, also show reduced limb morphologies, including fewer mesopodial and digital elements. These cases of reductions in urodeles are thought to evolve by three possible evolutionary mechanisms: reduction in size of

the limb mesenchyme(Alberch Gale, EA 1985), failure of digit primordium to separate, and fusion of initially separate condensations(Shubin N. 1996; Shubin 2002).

All urodeles have less than five digits in the manus, and in salamanders, four-toe pattern has evolved independently in several genera. Some species have as few as two digits, such as the cave-dwelling salamander *Proteus*.This species retains digits I and II, the first digits of the digital arch to form developmentally. Four-toed salamanders have all lost digit V. Indeed, in almost all cases of digit reduction, the last digits to develop are the first ones to be lost in evolution. This phenomenon explains why digits are lost in different sequences, specifically in urodeles which are distinct in their order of digit development.

However, it remains to be explored why digits are lost in the first place in all urodele species. A study by Alberch and Gale (1985) proposes two hypothesis for this, that digit loss in salamanders is associated with either a global developmental arrest (such as in dwarfism), or a global slow-down in cellular proliferation (such as in paedomorphosis)(Alberch Gale, EA 1985). Morphometric and phylogenetic analysis recently showed that both cases associate with digit loss in salamanders(Wiens J.J. J.T. 2008).

The association between the evolution of limb size and pattern is an interesting phenomenon, especially in the context of digit loss. Miniaturization of body size has significant morphological and developmental consequences, mostly because the morphogenetic mechanisms of pattern formation are size dependent. Therefore, size reduction in embryos is often accompanied by homoplasy, as in the case of digit loss.

Not just urodeles, but some frogs also lose digits as a result of miniaturization. Smaller limb primordial result in loss of the first digit of the hind limb in frogs, and fifth digit in salamanders in numerous cases(Alberch Gale, EA 1985; Hanken Wake, D. 1993). The difference in sequence of digit loss is, as previously discussed, a result of different developmental sequence during digit development.

Lizards

Lizards exhibit a wide range of reduction in digital elements, from loss of a single phalanx to complete limbness(Greer 1991). Perhaps the most striking case is that of the Australian skink from genus *Hemiergis*, which includes several closely related species that populate neighboring habitats but are geographically isolated, and display differences in digit numbers. The body plan and limb morphology of these lizards are almost identical except for the reduction in digit numbers. These isolated populations in close proximity display digit numbers ranging from 2 to 5 in the forelimbs and hindlimbs. Shapiro et al. have explored embryological gene expression in the four *Hemiergis* species, and specifically focused on factors involved in limb patterning and tissue quantity(Shapiro et al. 2003). They report a change in duration of Shh signaling in the ZPA, in correlation with digit reduction. Therefore, rather than a global truncation of growth or smaller limb primordium (as was suggested in urodeles), the skinks display shortened Shh signaling in limbs with fewer digits.

This scenario on the mechanistic of digit loss was only shown as correlation in Shapiro et al., but remains as a possible scenario, most notably due to some functional studies on *Ambystoma mexicanum* salamanders where Shh signaling was blocked with

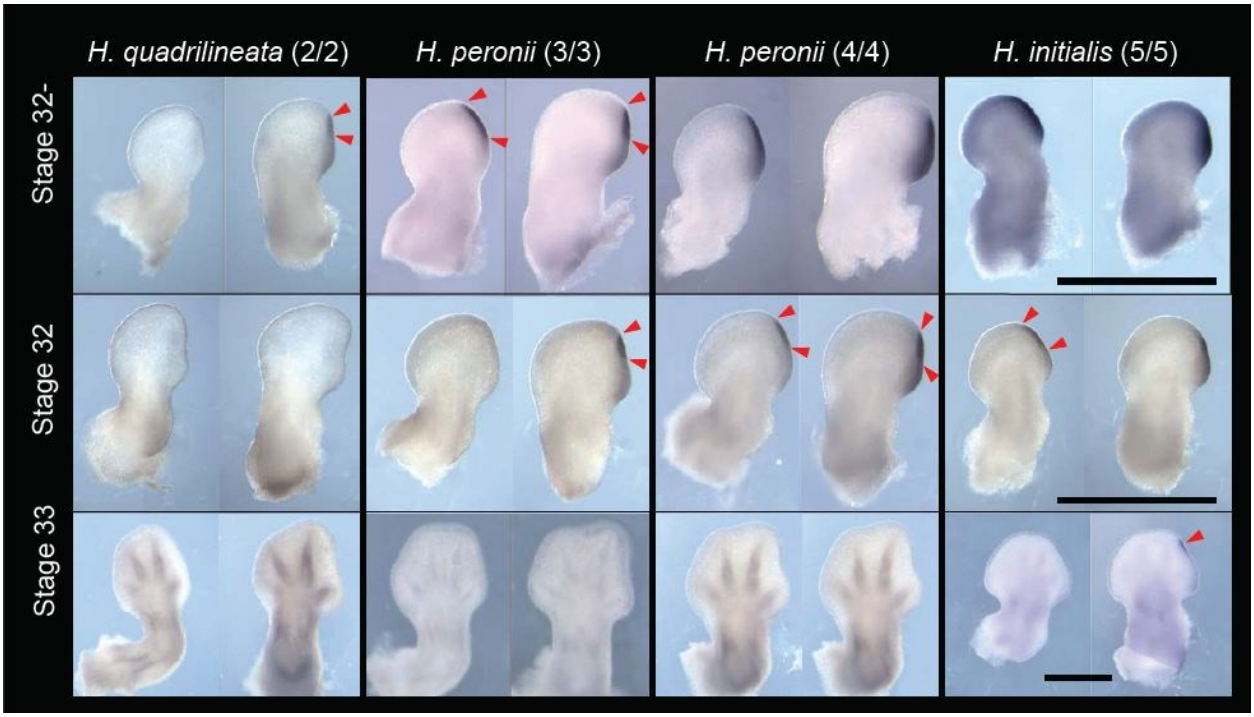

Figure 1.5:SHH duration in the limb correlated with digit loss in Australian skinks: Data from Shapiro et al., 2003 suggests that duration of SHH signaling in the limb is correlated with digit number reduction in skinks from genus *Hemiergis.*

drug cyclopamine and digit loss was attained in a pattern that mimicked the order of digit loss in natural variation for salamanders(Stopper GF 2007).

Studies on mechanics of movement in lizards of genus *Bachia* have lead to interesting theories on locomotion, body proportions and number of digits. If pleiotropic effects are overlooked and it is assumed that digit number and relative limb length are genetically independent, variation on the number of digits observed in Bachia lizards can be explained by natural selection for behavioral function of structurally reduced limbs(Lande 1978). For instance, rapid undulatory movements require lizards with long bodies to fold their limbs to their sides, in order to reduce friction during locomotion. This situation would benefit fewer digits. On the other hand, during slow movement or resting, digits are employed for balance and propping up the body. In this scenario, too few digits would be a hindrance. Thus, it is hypothesized that for a given body size and proportion, there is an optimum digit number, and that this is a selective force to stabilize digit number(Lande 1978).

Mammals

Numerous mammalian species have experienced some form of digital loss throughout evolution. Considering the wide range of habitats occupied by mammalian species, this is not a surprising strategy for locomotive adaptation. However, despite the many different strategies that mammalian species have lost digits, a common mechanism to digit loss has not been identified. Some of the current theories on digit loss suggest that digital condensations may never form in the first place, they may form and then disappear by tissue regression or destruction(Galis et al. 2002; Hamrick 2002),

they may fuse with other elements(Sears et al. 2007), they may develop at relatively slow rate or stall growth completely(Hamrick 2002).

One of the most prominent clades of mammals that have gone through different forms and stages of digit loss are undulates, the group animals that use the tips of their toes (usually hoofed) to support their weight. Some examples are pig, hippopotamus, deer, cattle, camel, giraffe, goat from the artiodactyla (even toed ungulates), and horse, tamir, rhinoceros from the perissodactyla (odd toed ungulates). The earliest known ungulates were pentadactyls, however, lineages went through stages of digit loss. Some species, such as the artiodactylous camel, retain only two digits (digits III and IV), while the perissodactylous horse has only a single digit (digit III)(K E Sears et al. 2011). This partial reduction or complete loss of lateral digits in different lineages of ungulates was an adaptation for increased cursoriality and speed, and was essential for the evolutionary success of the clade. The study of this phenomenon can provide insights into mechanisms that are employed to evolutionarily modify the constrained pentadactyl ground state in different mammalian species.

To date, the only detailed analysis of the ungulate digit formation has been undertaken on the pig (*Sus scrofa*). These studies have shown that for *S. scrofa*, digit reduction involves a process of pentadactyl patterning and initial condensation in both forelimbs and hindlimbs, followed by extreme reduction of digit I, and subsequent reductions of digits II and V. The digits that end up growing to full length are III and IV, but *S. scrofa* is still assumed to have four primary digits. Curiously, at the initial condensation stage, the relative sizes of digits are same as the adult form, and all digits continue to grow at similar rates. This suggests that it is the size of the initial

condensations that dictates the ultimate ratio of digits, with later growth occurring comparably. On a similar note, the early stage of the limb bud outgrowth, before the digital condensations are distinguishable, the pig bud appears to be significantly narrower in the A-P axis, compared to the mouse bud. Moreover, patterns of cell death zones in the limb palette are similar in the pig and pentadactyl mouse. These findings suggest that in pigs, digits I, II and V are reduced through evolutionary modifications in the earlier phase of limb development, rather than later differences in growth, regression or cell death. This does not rule out presence of other mechanisms for digit modifications to other ungulates, and a thorough examination of a range of digit loss in different mammalian species should be performed before reaching a conclusion on a common mechanism that is employed for digital loss(K E Sears et al. 2011).

Cetaceans (whales, dolphins and porpoises) are distant relatives of ungulates, and constitute another mammalian clade where digit loss and reduction is common. The first cetaceans originated in the Eocene era about 50 million years ago, branching off from the now extinct group of small artiodactyl ungulates(Bejder & Hall 2002; Thewissen et al. 2007). As an adaptation to the aquatic life, and as is the case in most secondarily aquatic tetrapods, cetaceans have evolved to hyperphalangy and digit loss(L N Cooper et al. 2007), along with embedding of the digits into the skin tissue and complete loss of the hindlimb(Thewissen et al. 2006). Odontocetes (toothed whales) and some mysticetes (baleen whales) have maintained their pentadactyous forelimbs, however, other cetaceans have lost digit I completely and retain only four digital rays in their flipper(L N Cooper et al. 2007). Another common digital modification in cetaceans is the loss of phalangeal elements in digits I and V, and increase in the number of phalanges

in digits II-IV. This unique morphology of the forelimbs provides to be suitable for the mammalian aquatic locomotion where a strong yet flexible, rigid, and narrow flippers function to steer the dorsoventral oscillatory locomotion.

A completely different clade of mammals, the rodents, also show examples of digit reduction. The jerboa, a close relative of the birch mice and jumping mice from the order Rodentia, is a family of rodents that comprise 33 species. They are distinguished with their drastically elongated hindlimbs, fused metatarsals and a range of hindlimb-specific digit reductions, adapted for a bipedal, jumping locomotion. While the forelimb morphology is highly comparable to the that of the *Mus musculus* and most other small rodents, the hindlimbs feature a range of digit reductions in different populations. Most remarkable is the *Jaculus jaculus* (the lesser Egyptian jerboa) which has lost its to lateral digits (digits I and V) and provides to be an excellent model system to study mechanisms of digit loss.

Human oligodactyly

Medical reports on supernumerary digits and loss of digits in humans date to many centuries ago(Klaassen et al. 2011), and digital malformations are still one of the most common congenital anomalies. In clinical medicine, human digital malformations are of special importance not only because it may necessitate surgical treatment, but also because it can be an easily recognizable indicator of another congenital anomaly syndrome(Biesecker 2010). Therefore, human cases of oligodactyly and polydactyly can be considered as natural experiments where a gene activity within the tight signaling network in the autopod is disrupted. So far, such mutations have helped dissect out the gene pathways and regulators that orchestrate limb patterning.

Biesecker et al., 2002 (updated 2010) have done cataloguing of clinical entities that include polydactyly as one of the manifestations(Biesecker 2002; Biesecker 2010). Among the 310 entities listed, 80 are associated with causative mutations in 99 genes. These genes include GLI2, GLI3, FGFR2, PTCH1, BMP4, HOXA13 and many others that have already been outlined in this review as part of the digital patterning network. Even though human oligodactyly is rarer and usually familial, there are also extensive studies on cases of digit loss in humans and the syndromes they are associated with, including Weyer's Ulnar Syndrome and Poland syndrome(Turnpenny et al. 1992; Bronfen et al. 1994). As one would expect, disruption of the intricate gene network in the autopod leads to different cases of patterning defects, when regulation of either the proliferation of limb tissue or patterning of digits is defective.

Etiology of human digital malformations has helped developmental biologists with the characterization of key pathways in limb development. An example is the Greig cephalopolysyndactyly syndrome (GCPS), which was recapitulated in a mouse model *extratoes* (Xt). As mentioned previously in this review, this mutation is a 3' deletion of the Gli3 gene, and its study has revealed key roles for Gli3 in cell cycle regulation and digit primordial proliferation. Other genes catalogued in the Biesecker report for polydactyly include proteins involved in cell signaling (21 genes), and genes that encode for proteins in the basal body and cilium (13 genes), DNA repair genes (15 genes) and transcription factors (16 genes). Genes encoding structural and catalytic proteins, immunoglobulin superfamily proteins, chaperones and gap junctions have also been identified. We can anticipate the study of these syndromes and causative mutations in model systems will reveal new insights into mammalian development.

In contrast to numerous cases of digit reduction throughout evolution, polydactyly is not a trait that has been evolutionary adapted, and it is not common for a species to increase its digit number from a pentadactyl ground state. Due to the high occurrence rate of polydactyly mutations in human and other mammalian populations, as well as the results of genetic manipulations, it appears to be a relatively easy process for an embryo to increase the number of its digits. Medical examinations of cases of random mutations that lead to polydactylous phenotypes suggests that pentadactyly may as well have a pleiotropic constraint where the genetic changes that lead to a polydactylous phenotype may be affecting another physical characteristic. Curiously, digital phenotypes can be manifestation of clinical cases that have also been associated with fertility problems or genital phenotypes, and therefore may be directly linked to reproductive success

Conclusion

From ancient fossil records to current human medical reports, the evolutionary and clinical perspectives to digit number and identitiy have significantly deepened our understanding of the developmental mechanisms that regulate limb formation. The non-lethal nature of digit number anomalies has also made it possible to examine experimental perturbations to model organisms, as well as a wide range of evolutionary adaptations among vertebrates, to study how an embryonic structure's form and function can be modified genetically. Therefore, digit patterning poses to be an excellent system to study form and function at cross roads of comparative morphology and novel genetic tools to study mechanism.

Therefore, any modifications to digit pattern, such as reduction in number of digits, can provide great insights into developmental mechanisms of evolutionary adaptation. Moreover, digit reduction is a convergent adaptation observed in different animals from a range of taxa, and it would be very important to see whether convergent developmental modifications are employed , or if animals display flexibility and mechanistic variation in generating the same phenotype.

References

Ahn, D., & Ho, R. K. (2008). Tri-phasic expression of posterior Hox genes during development of pectoral fins in zebrafish: implications for the evolution of vertebrate paired appendages. *Dev Biol*, *322*(1), 220–233.

Alberch Gale, EA, P. (1985). A Developmental Analysis of an Evolutionary Trend: Digital Reduction in Amphibians. *Evolution*, *39*(1), 8–23.

Alberch, P., & Gale, E. A. (1983). Size dependence during the development of the amphibian foot. Colchicine-induced digital loss and reduction. *J Embryol Exp Morphol*, *76*, 177–197.

Aza-Blanc, P., & Kornberg, T. B. (1999). Ci: a complex transducer of the hedgehog signal. *Trends Genet*, *15*(11), 458–462. doi:S0168-9525(99)01869-7 [pii]

Barkai, N., & Ben-Zvi, D. (2009). “Big frog, small frog”--maintaining proportions in embryonic development: delivered on 2 July 2008 at the 33rd FEBS Congress in Athens, Greece. *The FEBS Journal*, *276*(5), 1196–207. doi:10.1111/j.1742-4658.2008.06854.x

Bejder, L., & Hall, B. K. (2002). Limbs in whales and limblessness in other vertebrates: mechanisms of evolutionary and developmental transformation and loss. *Evol Dev*, *4*(6), 445–458.

Ben-Zvi, D., Fainsod, A., Shilo, B.-Z., & Barkai, N. (2014). Scaling of dorsal-ventral patterning in the Xenopus laevis embryo. *BioEssays : News and Reviews in Molecular, Cellular and Developmental Biology*, *36*(2), 151–6.

Bever, G. S., Gauthier, J. A., & Wagner, G. P. (2011). Finding the frame shift: digit loss, developmental variability, and the origin of the avian hand. *Evol Dev*, *13*(3), 269–279.

Biesecker, L. G. (2002). Polydactyly: how many disorders and how many genes? *Am J Med Genet*, *112*(3), 279–283.

Biesecker, L. G. (2010). Polydactyly: how many disorders and how many genes? 2010 update. *Dev Dyn*, *240*(5), 931–942.

Bretscher, A. (1949). Die Hinterbeinentwicklung von Xenopus laevis Daud. und ihre Beeinflussung durch Colchicin. *Revue Suisse Zool.*, *56*, 33–96.

Briscoe, J., Pierani, A., Jessell, T. M., & Ericson, J. (2000). A homeodomain protein code specifies progenitor cell identity and neuronal fate in the ventral neural tube. *Cell*, *101*(4), 435–445.

Bronfen, C., Rigault, P., Padovani, J. P., Touzet, P., Finidori, G., & Chaumien, J. P. (1994). [Foot deformities in longitudinal ectromelia of the lower limbs]. *Int Orthop*, *18*(3), 139–149.

Butterfield, N. C., McGlinn, E., & Wicking, C. (2010). The molecular regulation of vertebrate limb patterning. *Curr Top Dev Biol*, *90*, 319–341.

Caldwell, M. W. (2003). Without a leg to stand on'': on the volution and development of the axial elongation and limbnessness in tetrapods. *Canadian J Earth Sci*, (40), 573–588.

Chen, J. K., Taipale, J., Cooper, M. K., & Beachy, P. A. (2002). Inhibition of Hedgehog signaling by direct binding of cyclopamine to Smoothened. *Genes Dev*, *16*(21), 2743–2748.

Chen, M. H., Li, Y. J., Kawakami, T., Xu, S. M., & Chuang, P. T. (2004). Palmitoylation is required for the production of a soluble multimeric Hedgehog protein complex and long-range signaling in vertebrates. *Genes Dev*, *18*(6), 641–659.

Chen, Y., & Struhl, G. (1996). Dual roles for patched in sequestering and transducing Hedgehog. *Cell*, *87*(3), 553–563.

Chiang, C., Litingtung, Y., Harris, M. P., Simandl, B. K., Li, Y., Beachy, P. A., & Fallon, J. F. (2001). Manifestation of the limb prepattern: limb development in the absence of sonic hedgehog function. *Dev Biol*, *236*(2), 421–435.

Chiang, C., Litingtung, Y., Lee, E., Young, K. E., Corden, J. L., Westphal, H., & Beachy, P. A. (1996). Cyclopia and defective axial patterning in mice lacking Sonic hedgehog gene function. *Nature*, *383*(6599), 407–413.

Chuang, P. T., & McMahon, A. P. (1999). Vertebrate Hedgehog signalling modulated by induction of a Hedgehog-binding protein. *Nature*, *397*(6720), 617–621.

Clack, J. A. (2002). An early tetrapod from “Romer”s Gap’. *Nature*, *418*(6893), 72–76.

Clack, J. A. (2009). The Fish-Tetrapod Transition: New Fossils and Interpretations. *Evo Edu Outreach*, *2*, 213–223.

Coates, M. I. (1994). The origin of vertebrate limbs. *Dev Suppl*, 169–180.

Coates, M. I. (1996). The Devonian Tetrapod Acanthostega gunnari Jarvik: postcranial anatomy, basal tetrapod interrelationships and patterns of skeletal evolution. *Trans. R. Soc. Edinb.*, *87*, 363–421.

Coates M.I., C. J. A. (1990). Polydactyly in the earliest known tetrapod limbs. *Nature*, *347*, 66–69.

Cooke, J. (1981). Scale of body pattern adjusts to available cell number in amphibian embryos. *Nature*, *290*(5809), 775–778.

Cooper, L. N., Berta, A., Dawson, S. D., & Reidenberg, J. S. (2007). Evolution of hyperphalangy and digit reduction in the cetacean manus. *Anat Rec (Hoboken)*, *290*(6), 654–672. doi:10.1002/ar.20532

Corbit, KA, Singla, V, Norman, A.R., Stainier, D.Y., Reiter, J. F. (2005). Vertebrate Smoothened functions at the primary cilium. *Nature*, *437*, 1018–1021.

Dai, P., Akimaru, H., Tanaka, Y., Maekawa, T., Nakafuku, M., & Ishii, S. (1999). Sonic Hedgehog-induced Activation of the Gli1Promoter Is Mediated by GLI3. *J. Biol. Chem.*, *274*(12), 8143–8152.

De Robertis, E. M. (2009). Spemann's organizer and the self-regulation of embryonic fields. *Mechanisms of Development*, *126*(11-12), 925–41.

Dessaud, E., McMahon, A. P., & Briscoe, J. (2008). Pattern formation in the vertebrate neural tube: a sonic hedgehog morphogen-regulated transcriptional network. *Development*, *135*(15), 2489–2503.

Dessaud, E., Yang, L. L., Hill, K., Cox, B., Ulloa, F., Ribeiro, A., … Briscoe, J. (2007). Interpretation of the sonic hedgehog morphogen gradient by a temporal adaptation mechanism. *Nature*, *450*(7170), 717–20.

Ericson, J., Muhr, J., Jessell, T. M., & Edlund, T. (1995). Sonic hedgehog: a common signal for ventral patterning along the rostrocaudal axis of the neural tube. *Int J Dev Biol*, *39*(5), 809–816.

Ericson, J., Rashbass, P., Schedl, A., Brenner-Morton, S., Kawakami, A., van Heyningen, V., … Briscoe, J. (1997). Pax6 controls progenitor cell identity and neuronal fate in response to graded Shh signaling. *Cell*, *90*(1), 169–180.

Fior, R., & Henrique, D. (2005). A novel hes5/hes6 circuitry of negative regulation controls Notch activity during neurogenesis. *Developmental Biology*, *281*(2), 318–33.

Freitas, R., Zhang, G., & Cohn, M. J. (2007). Biphasic Hoxd gene expression in shark paired fins reveals an ancient origin of the distal limb domain. *PLoS One*, *2*(8), e754.

Galis F Metz JAJ, van A. J. J. M. (2001). Why five fingers? Evolutionary constraints on digit numbers. *TREE*, (16), 637–646.

Galis, F., Kundrat, M., & Metz, J. A. (2005). Hox genes, digit identities and the theropod/bird transition. *J Exp Zool B Mol Dev Evol*, *304*(3), 198–205.

Galis, F., van Alphen, J. J., & Metz, J. A. (2002). Digit reduction: via repatterning or developmental arrest? *Evol Dev*, *4*(4), 249–251.

Garrity, D. M., Childs, S., & Fishman, M. C. (2002). The heartstrings mutation in zebrafish causes heart/fin Tbx5 deficiency syndrome. *Development (Cambridge, England)*, *129*(19), 4635–45.

Gerard, M., Zakany, J., & Duboule, D. (1997). Interspecies exchange of a Hoxd enhancer in vivo induces premature transcription and anterior shift of the sacrum. *Dev Biol*, *190*(1), 32–40.

Goff, D. J., & Tabin, C. J. (1997). Analysis of Hoxd-13 and Hoxd-11 misexpression in chick limb buds reveals that Hox genes affect both bone condensation and growth. *Development*, *124*(3), 627–636.

Gonzalez, F., Duboule, D., & Spitz, F. (2007). Transgenic analysis of Hoxd gene regulation during digit development. *Dev Biol*, *306*(2), 847–859.

Goodrich, L. V, Johnson, R. L., Milenkovic, L., McMahon, J. A., & Scott, M. P. (1996). Conservation of the hedgehog/patched signaling pathway from flies to mice: induction of a mouse patched gene by Hedgehog. *Genes Dev*, *10*(3), 301–312.

Gould, S. J. (1978). The Panda's Peculiar Thumb. *Incorporating Nature Magazine*, *Vol. LXXXV*(No.9).

Greer, A. E. (1991). Limb reduction in squamates: Identification of the lineages and discussion of the trends. *J Herpetol*, *25*, 166–173.

Gritli-Linde, A., Lewis, P., McMahon, A. P., & Linde, A. (2001). The whereabouts of a morphogen: direct evidence for short- and graded long-range activity of hedgehog signaling peptides. *Dev Biol*, *236*(2), 364–386.

Guerrero, I., & Chiang, C. (2007). A conserved mechanism of Hedgehog gradient formation by lipid modifications. *Trends Cell Biol*, *17*(1), 1–5.

Gurdon, J. B., & Bourillot, P. Y. (2001). Morphogen gradient interpretation. *Nature*, *413*(6858), 797–803.

Hamrick, M. W. (2002). Developmental mechanisms of digit reduction. *Evol Dev*, *4*(4), 247–248.

Handler, M., Yang, X., & Shen, J. (2000). Presenilin-1 regulates neuronal differentiation during neurogenesis. *Development (Cambridge, England)*, *127*(12), 2593–606.

Hanken Wake, D., J. (1993). Miniaturization of body size: organismal consequences and evolutionary significance. *Annu. Rev. Ecol. Syst.*, *24*, 501–519.

Haramis, A. G., Brown, J. M., & Zeller, R. (1995). The limb deformity mutation disrupts the SHH/FGF-4 feedback loop and regulation of 5' HoxD genes during limb pattern formation. *Development*, *121*(12), 4237–4245.

Harfe, B. D., Scherz, P. J., Nissim, S., Tian, H., McMahon, A. P., & Tabin, C. J. (2004). Evidence for an expansion-based temporal Shh gradient in specifying vertebrate digit identities. *Cell*, *118*(4), 517–528.

Hatakeyama, J., Bessho, Y., Katoh, K., Ookawara, S., Fujioka, M., Guillemot, F., & Kageyama, R. (2004). Hes genes regulate size, shape and histogenesis of the nervous system by control of the timing of neural stem cell differentiation. *Development (Cambridge, England)*, *131*(22), 5539–50.

Hill, P., Gotz, K., & Ruther, U. (2009). A SHH-independent regulation of Gli3 is a significant determinant of anteroposterior patterning of the limb bud. *Dev Biol*, *328*(2), 506–516.

Holtz, A. M., Peterson, K. A., Nishi, Y., Morin, S., Song, J. Y., Charron, F., … Allen, B. L. (2013). Essential role for ligand-dependent feedback antagonism of vertebrate hedgehog signaling by PTCH1, PTCH2 and HHIP1 during neural patterning. *Development (Cambridge, England)*, *140*(16), 3423–34.

Huangfu, D., Liu, A., Rakeman, A. S., Murcia, N. S., Niswander, L., & Anderson, K. V. (2003). Hedgehog signalling in the mouse requires intraflagellar transport proteins. *Nature*, *426*(6962), 83–87.

Hui, C. C., & Joyner, A. L. (1993). A mouse model of greig cephalopolysyndactyly syndrome: the extra-toesJ mutation contains an intragenic deletion of the Gli3 gene. *Nat Genet*, *3*(3), 241–246.

Hutchinson, J. R., Delmer, C., Miller, C. E., Hildebrandt, T., Pitsillides, A. A., & Boyde, A. (2011). From flat foot to fat foot: structure, ontogeny, function, and evolution of elephant "sixth toes." *Science*, *334*(6063), 1699–1703.

Incardona, J. P., Gruenberg, J., & Roelink, H. (2002). Sonic hedgehog induces the segregation of patched and smoothened in endosomes. *Curr Biol*, *12*(12), 983–995.

Ingham, P. W., & McMahon, A. P. (2001). Hedgehog signaling in animal development: paradigms and principles. *Genes Dev*, *15*(23), 3059–3087.

Jeong, J., & McMahon, A. P. (2005). Growth and pattern of the mammalian neural tube are governed by partially overlapping feedback activities of the hedgehog antagonists patched 1 and Hhip1. *Development*, *132*(1), 143–154.

Jessell, T. M. (2000). Neuronal specification in the spinal cord: inductive signals and transcriptional codes. *Nat Rev Genet*, *1*(1), 20–29.

Jiang, J., & Hui, C. C. (2008). Hedgehog signaling in development and cancer. *Dev Cell*, *15*(6), 801–812.

Klaassen, Z., Shoja, M. M., Tubbs, R. S., & Loukas, M. (2011). Supernumerary and absent limbs and digits of the lower limb: a review of the literature. *Clin Anat*, *24*(5), 570–575.

Kraus, P., Fraidenraich, D., & Loomis, C. A. (2001). Some distal limb structures develop in mice lacking Sonic hedgehog signaling. *Mech Dev*, *100*(1), 45–58.

Kumar, S., & Hedges, S. B. (1998). A molecular timescale for vertebrate evolution. *Nature*, *392*(6679), 917–20.

Kutejova, E., Briscoe, J., & Kicheva, A. (2009). Temporal dynamics of patterning by morphogen gradients. *Curr Opin Genet Dev*, *19*(4), 315–322.

Lande, R. (1978). Evolutionary Mechanisms of Limb Loss in Tetrapods. *Evolution*, *32*(1), 73–92.

Larsson, H. C., Heppleston, A. C., & Elsey, R. M. (2010). Pentadactyl ground state of the manus of Alligator mississippiensis and insights into the evolution of digital reduction in Archosauria. *J Exp Zool B Mol Dev Evol*, *7*, 571–9.

Laurin, M. (1998). A reevaluation of the origin of pentadactyly. *Evolution*, *52*, 1476–1482.

Lebedev, O. A. (1984). The first find of a Devonian tetrapod in the U.S.S.R. *Dokl. Akad. Nauk. SSSR*, *278*, 1407–1473.

Li, Y., Zhang, H., Litingtung, Y., & Chiang, C. (2006). Cholesterol modification restricts the spread of Shh gradient in the limb bud. *Proc Natl Acad Sci U S A*, *103*(17), 6548–6553.

Litingtung, Y., Dahn, R. D., Li, Y., Fallon, J. F., & Chiang, C. (2002). Shh and Gli3 are dispensable for limb skeleton formation but regulate digit number and identity. *Nature*, *418*(6901), 979–983.

Liu, A., Wang, B., & Niswander, L. A. (2005). Mouse intraflagellar transport proteins regulate both the activator and repressor functions of Gli transcription factors. *Development*, *132*(13), 3103–3111.

Lopez-Rios, J., Speziale, D., Robay, D., Scotti, M., Osterwalder, M., Nusspaumer, G., … Zeller, R. (2012). GLI3 constrains digit number by controlling both progenitor proliferation and BMP-dependent exit to chondrogenesis. *Dev Cell*, *22*(4), 837–848.

Macias, D., Ganan, Y., Rodriguez-Leon, J., Merino, R., & Hurle, J. M. (1999). Regulation by members of the transforming growth factor beta superfamily of the digital and interdigital fates of the autopodial limb mesoderm. *Cell Tissue Res*, *296*(1), 95–102.

Marigo, V., Scott, M. P., Johnson, R. L., Goodrich, L. V, & Tabin, C. J. (1996). Conservation in hedgehog signaling: induction of a chicken patched homolog by Sonic hedgehog in the developing limb. *Development*, *122*(4), 1225–1233.

Martinelli, D. C., & Fan, C. M. (2007). Gas1 extends the range of Hedgehog action by facilitating its signaling. *Genes Dev*, *21*(10), 1231–1243.

Masuya, H., Sagai, T., Wakana, S., Moriwaki, K., & Shiroishi, T. (1995). A duplicated zone of polarizing activity in polydactylous mouse mutants. *Genes Dev*, *9*(13), 1645–1653.

Meyer, N. P., & Roelink, H. (2003). The amino-terminal region of Gli3 antagonizes the Shh response and acts in dorsoventral fate specification in the developing spinal cord. *Dev Biol*, *257*(2), 343–355.

Michos, O., Panman, L., Vintersten, K., Beier, K., Zeller, R., & Zuniga, A. (2004). Gremlin-mediated BMP antagonism induces the epithelial-mesenchymal feedback signaling controlling metanephric kidney and limb organogenesis. *Development*, *131*(14), 3401–3410.

Mitgutsch, C., Richardson, M. K., Jimenez, R., Martin, J. E., Kondrashov, P., de Bakker, M. A., & Sanchez-Villagra, M. R. (2012). Circumventing the polydactyly “constraint”: the mole’s “thumb.” *Biol Lett*, *8*(1), 74–77.

Montavon, T., Soshnikova, N., Mascrez, B., Joye, E., Thevenet, L., Splinter, E., … Duboule, D. (2011). A regulatory archipelago controls Hox genes transcription in digits. *Cell*, *147*(5), 1132–1145.

Morgan, T. (1895). Half embryos and whole embryos from one of the first two blastomeres of the frog’s egg. *Anat. Anz*, *10*, 623–638.

Nelson, C. E., Morgan, B. A., Burke, A. C., Laufer, E., DiMambro, E., Murtaugh, L. C., … Tabin, C. (1996). Analysis of Hox gene expression in the chick limb bud. *Development*, *122*(5), 1449–1466.

Nishi, Y., Ji, H., Wong, W. H., McMahon, A. P., & Vokes, S. A. (2009). Modeling the spatio-temporal network that drives patterning in the vertebrate central nervous system. *Biochim Biophys Acta*, *1789*(4), 299–305.

Ohtsuka, T., Ishibashi, M., Gradwohl, G., Nakanishi, S., Guillemot, F., & Kageyama, R. (1999). Hes1 and Hes5 as notch effectors in mammalian neuronal differentiation. *The EMBO Journal*, *18*(8), 2196–207.

Ohtsuka, T., Sakamoto, M., Guillemot, F., & Kageyama, R. (2001). Roles of the basic helix-loop-helix genes Hes1 and Hes5 in expansion of neural stem cells of the developing brain. *The Journal of Biological Chemistry*, *276*(32), 30467–74.

Owen, R. (1848). *On the Archetype and Homologies of the Vertebrate Skeleton*. London: John van Voorst , Paternoster Row.

Paganelli Olszowka, A., Ar, A, C. V. (1974). The avian egg: surface area, volume and density. *The Condor*, (76), 319–325.

Pan, A., Chang, L., Nguyen, A., & James, A. W. (2013). A review of hedgehog signaling in cranial bone development. *Frontiers in Physiology*, *4*, 61.

Perrimon, N., & McMahon, A. P. (1999). Negative feedback mechanisms and their roles during pattern formation. *Cell*, *97*(1), 13–16.

Robert, B. (2007). Bone morphogenetic protein signaling in limb outgrowth and patterning. *Dev Growth Differ*, *49*(6), 455–468.

Saha, K., & Schaffer, D. V. (2006). Signal dynamics in Sonic hedgehog tissue patterning. *Development*, *133*(5), 889–900.

Schneider, I., Aneas, I., Gehrke, A. R., Dahn, R. D., Nobrega, M. A., & Shubin, N. H. (2011). Appendage expression driven by the Hoxd Global Control Region is an ancient gnathostome feature. *Proc Natl Acad Sci U S A*, *108*(31), 12782–12786.

Sears, K. E., Behringer, R. R., Rasweiler, J. J. th, & Niswander, L. A. (2007). The evolutionary and developmental basis of parallel reduction in mammalian zeugopod elements. *Am Nat*, *169*(1), 105–117.

Sears, K. E., Bormet, A. K., Rockwell, A., Powers, L. E., Noelle Cooper, L., & Wheeler, M. B. (2011). Developmental basis of mammalian digit reduction: a case study in pigs. *Evol Dev*, *13*(6), 533–541.

Shapiro, M. D., Hanken, J., & Rosenthal, N. (2003). Developmental basis of evolutionary digit loss in the Australian lizard Hemiergis. *J Exp Zool B Mol Dev Evol*, *297*(1), 48–56.

Shubin N., A. P. (1986). A morphogenetic approach to the origin and basic organisation of the tetrapod limb. *Evolutionary Biology*, *20*, 319–387.

Shubin, N. H. (2002). Origin of evolutionary novelty: examples from limbs. *J Morphol*, *252*(1), 15–28.

Shubin, N., Tabin, C., & Carroll, S. (2009). Deep homology and the origins of evolutionary novelty. *Nature*, *457*(7231), 818–823. doi:nature07891 [pii] 10.1038/nature07891

Shubin N., W. D. B. (1996). Phylogeny, variation, and morphological integration. *Am Zool*, (36), 51–60.

Sordino, P., & Duboule, D. (1996). A molecular approach to the evolution of vertebrate paired appendages. *Trends Ecol Evol*, *11*(3), 114–119.

Sordino, P., Duboule, D., & Kondo, T. (1996). Zebrafish Hoxa and Evx-2 genes: cloning, developmental expression and implications for the functional evolution of posterior Hox genes. *Mech Dev*, *59*(2), 165–175.

Sordino, P., van der Hoeven, F., & Duboule, D. (1995). Hox gene expression in teleost fins and the origin of vertebrate digits. *Nature*, *375*(6533), 678–681.

Spemann H, H. ; M. (1924). Induction of embryonic primordia by implantation of organizers from a different species. *Roux's Arch Entw Mech*, (100), 599–638.

Spemann, H. (1938). *Embryonic Development and Induction*. New Haven, CT: Yale University Press.

Spitz, F., Gonzalez, F., & Duboule, D. (2003). A global control region defines a chromosomal regulatory landscape containing the HoxD cluster. *Cell*, *113*(3), 405–417.

Stamataki, D., Ulloa, F., Tsoni, S. V, Mynett, A., & Briscoe, J. (2005). A gradient of Gli activity mediates graded Sonic Hedgehog signaling in the neural tube, 626–641.

Stamataki, D., Ulloa, F., Tsoni, S. V, Mynett, A., & Briscoe, J. (2005). A gradient of Gli activity mediates graded Sonic Hedgehog signaling in the neural tube. *Genes Dev*, *19*(5), 626–641.

Stopper GF, W. G. P. (2007). Inhibition of Sonic hedgehog Signaling Leads to Posterior Digit Loss in Ambystoma mexicanum: Parallels to Natural Digit Reduction in Urodeles. *Developmental Dynamics*, *236*, 321–333.

Tabin, C. J. (1992). Why we have (only) five fingers per hand: hox genes and the evolution of paired limbs. *Development*, *116*(2), 289–296.

Tarchini, B., & Duboule, D. (2006). Control of Hoxd genes' collinearity during early limb development. *Dev Cell*, *10*(1), 93–103.

Teleman, a a, & Cohen, S. M. (2000). Dpp gradient formation in the Drosophila wing imaginal disc. *Cell*, *103*(6), 971–80.

Tenzen, T., Allen, B. L., Cole, F., Kang, J.-S., Krauss, R. S., & McMahon, A. P. (2006). The cell surface membrane proteins Cdo and Boc are components and targets of the Hedgehog signaling pathway and feedback network in mice. *Developmental Cell*, *10*(5), 647–56.

The, I., Bellaiche, Y., & Perrimon, N. (1999). Hedgehog movement is regulated through tout velu-dependent synthesis of a heparan sulfate proteoglycan. *Mol Cell*, *4*(4), 633–639.

Thewissen, J. G., Cohn, M. J., Stevens, L. S., Bajpai, S., Heyning, J., & Horton Jr., W. E. (2006). Developmental basis for hind-limb loss in dolphins and origin of the cetacean bodyplan. *Proc Natl Acad Sci U S A*, *103*(22), 8414–8418.

Thewissen, J. G., Cooper, L. N., Clementz, M. T., Bajpai, S., & Tiwari, B. N. (2007). Whales originated from aquatic artiodactyls in the Eocene epoch of India. *Nature*, *450*(7173), 1190–1194.

Tickle, C., Summerbell, D., & Wolpert, L. (1975). Positional signalling and specification of digits in chick limb morphogenesis. *Nature*, *254*(5497), 199–202.

Turnpenny, P. D., Dean, J. C., Duffty, P., Reid, J. A., & Carter, P. (1992). Weyers' ulnar ray/oligodactyly syndrome and the association of midline malformations with ulnar ray defects. *J Med Genet*, *29*(9), 659–662.

Vargas AO, F. J. F. (2005a). Birds have dinosaur wings: the molecular evidence. *J Exp Zool*, (304B), 86–90.

Vargas AO, F. J. F. (2005b). The digits of the wing of birds are 1,2, and 3. A review. *J Exp Zool*, (304B), 206–219.

Wagner Misof, B.Y., G. P. (1993). How can a character be developmentally constrained despite variation in developmental pathways. *J. Evol. Biol.*, *6*, 449–455.

Wagner, G. P., & Chiu, C. H. (2001). The tetrapod limb: a hypothesis on its origin. *J Exp Zool*, *291*(3), 226–240.

Wake Shubin, N., D. B. (1998). Limb development in the Pacific giant salamanders, Dicamptodon (Amphibia, Caudata, Dicamptodontidae). *Can J Zool*, *76*, 2058–2066.

Wang, B., Fallon, J. F., & Beachy, P. A. (2000). Hedgehog-regulated processing of Gli3 produces an anterior/posterior repressor gradient in the developing vertebrate limb. *Cell*, *100*(4), 423–434.

Wang, Z., Young, R. L., Xue, H., & Wagner, G. P. (2011). Transcriptomic analysis of avian digits reveals conserved and derived digit identities in birds. *Nature*, *477*(7366), 583–586.

Wiens J.J. J.T., H. (2008). Digit Reduction, body size, and paedomorphosis in salamanders. *Evolution & Development*, *10*(4), 449–463.

Wolpert, L. (2011). Positional information and patterning revisited. *Journal of Theoretical Biology*, *269*(1), 359–65.

Yamada, T., Pfaff, S. L., Edlund, T., & Jessell, T. M. (1993). Control of cell pattern in the neural tube: motor neuron induction by diffusible factors from notochord and floor plate. *Cell*, *73*(4), 673–686.

Yokouchi, Y., Nakazato, S., Yamamoto, M., Goto, Y., Kameda, T., Iba, H., & Kuroiwa, A. (1995). Misexpression of Hoxa-13 induces cartilage homeotic transformation and changes cell adhesiveness in chick limb buds. *Genes Dev*, *9*(20), 2509–2522.

Zakany, J., & Duboule, D. (1996). Synpolydactyly in mice with a targeted deficiency in the HoxD complex. *Nature*, *384*(6604), 69–71. doi:10.1038/384069a0

Zakany, J., & Duboule, D. (1999). Hox genes in digit development and evolution. *Cell Tissue Res*, *296*(1), 19–25.

Zakany, J., Fromental-Ramain, C., Warot, X., & Duboule, D. (1997). Regulation of number and size of digits by posterior Hox genes: a dose-dependent mechanism with potential evolutionary implications. *Proc Natl Acad Sci U S A*, *94*(25), 13695–13700.

Zakany, J., Kmita, M., & Duboule, D. (2004). A dual role for Hox genes in limb anterior-posterior asymmetry. *Science*, *304*(5677), 1669–1672.

Zeller, R., López-Ríos, J., & Zuniga, A. (2009). Vertebrate limb bud development: moving towards integrative analysis of organogenesis. *Nature Reviews. Genetics*, *10*(12), 845–58.

Zeng, X., Goetz, J. A., Suber, L. M., Scott Jr., W. J., Schreiner, C. M., & Robbins, D. J. (2001). A freely diffusible form of Sonic hedgehog mediates long-range signalling. *Nature*, *411*(6838), 716–720.

Chapter Two

Scaling Pattern to Variations in Size during Vertebrate Neural Tube Development

“It was much pleasanter at home," thought poor Alice, "when one wasn't always growing larger and smaller, and being ordered about by mice and rabbits. I almost wish I hadn't gone down the rabbit-hole -and yet- it's rather curious you know, this sort of life.”
— **Lewis Carroll, *Alice in Wonderland***

Scaling Pattern to Variations in Size during Vertebrate Neural Tube Development

Aysu Uygur[1], James Briscoe[2] and Clifford J. Tabin[1#]

1. *Harvard Medical School, Department of Genetics, 77 Avenue Louis Pasteur, Boston, Massachusetts, 02115, USA*
2. *MRC National Institute for Medical Research, Mill Hill, London NW7 1AA*

[#]*Corresponding author, email: tabin@genetics.med.harvard.edu*

The work in this chapter was originally conceived by Cliff Tabin and Aysu Uygur. All experiments were designed by AU and CT with intellectual input from JB. Experiments and analysis were conducted by AU. Text, figures and tables were produced by AU.

Summary

Mechanisms of morphogen mediated pattern formation are largely conserved across vertebrate species, however, little is known about how they are adapted to generate essentially identical morphological structures in varying embryonic sizes. We explored this question using a comparative approach and analyzed the dynamics of patterning in chick (*Gallus gallus*), zebra finch (*Taeniopygia guttata*) and emu (*Dromaius novaehollandiae*), three species that are drastically different in embryonic size starting at a very early time point in development. We focused on the patterning dynamics of the neural tube dorso-ventral axis, where neuronal cell fate specification induced by Sonic hedgehog is one of the best-studied examples of morphogen mediated organization and expression domains of distinct transcription factors provide an excellent read out for morphogen response.

Our findings suggest that there is a difference to cellular morphogen response in the three avian species, observed both *in vivo* and *in vitro*. *In vivo*, temporal dynamics of patterning are shifted, where the neural tube of the smaller bird, the zebra finch, is patterned fastest and the neural tube of the bigger bird, the emu, is patterned slowest. *In vitro,* naive neural plate explant assays suggest that morphogen sensitivity decreases as embryonic size increases: Finch cells are most sensitive to a given Shh concentration or duration, while the emu cells are the least sensitive. This differential response is intrinsic, as suggested by generation of chimeric embryos at 12 hr of development. Cells from different species in the neural tubes of chimeric embryos retain their potential of differential response.

We believe this difference in response is crucial to scaling pattern to size in three species and that temporal adjustment is essential for conserving spatial organization of cell types in the neural tube dorso-ventral axis. We are further exploring the mechanism of this and have strong evidence that the differential it is due to intrinsic differences in GLI activity. A mechanistic understanding of differences in morphogen mediated patterning in species of different sizes will provide important insights into how pattern is adapted to size throughout evolution.

Introduction

There is an enormous variation in size throughout the animal kingdom. Across species, embryonic development is orchestrated by conserved signaling events, yet morphological patterns arise in proportion with the size of the developing embryo. Scaling form and function to size is a fundamental question that arises repeatedly when we think about evolution of size variation across species at time of patterning, embryogenesis.

In many species ranging from cnidarians to humans, morphological patterning is guided by a spatial gradient of morphogens, long-range extracellular effectors that induce different cell fates in a concentration dependent manner. During embryonic development, morphogen gradients are launched by evolutionarily conserved molecular networks, and correct morphological patterning is established proportional to the embryonic size, within or across species. Work on morphogen mediated patterning dates back to theoretical studies of Lewis Wolpert(Wolpert 1969) several decades ago, where the term ‘French flag model’ was first coined. According to this classical view of morphogens, distance from source is an integral component of positional information

and cell fate specification, as it dictates the concentration and duration of morphogen exposure (**Fig 2.1a**). However, an interesting problem arises when same pattern is to be established in tissues of different sizes. How do we integrate inter-species size differences at time of patterning to the classical view of morphogen? We set out to explore this question, and suggest two different strategies through which this can be achieved. Our first model is to alter shape of the gradient, such that each threshold concentration is reached at a shorter distance from morphogen source. A faster decay rate of the morphogen molecule along the tissue is one way to achieve this. Another possibility is to alter the threshold concentration values at which cell type induction occurs, such that, regardless of the amplitude or shape of the morphogen concentration gradient, same pattern can be established.**(Fig 2.1b)**

We set out to explore this question in a model system that is widely used to study morphogen mediated patterns, the vertebrate neural tube. The ventral neural tube is an excellent system to study different aspects of morphogen mediated patterning due to the availability of a molecular read-out for morphogen activity. During neural tube development, morphogen Sonic hedgehog is secreted by the ventrally located notochord and floorplate, and diffuses to form a concentration gradient across the dorso-ventral axis(Jessell 2000). Distinct sets of transcription factors are expressed in progenitor domains as cell fate specification occurs at threshold concentrations(Yamada et al. 1991; Yamada et al. 1993; Dessaud et al. 2007). Dorsal expansion of these domains are also markers of stronger morphogen response in the tissue: as the tissue is exposed to a higher concentration of SHH for a longer duration, cells that are more dorsally located from the source can reach a specific threshold concentration and

undergo cell type specification. At the end of patterning, 5 distinct ventral cell types are produced, with the more ventrally located cells reaching higher threshold concentrations, and more dorsally located cells reaching lower threshold values. Availability of an *in vitro* explant technique pioneered by the Jessell and Briscoe groups makes it possible to study morphogen activity in a more controlled environment and assess response with known molecular markers(Yamada et al. 1993).

To explore dynamics of size and pattern in the developing ventral neural tube, we picked three different avian species that are remarkably different in egg size. Members of Class Aves show a large variation in egg size, and therefore an expected variation in embryonic size, but are still related close enough that we can expect general mechanisms governing morphogen mediated patterning to be conserved. Zebra Finch (*Taeniopygia guttata*), Chick (*Gallus gallus*) and the Emu bird (*Dromaius novaehollandiae*) lay eggs that cover a large range of sizes, making it possible to perform comparative and molecular studies in varying embryonic sizes **(Supplementary Figure S1.1 and S1.2)**.

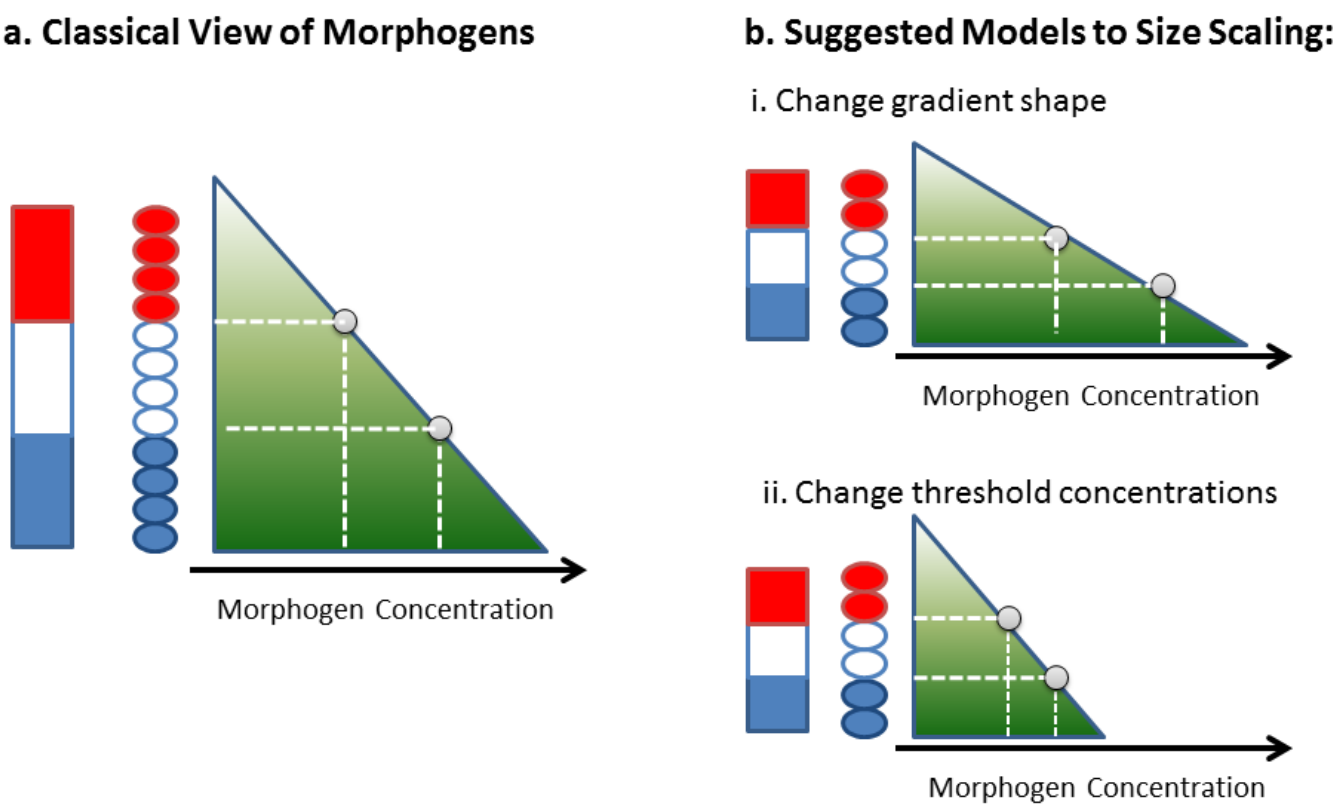

Figure 2.1: Classical morphogen model and suggested models on pattern scaling: a. According to the classical french flag model of morphogen mediated patterning, distance of a cell from morphogen source dictates the concentration and duration of morphogen exposure, where cells closer to the source are exposed to higher level of the morphogen protein, which forms a concentration gradient along the tissue. At specific threshold concentrations, cells are induced to specific fates. Therefore, size of the tissue is an integral component of pattern. **b.** We have come up with two distinct models to resolve pattern scaling problem in systems where size is different but eventual pattern is proportionate. First strategy is to change the shape of the gradient but keep threshold values the same. A second strategy is to alter threshold concentration values, such that pattern can be conserved regardless of the amplitude or shape of the gradient.

Results

Before assessing dynamics of patterning in the neural tubes of the Finch, Chick and Emu, we wanted to quantify size and growth across the D-V axis at comparable stages. As the size of the neural tube D-V axis is not uniform along the antero-posterior axis, we picked somite 15 as reference point for all developmental time points in the three species, and analyzed patterning at this A-P level so as to stay consisted between samples and species. Formation of somite 15 was designated as t=0, and data for subsequent time points are plotted as hours after formation of this somite.

Size measurements show that growth along D-V axis is not comparable in the three species (**Figure 2.2a**). Towards the end of neural tube development the biggest bird, Emu, has the largest number of neurons in the neural tube, while the smallest bird, Zebra Finch, has the smallest. Surprisingly, for a brief time at the very early stages of development, size is comparable in three species. However, our analysis of % PH3 in neural tube progenitors of the three species shows that the smallest bird Zebra Finch goes through growth arrest earlier, while the biggest bird has prolonged proliferation in the ventral neural tube, even at time points at which cellular proliferation in Zebra Finch ventral neural tube has completely stopped (**Figure 2.2b**). Size of the progenitor cells, analyzed by membrane-GFP as well as DAPI stainings show that it is comparable in all three species (data not shown).

Figure 2.2: Neural tube dorso ventral axis growth dynamics in Finch, Chick and Emu a. Cell number along dorso-ventral axis in is plotted against time, and hours after formation of somite 15. All sections are along the level of somite 15, and t=0 is when somite 15 forms. Surprisingly, within the first few hours, size of the neural tube is comparable among the three species. Shortly after, chick neural tube grows bigger than Finch and ends up becoming significantly larger. Emu, on the other hand, grows more gradually but surpasses chick (at the latest stage we were able to sample). **b.** Analysis of cellular proliferation (%PH3 in progenitors) in ventral neural tube shows that this difference in size stems from early growth arrest in the Finch ventral neural tube, and prolonged growth in the Emu ventral neural tube. * $p<0.05$

a.

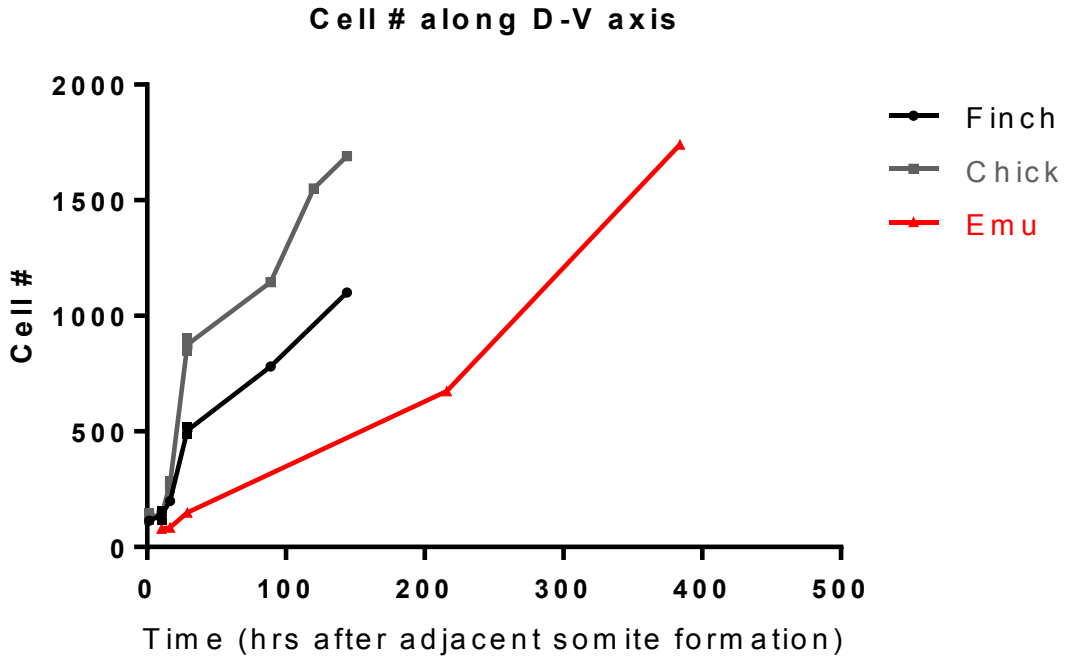

b.

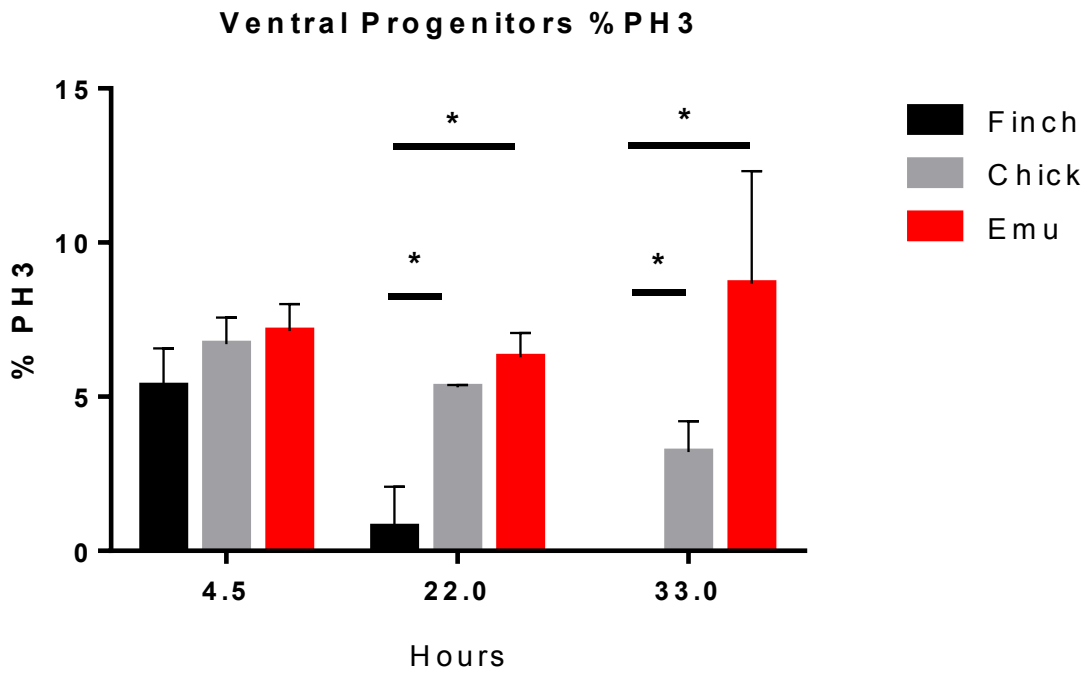

Figure 2.2, continued

Knowing that the growth dynamics are different in three species, we wanted to map out patterning dynamics. In order to characterize progression of pattern, we analyzed the expression domains of several transcription factors that mark distinct neuronal progenitors. OLIG2 expression marks motor neuron progenitors (pMN), NKX2.2 expression marks ventral-most v3 inter neuron progenitors (pV3) and NKX6.1 expression marks all ventral progenitor domains (pV3-pV0). We collected neural tube tissue at the antero-posterior position adjacent to somite 15 across developmental stages (roughly forelimb level for all species), thereby avoiding stage specific differences in timing or differences in signaling dynamics across the A-P axis. Expansion of the signal in progenitor domains was measured from the ventral midline.

A prevailing notion on scaling of morphogen mediated patterning events is that pattern is inherently scaled to size throughout growth. In the three species we analyzed, we realized that progression of pattern does not necessarily scale to D-V axis size, except for at the end of patterning process. (**Figure 2.3**) We noticed that even though all three species end up with proportionate patterning of their progenitor domains to their final size before differentiation begins, the speed at which progenitor domains expand is entirely different. For all transcription factors we analyzed, domain expansion and patterning is accelerated in the smaller bird Zebra Finch and drastically decelerated in the Emu. This is true not only for the percent dorsal expansion of the domains, but also for the total number of cells that are induced to express any specific marker gene (**Figure 2.3e, Supplementary Figure S1.3 and S1.4**). This indicates that progression of pattern is not scaled among species throughout the process of patterning, but rather,

Figure 2.3: Dorsal expansion of distinct progenitor domains across developmental time Percent dorsal expansion of progenitor domains along the D-V axis of neural tube shows accelerated domain progression in the Finch neural tube, in contrast to a dramatically decelerated Emu patterning process**. a-c**: Dorsal expansion of the domains of specific transcription factors that are known to be upregulated by Shh exposure. All follow a similar pattern where patterning is most rapid in the Finch tissue and slowest in the Emu**. d**. We also wanted to analyze a dorsal transcription factor, Pax7, whose expression is initially suppressed by exposure to Shh. Indeed, Pax7 is excluded from ventral domains in the Finch tissue, while it can expand more ventrally in the chick. **e.** Olig2 pattern progression by cell number, not percent expansion. Again, progenitors expressing Olig2 are greater in number in the Finch neural tube from an earlier time point.

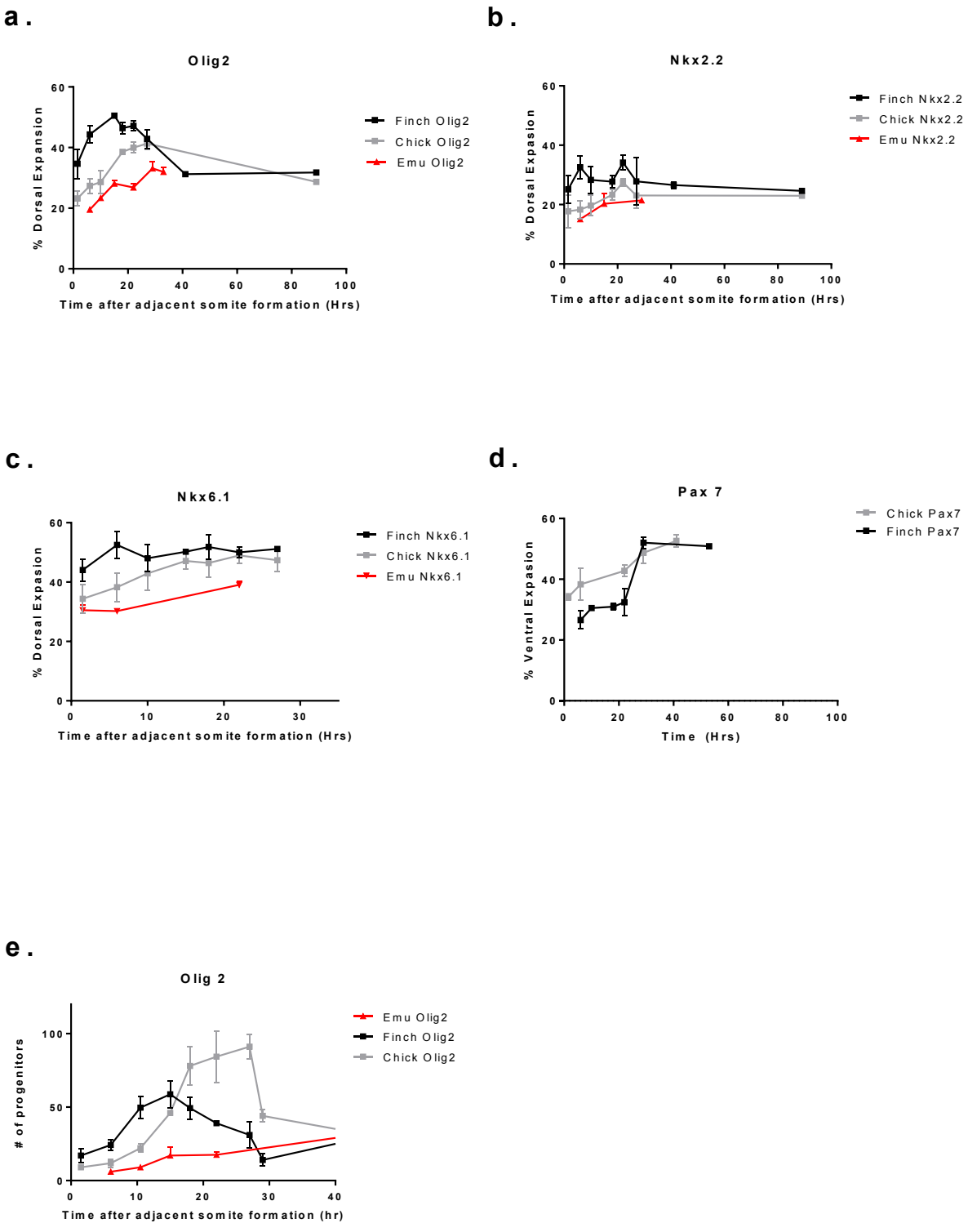

Figure 2.3, continued

regulated differently such that final outcome to scale. Since we know the growth dynamics are also entirely different between these embryos, this strategy may help the smaller bird couple patterning to an early arrested growth, while the bigger bird can slow down its patterning process so as to accommodate an elongated growth period.

Interestingly, we also observe the expression of motor neuron differentiation marker isl-1 earliest in the Finch neural tube and latest in the Emu (**Supplemental Figure S1.5**). However, it remains to be explored whether the difference in timing of differentiation is due to species-specific differences in rate of differentiation, or simply due to the differences in the patterning phase. When assessed with OLIG2 expressing progenitor numbers throughout development, it seems that an earlier expression of Isl-1 may be a result of Olig2 expression that is induced earlier in Finch progenitors, as opposed to differences in rate of differentiation.

The observation that the three different species regulate patterning differently lead us question differences in source of morphogen. Both the notochord size and notochord cell number increases as we move from the smaller bird to the bigger bird. If we assume each cell in the notochord to secrete comparable levels of SHH, we would expect the Zebra Finch notochord to produce the least amount of the morphogen, and the Emu to produce the most. To address this, we performed an *in vitro* assay where we plant a naïve Chick neural plate intermediate explant adjacent to the same length of either Zebra Finch, Chick or Emu notochord (**Figure 2.4**). Embedded in collagen and grown *in vitro* in media for 24 hr, the initially naïve explants are later assayed for expression of NKX2.2 and OLIG2. We chose these two transcription factors in particular because previous studies have shown that NKX2.2 is a higher threshold response gene

Figure 2.4:Exposure of tissues to the morphogen Shh is lowest in the Finch and highest in the Emu: a. Size of the notochords in the three species at two different developmental time points**. b.** Notochord-naïve chick explant incubations are immunostained after 24 hours for transcription factors Nkx2.2 (higher response) and Olig2 (lower response).

a.

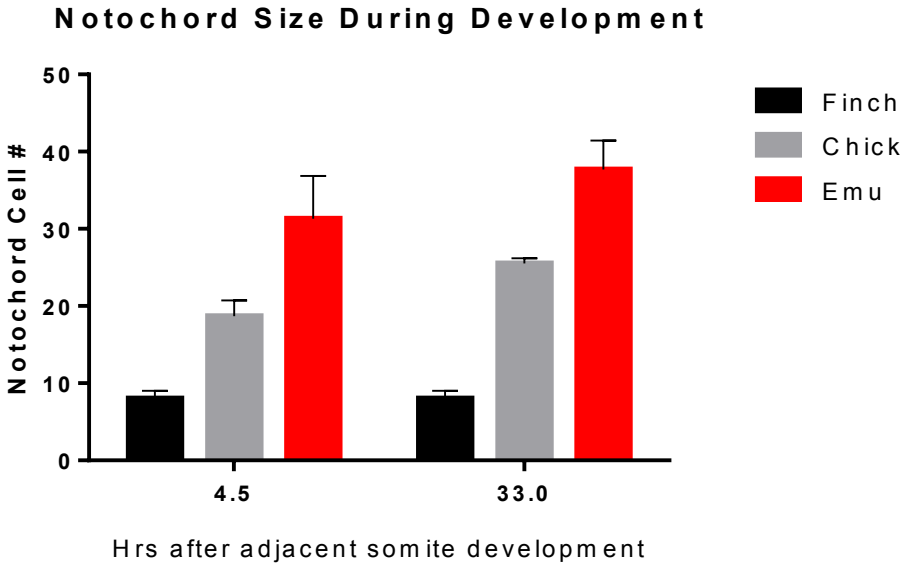

b.

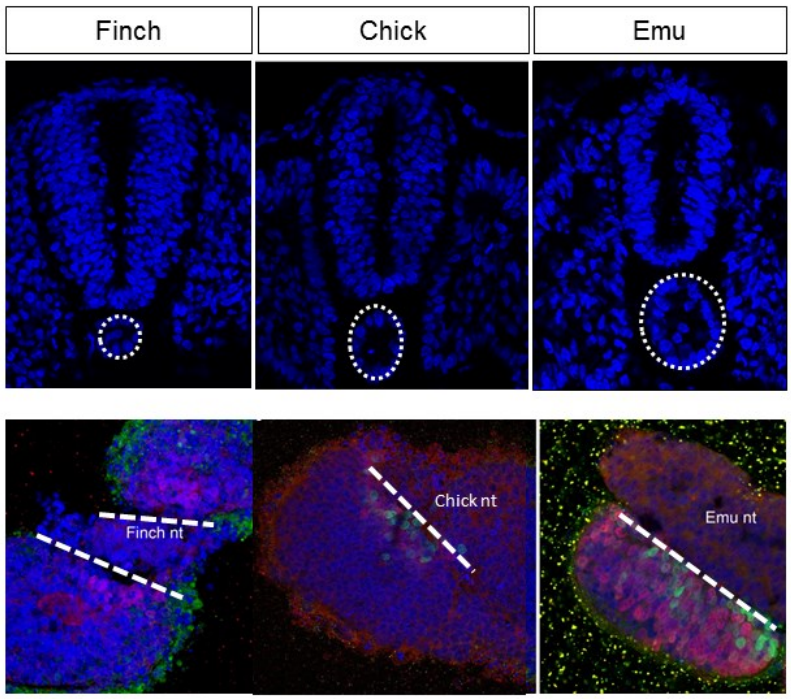

Figure 2.4, continued

and requires a higher concentration of SHH for longer, whereas Olig2 is a lower threshold response gene(Dessaud et al. 2008). Thus, we have a direct molecular read out for morphogen response in explants, and both of these antibodies work equally well for the three species, as shown *in vivo*. The expression analysis of the *in vitro* chick explants show that when a naïve intermediate neural plate tissue is incubated with notochords from all three species, Finch notochords induce the lowest morphogen response, and the Emu notochords induce the strongest. As shown in **Figure 2.4**, cells in the explants planted adjacent to the Finch notochord express the lower threshold response gene OLIG2, while the explants planted adjacent to the Chick notochord has higher threshold response gene NKX2.2 expression as well as OLIG2. The emu notochord, on the other hand, induces very strong Nkx2.2 and Olig2 response in the explant tissues. Thus, we can conclude that the morphogen activity the naïve neural tube tissue is exposed to is least potent in the smallest bird Finch, and most potent in the biggest bird Emu.

These findings so far present a paradoxical situation such that the Finch has the smallest notochord and lowest morphogen activity but patterns its neural tube tissue most rapidly, whereas the Emu has the largest notochord and strongest morphogen activity, but patterns most gradually. This prompted us to explore the *response* of the tissue in the three species to the morphogen SHH. We isolated naïve intermediate neural plate explants from Finch, Chick and Emu embryos and incubated *in vitro* with different concentrations of recombinant SHH-N. After 24 hours, explants were harvested and immunostained for NKX2.2 and OLIG2 expression (**Figure 2.5**). Lower concentrations of SHH were sufficient to induce high threshold response gene NKX2.2

in the Finch explants, while same concentrations induced OLIG2 expression in the Chick explants and no response in the Emu. At higher concentrations, both Finch and Chick were saturated for NKX2.2 response, however, emu explants still did not upregulate expression of either OLIG2 or NKX2.2. At a much higher concentration, we were able to see NKX2.2 induction in the Emu explants. We also assayed for PAX7 expression in the explants for a lower threshold concentration, and observed that Emu explants continue to express Pax7 upon exposure to SHH at 60 nM, a concentration that is high enough to suppress PAX7 in both Finch and Chick tissues, which are more sensitive to the same level of the morphogen. *In vitro* assays show us that the Zebra Finch is most sensitive to a given concentration of SHH, while Emu is the least sensitive. This differential response to morphogen can explain why the smaller bird has accelerated patterning, while the overall process is slower in the Chick and drastically slower in the Emu.

Previous studies have shown that it is not only the absolute concentration of the morphogen, but also the duration of exposure that is integrated into a cell's interpretation of the morphogen signal(Harfe et al. 2004; Dessaud et al. 2007). Therefore, we wanted to test how different tissues behaved when exposed to the same concentration of morphogen, but for varying durations. At 12 hours of exposure to a fixed concentration of SHH, the Finch tissue was saturated for the high threshold NKX2.2 response, whereas for the same duration of exposure at same concentration the Chick tissue only expressed the low threshold OLIG2 (**Supplementary Figure S1.6**). At 24 hr, explants from both species were saturated for NKX2.2. It is evident that differential response also has a temporal component.

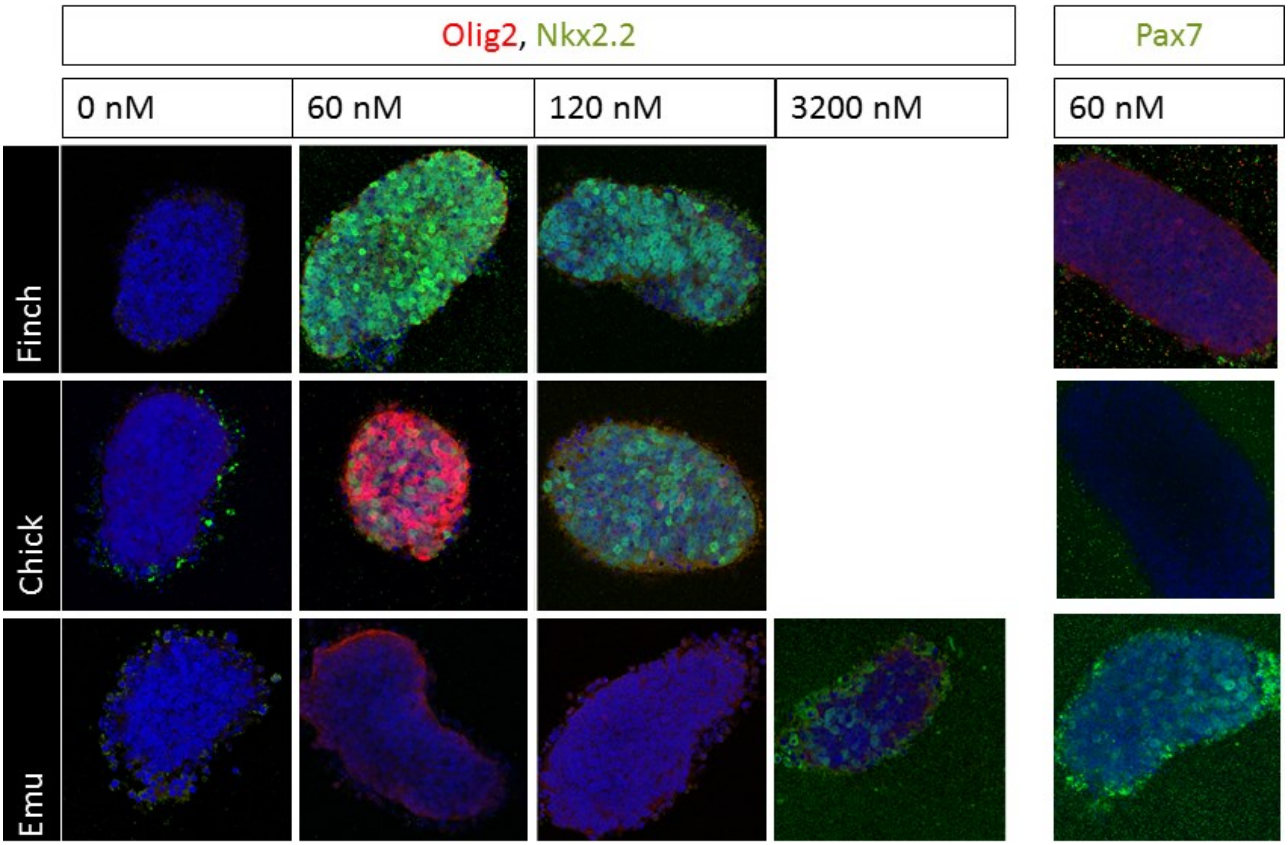

Figure 2.5: Naïve intermediate neural plate explants: Naïve neural plate tissue from all three species is isolated and grown *in vitro* in presence of recombinant Shh-N at different concentrations. Tissues are then stained for Olig 2 and Nkx2.2, or Pax7. Finch tissue is most sensitive to any given concentration, while Emu is the least sensitive. n>10 for each Finch and Chick panel, results are representative. n>5 for each emu panel, results are representative.

Next, we wanted to test whether the differential response we observe in species is intrinsic to the cells, or due to other signals that the cells may be exposed to throughout development. We generated chimeric animals so that the developing neural tube can incorporate cells from different species, and that throughout development these cells get exposed to the exact same signals. As shown in **Figure 2.6a**, at first 12 hours of development (HH stage 3) a piece from the tip of the Hensen's node is dissected out from a GFP-Chick donor and transplanted into Finch host. In the neural tube tissue of the resulting chimeric animal, any cell expressing GFP is from the Chick-GFP donor, while non-GFP cells belong to the Finch host. Strikingly, as was observed in the *in vitro* explant assays, Finch cells in the chimeric animals are much more sensitive to the endogenous morphogen compared to the chick cells. As shown in **Figure 2.6**, Finch cells much further away from the source can upregulate expression of SHH target gene NKX6.1, while Chick cells are still expressing PAX7, a gene that is repressed by SHH. Differential response appears to be cell autonomous, since not just clones of cells but also isolated single Chick cells appear to be less sensitive to morphogen (**arrow, Figure 2.6b**). We repeated the same chimeric experiments using Finch-GFP donors and Chick hosts, and saw similar results in this reciprocal experiment. GFP expressing Finch donors were more responsive to SHH, while Chick host cells were less responsive. These results confirm that the effects we see with *in vitro* explants are intrinsic to cells, and that species show differential response to a morphogen as an intrinsic property of the cells.

These findings prompted us to investigate the mechanism of differential response that is intrinsic to cells. The Sonic hedgehog signaling pathway has extracellular and

Figure 2.6: Chimeric embryos show differential response is an intrinsic property of cells. a. At 12 hours of development, tip of the Hensen's node from a GFP donor embryo is transplanted into a host embryo to generate a chimeric animal with cells from both species inside a chimeric neural tube. **b.** A chimeric neural tube with GFP cells from the Chick donor and non-GFP cells from the Finch host. Expression of Shh target genes is differential**. n>3**, results representative for all embryos we assayed **c.** The reciprocal experiments, with GFP cells coming from a Finch-GFP donor and non-GFP cells from the Chick host**. n=2** due to unavailability of Fch-GFP embryos, results representative for all embryos we assayed. Scale bar: 100 um, same for all panels

a.

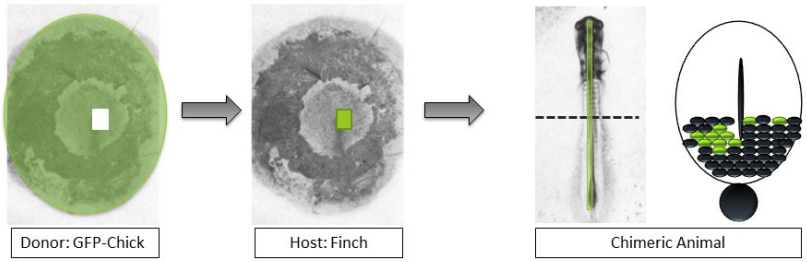

b.

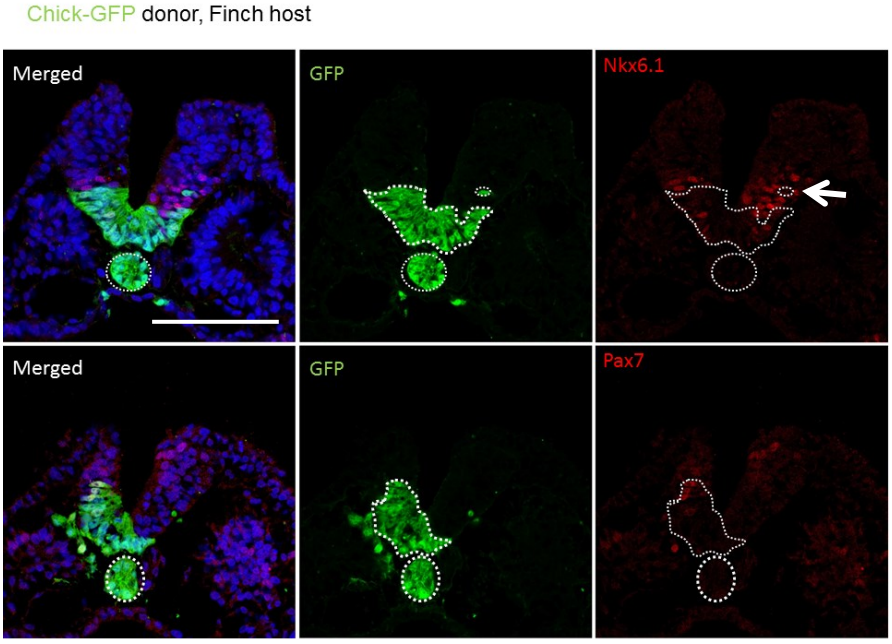

c.

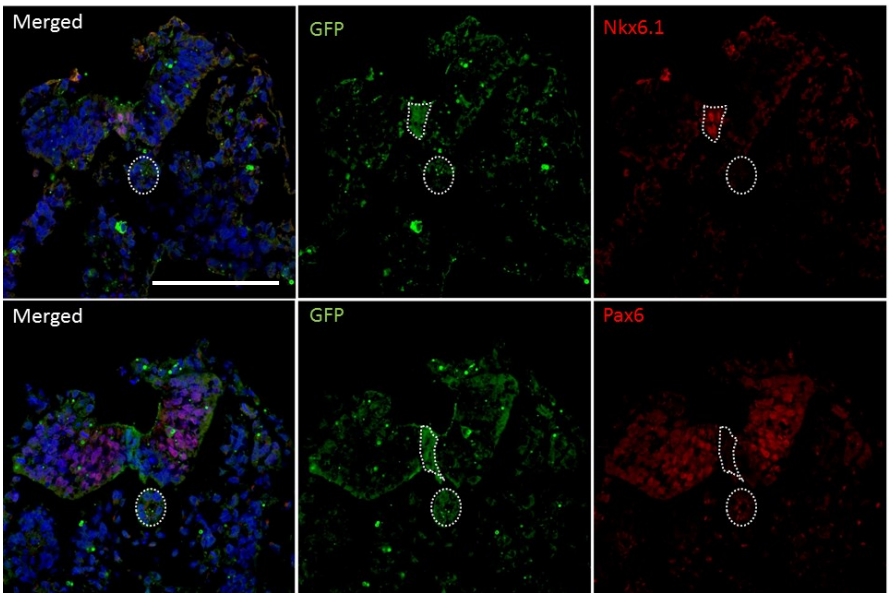

Figure 2.6, continued

intracellular components, but Smoothened receptor is the pivot point between these two. We activated the SHH pathway in all species with a Smoothened agonist, SAG, to test if differential response is upstream of SMO (extracellular components) or downstream of SMO (intracellular components including SMO receptor) (**Figure 2.7**). SAG treated explant assays indicated that mechanisms of differential response are downstream of the receptor Smoothened, as Finch cells are still more sensitive to a given concentration of SAG, whereas the Emu is the least sensitive. At a lower concentration of SAG, Finch tissue expresses OLIG2 and NKX2.2, while the Chick tissue is saturated with OLIG2 response. At a higher concentration, Finch tissue is expressing mainly NKX2.2, while the Chick has mainly OLIG2 and a few cells expressıng NKX2.2. The emu explants are have upregulated the expression of neither, as was observed with recombinant SHH-N concentrations that induced similar response in Finch and Chick.

We extended our analysis of the mechanisms that are responsible for the differential response and focused on SHH target genes and pathway effectors. Naïve explants from Finch, Chick and Emu were incubated at a fixed Shh-N concentration and harvested at various time points (t= 0, 6, 8, 12 and 24 hr). We then tested target gene upregulation with qRT-PCR using species specific primers**.** For each species specific primer set, we ran standard curves to interpret relative amounts of transcripts precisely, and normalized each experimental data point to actin levels (Therefore, each data point represents units of transcript per units of actin).

As shown in **Figure 2.8** and **Supplemental Figure S1.7**, for all time points, levels of Smoothened in all three species appear to be comparable, as well as the initial

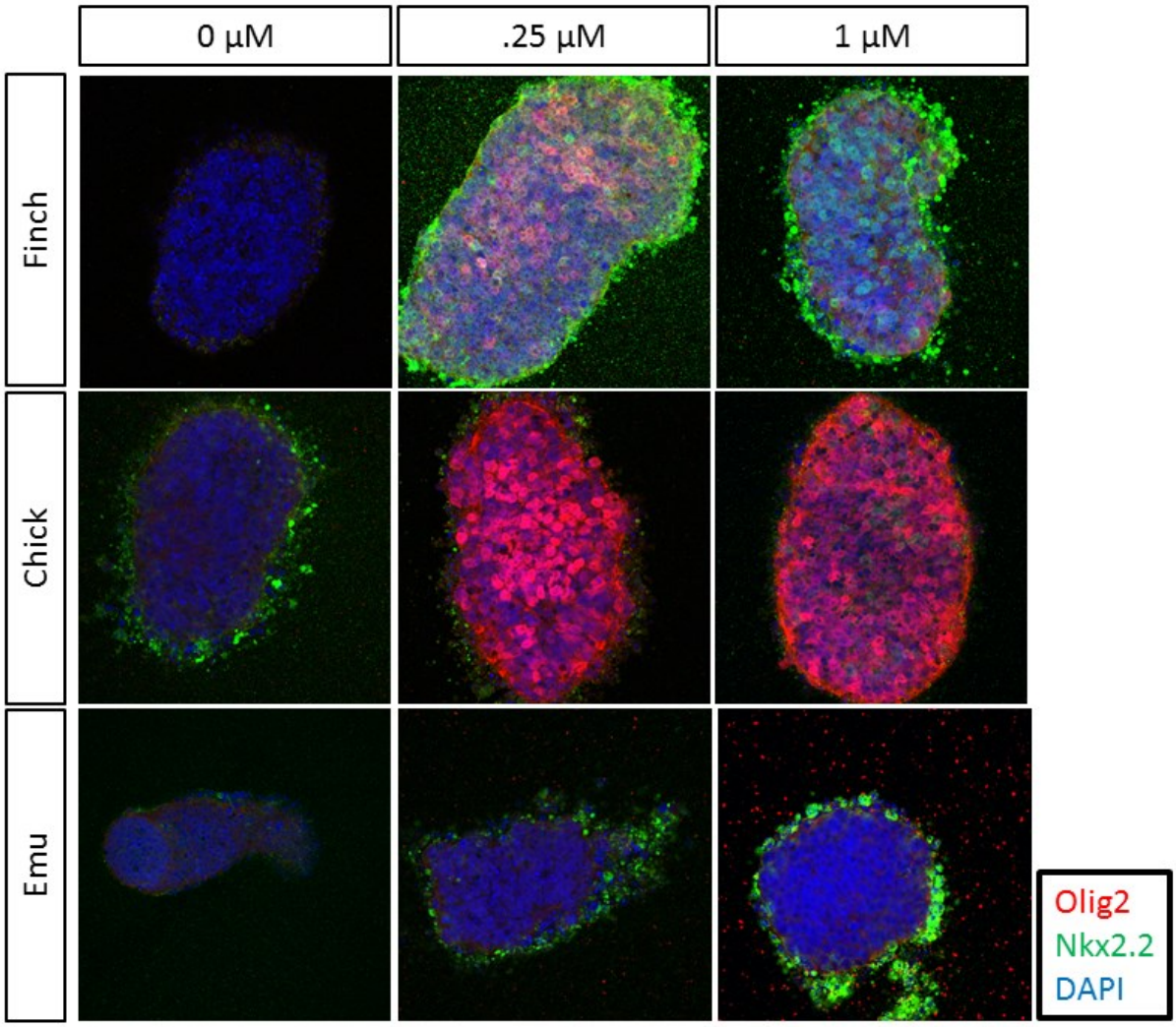

Figure 2.7: Differential respond persists when pathway is activated through Smoothened. Naïve intermediate neural tube explants from the three species were grown *in vitro*. Shh pathway was activated with Smoothened agonist, SAG. Differential response persists, Finch cells are expressing the higher response transcription factor, NKX2.2, at 0.25 mM. n>5 for each panel.

Figure 2.8: Expression profiles of SHH target genes upon exposure to the morphogen. a. PTC1 transcript upregulation in three species across time. **b.** OLIG2 in Finch and Chick. **c.** NKX2.2 in Finch and Chick. Each data point in graphs represents 15-25 explants pooled together for analysis.

a.

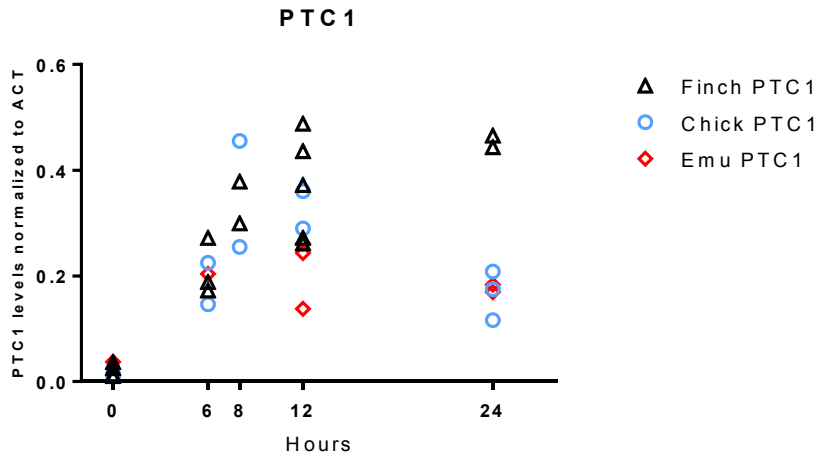

b.

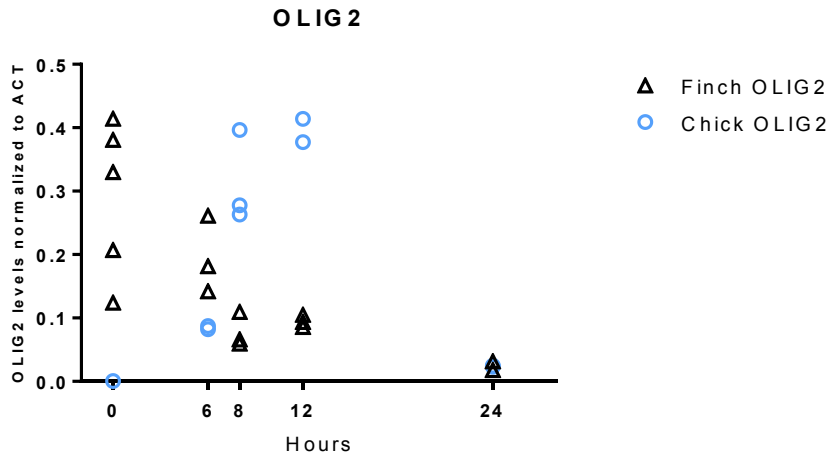

c.

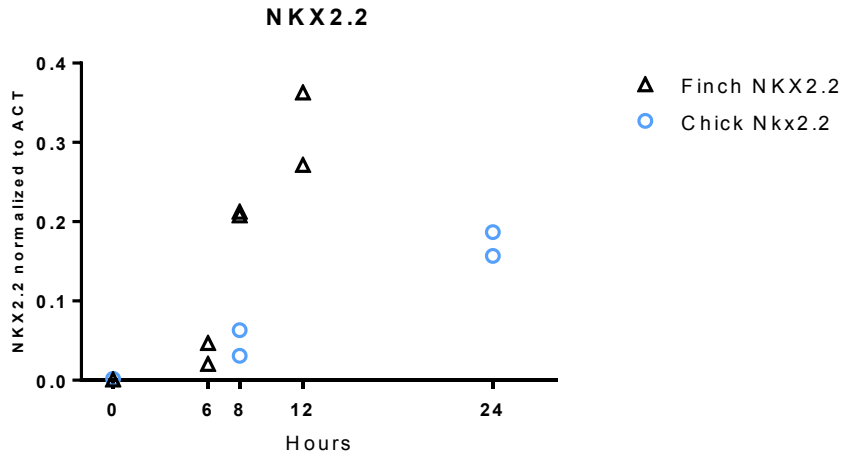

Figure2.8, continued

levels of Ptc1 at t=0. Interestingly, Ptc1 upregulation in all three species follows a similar trend. Similar starting levels of Ptc1 in Finch, Chick and Emu are upregulated to comparable levels as early as t=6. Notably, levels stay elevated in the Finch at 24 hrs, whereas they decline sharply in the Chick, as was shown previously in literature(Dessaud et al. n.d.; D Stamataki et al. 2005b).

Next, we narrowed down our analysis to two species, Zebra Finch and Chick, as availability of Emu embryos is limited. We assayed levels of GLI transcription and SHH target transcription factors, *OLIG2* and *NKX2.2.* As expected, expression of both OLIG2 and NKX2.2 peaked earlier in the Finch (**Figure 2.9**), which is what we observed with the *in vitro* explant immunostaining assays **(Supplemental Figure S1.6)**. Interestingly, Finch naïve explants at t=0 have relatively high levels of OLIG2 transcript, the expression of which is only induced upon SHH exposure in the chick. We are confident that Finch explants at t=0 have not been exposed to SHH, since levels of Ptc1 transcript are basal.

Genetic data from literature suggests that mice with *Shh-/- Gli3*$^{xt/xt}$ double mutant background have spontaneous OLIG2 expression in intermediate neural tube(Persson et al. 2002; Litingtung & Chiang 2000). This phenotype is not surprising because OLIG2 activity is mainly repressed by GLI3. In chick neural tube, SHH morphogen activity functions to deplete levels of GLI3 and relieve the repression from *OLIG2* locus (Bai et al. 2004). In the absence of both SHH and GLI3, spontaneous OLIG2 expression is observed in these mice. Importantly, when we assayed GLI transcription levels in Finch and Chick, we found that while GLI2 levels were not significantly different in the two species, GLI3 levels were strikingly low in the Finch, when tested with two different sets

Figure 2.9: Dynamics of Gli signaling and Gli3 activity in the Finch versus Chick neural tube. a. Electroporation of GBS-GFP gli reporter construct into the Finch neural tube shows GFP activity in more than 50% of the neural tube tissue. Green: GFP, Red: β-gal electroporation control **b.** Electroporation of the GBS-GFP Gli reporter construct in the chick shows activity only up to 40% in the Chick neural tube, as was shown previously in literature. **c-d.** Electroporation of Gli3-ires-GFP construct into chick neural tube down-regulates expression of Olig2 and attenuates patterning in the electroporated side. **e.** Electroporation of CAGG-GFP control construct in the Finch neural tube does not alter Gli3 expression. **f.** Preliminary data on Gli3-ires-GFP electroporation into Finch neural tube down-regulated expression of Olig2 in one cell where it is expressed.

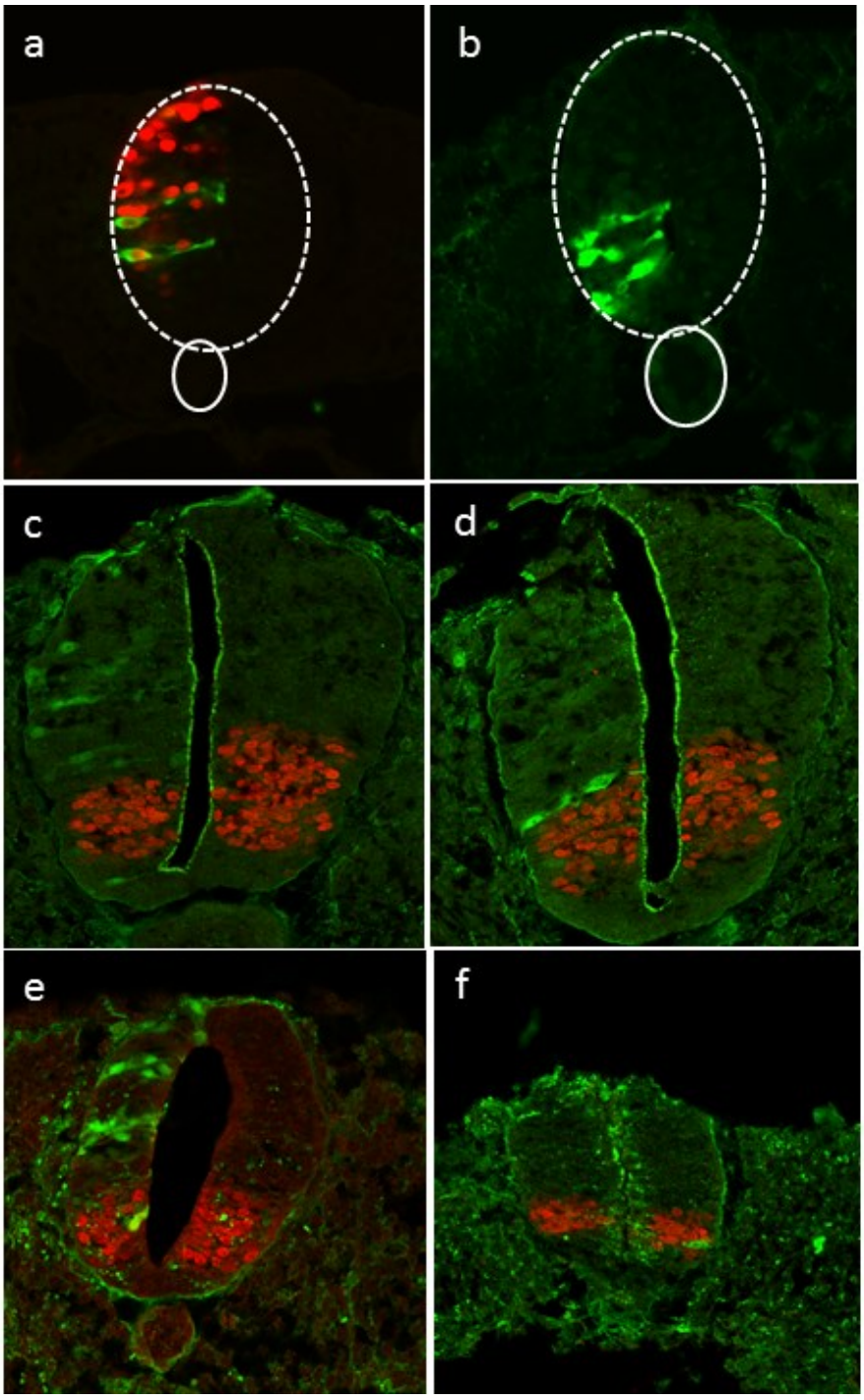

Figure 2.9, continued

of species specific primers **(Supplemental Figure S1.7).** In chick samples, initially high GLI3 levels are eventually depleted to basal levels within 24 hours of SHH exposure. In Finch neural tube tissue, initial levels of GLI3 appear to be basal.

Initial differences of OLIG2 and GLI3 levels in the naïve explants and the genetic data from mice led us to hypothesize that globally lower GLI3 levels in the Finch neural tube progenitor cells could explain intrinsic differential response at a GLI activity level. This prompted us to further investigate and test GLI activity *in vivo*. We used a GBS-GLI reporter construct to electroporate Finch and Chick neural tube. We found that while we can detect GFP activity from the GLI reporter only up to 50% of the neural tube in the Chick, we could detect reporter activity much dorsally in the Finch neural tube **(Figure 2.9a-b)**. Since GBS reporter is sensitive to both GLI2 activation and GLI3 repression(Tsanev et al. 2009), these results agree with our previous findings that Chick and Finch tissues have differential levels of GLI activity along the D-V axis, due to lower levels of GLI3 in the Finch.

To confirm that levels of GLI3 can affect dynamics of patterning in the neural tube, we moved on to functional tests. We hypothesized that if globally higher levels of GLI3 can alter patterning dynamics in the Chick neural tube, then electroporation of full length GLI3 into the developing neural tubes of Chick and Finch should similarly alter patterning dynamics. As expected, a GLI3-ires-GFP reporter, when injected, down-regulated cellular response to SHH, in both Chick and Finch embryos **(Figure 2.9c-f)**. In cells that uptake the construct, OLIG2 expression is repressed especially in more dorsally located cells, while this never happens in CAGG-GFP control electroporations. Due to less efficient electroporation in the Finch neural tube as well as weak GFP

expression from the IRES promoter, these assays need to be repeated and quantified. Preliminary results, however, are promising that increased levels of GLI3 affect cellular response and overall patterning.

Discussion

In summary, we provide a comprehensive view of how embryos with neural tubes of different sizes regulate their patterning dynamics in order to attain proportionate morphology at the end of development.

An interesting property of all three embryos is that at the first few hours of patterning, initial size is similar across species, but rate at which pattern is established is not. This may be due to constrains on size of the embryo at earlier patterning events, when the neural plate is first formed. Alternatively, size similarity may have significance for the formation and initial activity of the morphogen gradients, both the SHH gradient emanating from the notochord and the BMP gradient diffusing out from the roof plate. However, soon after the establishment of gradients, we do observe differences in progression of pattern. With *in vitro* explant assays and *in vivo* chimera analysis, we were able to pinpoint this difference to to a cell-autonomous and intrinsic differential response to the morphogen. The chimeras present solid evidence that even when the cells from two different species are exposed to identical developmental signals, they retain differential response to SHH.

Due to the limited availability of the Emu embryos, we tried to define a general trend using all three species, and narrowed down our mechanistic analysis between finch and chick. For all three species, we know the differential response to be downstream of SMO receptor, and specific to either the intracellular component of SHH

pathway, or at level of gene regulatory network. Our findings on OLIG2 expression in naïve Finch explants at t=0, as well as similarities in PTC1 upregulation and differences in GLI3 levels suggest that the differential response may be controlled at the GLI repressor levels. Our functional data with GBS-GFP reporter constructs and full length GLI3 electroporations further strengthen our hypothesis. While alteration to morphogen response through modifications to GLI activator or repressor activity is not new in literature, this is a novel finding for its employment in evolutionary adaptations.

Our work presents an alternative to scaling models that focus on scaling of the morphogen gradient itself(Hamaratoglu et al. 2011; De Robertis 2009). While gradient scaling can still be occurring in the three species, we are also confident that differential response contributes to rate and timing of patterning, and that intrinsic difference in repressor levels can be a strategy to scale spatio-temporal organization of cells at different embryonic sizes. Whether if such modifications at the level of intrinsic and cell-autonomous differential response can account for pattern scaling in more evolutionary distant vertebrates remains as an open question. However, scaling at the level of morphogen response, rather than morphogen gradient is a distinct alternative that we are proposing with the nuerual tube SHH mediated patterning in vertebrates, and suggests that it recapitulates our second model in Figure 2.1b, where we theoretically outlined strategies to overcome pattern scaling problem in embryos of different sizes.

Materials and Methods

Emrbyos and Embryonic staging

Finch eggs were obtained from Dr. Tim Gardner at Boston University, and Chick and Emu eggs were obtained from commercial sources (Charles River, MA and Floeck

Farm, NM). All eggs were incubated at 38°C and embryos were staged with reference to Hamburger Hamilton (chick), Zebra Finch and Emu staging series(Hamburger & Hamilton 1992; Murray et al. 2013; Nagai et al. 2011). However, for comparing growth and pattern in earlier stages, somite number was the main reference point. To stay consistent across antero-posterior level and across species, all measurements were made at the level of somite 15. Formation of somite 15 is time zero, and developmental time after 15 somite stage is calculated as measure of 'time after adjacent somite formation'. Somite 15 is also roughly where forelimb forms in all three species, and Dye-I analysis show that during development, neural tube tissue and adjacent somite remain relatively close to each other, in other words, tissues do not shift (data not shown).

Immunohistochemistry and imaging

Embryos were fixed in 4%PFA at 4 °C for 1 hr for stages up to HH 20, and 2-3 hrs for older stages. After 3x PBS washes, they incubated in 15% sucrose overnight at 4 °C. Next day, sample were embedded in 7.5% gelatin/ 15%sucrose/PBS, flash frozen in cold isopentane and cryosectioned at 14 um.

For immunostaining, gelatin was cleared from slides by incubation at 42 °C waterbath for 3 x 5 min. Blocking solution (1%BSA in PBS 0.1% Triton) for 1 hr, primary antibody (in blocking solution) overnight at 4 °C and secondary antibody (in blocking solution) for 2 hr at room temperature were performed. **Table 2.1** shows the list of antibodies used for neural tube staining.

Imaging was performed using Zeiss Confocal and analyzed with NIH ImageJ.

Naïve neural plate explant surgery

Neural plate tissue was isolated from 10-13 somite stage Chick, Finch and Emu embryos as described previously in chick(Yamada et al. 1993). Recombinant Mouse Shh-N from R&D Systems C25II (464-SH-025) and SAG (Millipore, 364590-63-6) were dissolved as instructed added to the medium.When harvested (t= 0,6,8,12 or 24) explants were either processed for qRT-pcr or immunostained as described.

qRT-PCR on explants

Naive explants embedded in collagen (PureCol, Advanced Biomatrix) were dissociated with extration buffer (Buffer XB) in PicoPure RNA Extraction kit and RNA isolation was performed as described in kit protocol. Immediately following RNA extraction, cDNA was made using superscript II kit. Species specific primers were used for each set, as listed in table X.

Chimera Transplants

To generate embryos with chimeric neural tubes, GFP-Chick donor and Finch host, or GFP-Finch donor and Chick host embryos were dissected in Thyrode's saline(Voiculescu et al. 2008) at 12 hrs of development (Stage HH 3). One half of the tip of the Hensen's node was transplanted from the donor into the host embryo, as described previously(Selleck & Stern 1992). Embryos were placed on stretched out vitelline membranes, and incubated on albumin containing petri dishes for 24 hrs in a humidified chamber at 38°C. They were fixed at 4% paraformaldehyde, embedded in gelatin and cryosectioned at 12-14 um.

Electroporations

Constructs CMV-Gli3-flag, CAGG-Gli3 and 8XGBS-GFP Gli reporter were obtained from James Briscoe, and used with control CAGG-GFP construct to electroporate

embryos at stage HH11-12. For Finch electroporations, we let the egg sit in a 12-well humidified dish, since sealing the delicate shell was tricky. Both chick and finch were harvested 24 hours post electroporation, fixed at 4%PFA and immunostained.

Table 2.1: List of Antibodies Used for This Project

Antibody	Source	Cat. #	Concentration Used
Nkx 2.2	DSHB	74.5A5	1:25
Olig 2	Millipore	AB9610	1:1000
Nkx6.1	DSHB	F55A10	1:1000
Pax 7	DSHB	PAX7	1:20
Isl-1	DSHB	39.4D5	1:1000
PH3	Millipore	06-570	1:250
GFP	Millipore	AB16901	1:1500
Shh	DSHB	5E1	1:20

References

Bai, C. B., Stephen, D., & Joyner, A. L. (2004). All Mouse Ventral Spinal Cord Patterning by Hedgehog Is Gli Dependent and Involves an Activator Function of Gli3. *Developmental Cell*, *6*(1), 103–115.

De Robertis, E. M. (2009). Spemann's organizer and the self-regulation of embryonic fields. *Mechanisms of Development*, *126*(11-12), 925–41.

Dessaud, E., McMahon, A. P., & Briscoe, J. (2008). Pattern formation in the vertebrate neural tube: a sonic hedgehog morphogen-regulated transcriptional network. *Development*, *135*(15), 2489–2503.

Dessaud, E., Ribes, V., Balaskas, N., Yang, L. L., Pierani, A., Kicheva, A., … Sasai, N. (n.d.). Dynamic assignment and maintenance of positional identity in the ventral neural tube by the morphogen sonic hedgehog. *PLoS Biol*, *8*(6), e1000382.

Dessaud, E., Yang, L. L., Hill, K., Cox, B., Ulloa, F., Ribeiro, A., … Briscoe, J. (2007). Interpretation of the sonic hedgehog morphogen gradient by a temporal adaptation mechanism. *Nature*, *450*(7170), 717–20.

Hamaratoglu, F., de Lachapelle, A. M., Pyrowolakis, G., Bergmann, S., & Affolter, M. (2011). Dpp signaling activity requires Pentagone to scale with tissue size in the growing Drosophila wing imaginal disc. *PLoS Biology*, *9*(10), e1001182.

Hamburger, V., & Hamilton, H. L. (1992). A series of normal stages in the development of the chick embryo. 1951. *Dev Dyn*, *195*(4), 231–272.

Harfe, B. D., Scherz, P. J., Nissim, S., Tian, H., McMahon, A. P., & Tabin, C. J. (2004). Evidence for an expansion-based temporal Shh gradient in specifying vertebrate digit identities. *Cell*, *118*(4), 517–528.

Jessell, T. M. (2000). Neuronal specification in the spinal cord: inductive signals and transcriptional codes. *Nat Rev Genet*, *1*(1), 20–29.

Litingtung, Y., & Chiang, C. (2000). Specification of ventral neuron types is mediated by an antagonistic interaction between Shh and Gli3. *Nature Neuroscience*, *3*(10), 979–85.

Murray, J. R., Varian-Ramos, C. W., Welch, Z. S., & Saha, M. S. (2013). Embryological staging of the Zebra Finch, Taeniopygia guttata. *Journal of Morphology*, *274*(10), 1090–110.

Nagai, H., Mak, S.-S., Weng, W., Nakaya, Y., Ladher, R., & Sheng, G. (2011). Embryonic development of the emu, Dromaius novaehollandiae. *Developmental*

Dynamics : An Official Publication of the American Association of Anatomists, *240*(1), 162–75.

Persson, M., Stamataki, D., te Welscher, P., Andersson, E., Böse, J., Rüther, U., … Briscoe, J. (2002). Dorsal-ventral patterning of the spinal cord requires Gli3 transcriptional repressor activity. *Genes & Development*, *16*(22), 2865–78.

Selleck, M. A. J., & Stern, C. D. (1992). Commitment of mesoderm cells in Hensen ' s node of the chick embryo to notochord and somite, *415*, 403–415.

Stamataki, D., Ulloa, F., Tsoni, S. V, Mynett, A., & Briscoe, J. (2005). A gradient of Gli activity mediates graded Sonic Hedgehog signaling in the neural tube. *Genes Dev*, *19*(5), 626–641.

Tsanev, R., Tiigimägi, P., Michelson, P., Metsis, M., Østerlund, T., & Kogerman, P. (2009). Identification of the gene transcription repressor domain of Gli3. *FEBS Letters*, *583*(1), 224–8.

Voiculescu, O., Papanayotou, C., & Stern, C. D. (2008). Spatially and temporally controlled electroporation of early chick embryos. *Nature Protocols*, *3*(3), 419–26.

Wolpert, L. (1969). Positional information and the spatial pattern of cellular differentiation. *Journal of Theoretical Biology*, *25*(1), 1–47.

Yamada, T., Pfaff, S. L., Edlund, T., & Jessell, T. M. (1993). Control of cell pattern in the neural tube: motor neuron induction by diffusible factors from notochord and floor plate. *Cell*, *73*(4), 673–686.

Yamada, T., Placzek, M., Tanaka, H., Dodd, J., & Jessell, T. M. (1991). Control of cell pattern in the developing nervous system: polarizing activity of the floor plate and notochord. *Cell*, *64*(3), 635–647.

Chapter Three

Patterning and Post-patterning Modes of Evolutionary Digit Loss in Mammals

"I think that the fascination so many people feel for evolutionary theory resides in […] its properties. […] It stands in the middle in a continuum stretching from sciences that deal in timeless, quantitative generality to those that work directly with the singularities of history. Thus, it provides a home for all styles and propensities, from those who seek the purity of abstraction (the laws of population growth and the structure of DNA) to those who revel in the messiness of irreducible particularity (what, if anything, did *Tyrannosaurus* do with its puny front legs anyway?). […] And then, of course, there are all those organisms: more than a million described species, from bacterium to blue whale, with one hell of a lot of beetles in between—each with its own beauty, and each with a story to tell."

Stephan Jay Gould, The Panda's Thumb

Patterning and post-patterning modes of evolutionary digit loss in mammals

Kimberly L. Cooper*[1,6], Karen E. Sears*[2], Aysu Uygur*[1], Jennifer Maier[2], Karl Stephan-Backowski[3], Margaret Brosnahan[4], Doug Antczak[4], Julian A. Skidmore[5], Clifford J. Tabin[1]

*These authors contributed equally to this work.

[1]*Department of Genetics, Harvard Medical School, Boston MA 02115*

[2]*Department of Animal Biology, University of Illinois Urbana-Champaign, Urbana IL 61801*

[3]*École Normale Supérieure de Lyon, France*

[4]*Department of Molecular Biology and Genetics, Cornell University, Ithaca NY 14853*

[5]*The Camel Reproduction Centre, Dubai, United Arab Emirates*

[6]*Present address: Division of Biological Sciences, University of California, San Diego, La Jolla CA 92138*

The work in this chapter was originally conceived by Kim Cooper and Cliff Tabin. Aysu Uygur is a co-first author on this paper. Species specific probes were generated by A. Uygur and K. Cooper. Whole mount in situ stainings and skeletal stainings were done by K. Cooper. Antibody stainings and cell death analysis were done by A. Uygur. Text was written by K. Cooper and Cliff Tabin, figures prepared by K. Cooper and A. Uygur.

Summary

A reduction in the number of digits has evolved multiple times in tetrapods, particularly in cursorial mammals that travel over deserts and plains, yet the underlying developmental mechanisms have remained elusive. Here we show that digit loss can occur both during early limb patterning and at later post-patterning stages of chondrogenesis. In the “odd-toed” jerboa and horse and the “even-toed” camel, expansive cell death sculpts the tissue around the remaining toes. In contrast, digit loss in the pig is orchestrated by earlier limb patterning mechanisms including down regulation of *Ptch1* expression but no increase in cell death. Together these data demonstrate remarkable plasticity in the mechanisms of vertebrate limb evolution and shed light on the complexity of morphological convergence, particularly within the artiodactyl lineage.

Introduction

Tetrapod limbs evolved adaptations for running, swimming, flying, and a myriad of other tasks, each reflected in functional modifications to their morphology. Digit reduction, a decrease in the number of digits from the basal pentadactyl, or five-digit, morphology, arose repeatedly in tetrapod evolution(Jennifer A. Clack 2009). In broad strokes, there are two plausible developmental mechanisms by which this could take place. The first would be to specify fewer digit primordia during the time when developmental fates are patterned in the early limb bud. The second would be to initially organize the limb bud in a normal pentadactyl pattern but then fail to elaborate the full set of digits by resculpting the nascent limb through differential proliferation or cell death.

To date, the molecular developmental mechanism of evolutionary digit reduction has been explored in only one tetrapod group - the skinks of the genus *Hemiergis*. Distinct species of *Hemiergis* range in digit number from two to five(Skinner et al. 2008; Shapiro 2002) with evolutionary progression to fewer digits correlating with increasingly early termination of *Sonic hedgehog* (*Shh*) expression in the posterior limb bud(Shapiro et al. 2003). *Shh* serves a dual purpose in limb development, both to pattern the digits and to expand the hand/foot plate to allow for the formation of a full complement of digits(Harfe et al. 2004; Towers et al. 2008; Zhu et al. 2008). Experimental truncation of the developmental timing of *Shh* expression removes digits in the reverse order of their formation(Zhu et al. 2008) thus providing a convenient way to evolutionarily tweak digit number without disturbing the overall structure of the limb, a mechanism first suggested by Alberch and Gale(Alberch & Gale 1983). However, this mechanism would not, in a simple manner, generate the symmetrical reduction of anterior (pre-axial) and posterior (post-axial) digits seen, for example, in the evolution of the horse lineage.

Results

To investigate how digit reduction evolved in other adaptive contexts we examined the mode of digit loss in a bipedal three-toed rodent and in three ungulates: the single-toed horse, an odd-toed ungulate or perissodactyl, and the pig with four toes and the camel with two, each representing the even-toed ungulates or artiodactyls (**Figure 3.1a, b**).

We first focused on the three-toed jerboa, *Dipus sagitta* (**Figure 3.1f**). This species has several advantages in identifying meaningful alterations to ancestral developmental mechanisms. First, it has a close evolutionary relationship to the

laboratory mouse and to a five-toed species of jerboa, *Allactaga elater*(Walker 1964) (**Figure 3.1d**). Moreover, digit loss in *D sagitta* is limited to the hind limb while fore limbs maintained five fully formed fingers(Shenbrot et al. 2008; Cooper 2011). This provides a unique opportunity to identify differences specific to morphological divergence of the hind limb among a potential plethora of species-specific modifications shared in the development of both sets of paired appendages.

In the adult *D sagitta*, the three central metatarsals are fused into a single element that trifurcates distally and articulates with each of the three digits(Shenbrot et al. 2008). However, in the neonate, alcian blue and alizarin red staining of the chondrogenic skeleton reveals that the three complete digits and their associated metatarsals are flanked by small, truncated cartilage remnants of the first and fifth metatarsals (**Figure 1c; Supplemental Figure S2.1**). This suggests that at least the proximal-most portion of each of the five digit rays is patterned early in development and that digits I and V are either not fully patterned distally or are truncated at a subsequent differentiation stage.

To gain a better sense of when the patterning and/or morphogenesis of the lateral digits begins to diverge in the three-toed jerboa hind limb, we compared the contours of various staged limb buds between mice and *D sagitta*. We found that when scaled for size, the fore limbs of mice and three-toed jerboas are consistently identical in morphology. In contrast, the *D sagitta* hind limb starts to be noticeably narrower as early as E11.5 (**Supplemental Figure S2.2**).

Figure 3.1: Convergent evolution of the embryonic limb skeleton in multiple mammal species. a-b, Phylogeny of (a) mammals and of (b) artiodactyls representing the major groups that have independently lost digits, based on Meredith et al(Meredith et al. 2011). Parenthetical lettering references skeletons in accompanying panels. Orange circles indicate an evolutionary incidence of digit loss. Purple circles represent the shift from mesaxonic to paraxonic limbs in basal artiodactyls. Species that sculpt the limb by cell death are highlighted in red, and those that show a restriction of *Ptch1* expression are highlighted in green. **C** Alcian blue and alizarin red stained skeleton of postnatal day 0 three-toed jerboa, *D sagitta* with the ankle (proximal) at the top. Posterior view (left) highlights the fifth metatarsal (arrow). Anterior view (right) highlights the first metatarsal (arrow head). **d,** Alcian blue stained skeletons of the approximately 16 dpc five-toed jerboa, *A elater,* hind foot; **e,** 30 dpc pig fore foot; **f,** approximately16 dpc *D sagitta* hind foot; **g,** 50 dpc camel hind foot; **h,** 34 dpc horse fore foot; **c, d, f,** scalebar = 0.5 mm. **e, g, h**, scalebar = 1 mm.

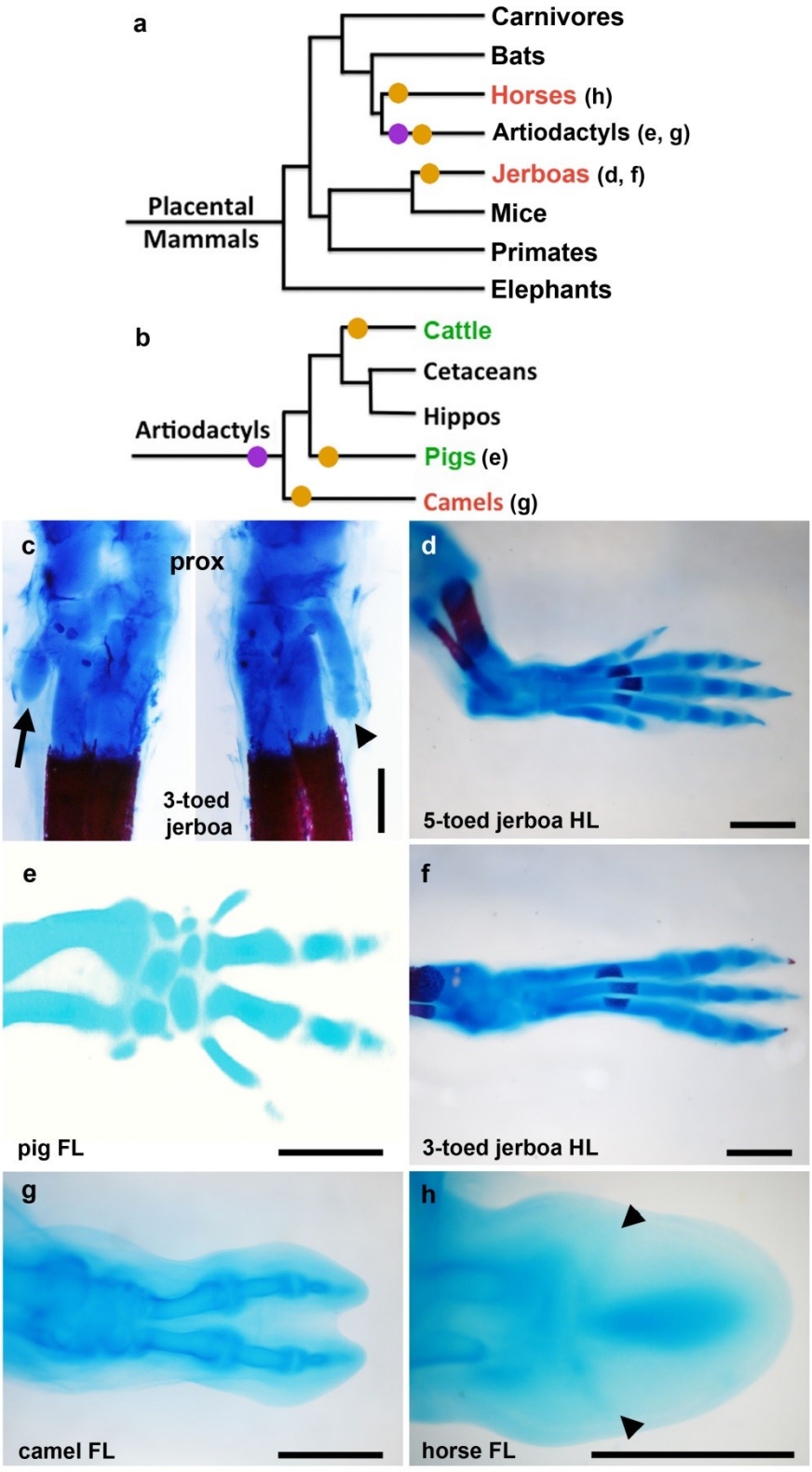

Figure 3.1, continued

Accordingly, we conducted an expression screen of a series of genes known to be involved in limb patterning just prior to and at the time of morphological divergence in hind limb bud shape. None of the patterning genes we examined showed a significant difference in expression in the *D sagitta* hind limb, including *SHH*, *PTCH1, GLI1,* and *HoxD13* (**Figure 3.2a, b**). Turning to post-patterning stages, cell proliferation was assessed by phospho-histone H3 antigen detection. However, we did not see a decrease in proliferation in the hind limb of the three-toed jerboa, either at early stages of autopod expansion or later during digit out growth in any domain of the developing limbs (**Supplemental Figure S2.3**). In contrast, we saw derived expanded domains of TUNEL positive nuclei, a marker for programmed cell death, specific to the jerboa hindlimb as early as 12.5 days post conception (dpc) (**Supplemental Figure S2.6**). These domains further expand by 13.5 dpc to encompass all of the tissue distal to what would become the truncated cartilage condensations (**Figure 3.3b**). Thus digit loss in this species appears to result from the sculpting of anterior (pre-axial) and posterior (post-axial) tissues at the distal ends of properly patterned nascent digits.

Apoptosis is used in basal tetrapods to sculpt the digits, removing interdigital tissue late in limb development(Zuzarte-Luis & Hurle 2005). This suggests that a potential evolutionary route for achieving cell death in the *D sagitta* hind limb digit I and V primordia might be through cooption of the apoptotic pathways normally used to direct interdigital cell death. The transcription factor *Msx2* is strongly expressed in the interdigital tissue of the embryonic mouse and chicken(Fernández-Terán et al. 2006), and retroviral misexpression in chicken embryos induces a dramatic increase in cell death and loss of digit condensations(Marazzi et al. 1997; Ferrari et al. 1998, p.2).

Figure 3.2: Expression of early patterning genes: *Shh, Ptch1, Gli1,* and *HoxD13*. a, mouse hind limb (HL). **b,** three-toed jerboa, *D sagitta,* hind limb. **c,** horse hind limb. **d,** mouse fore limb (FL). **e,** camel fore limb. **f,** pig fore limb. Scalebars = 1 mm.

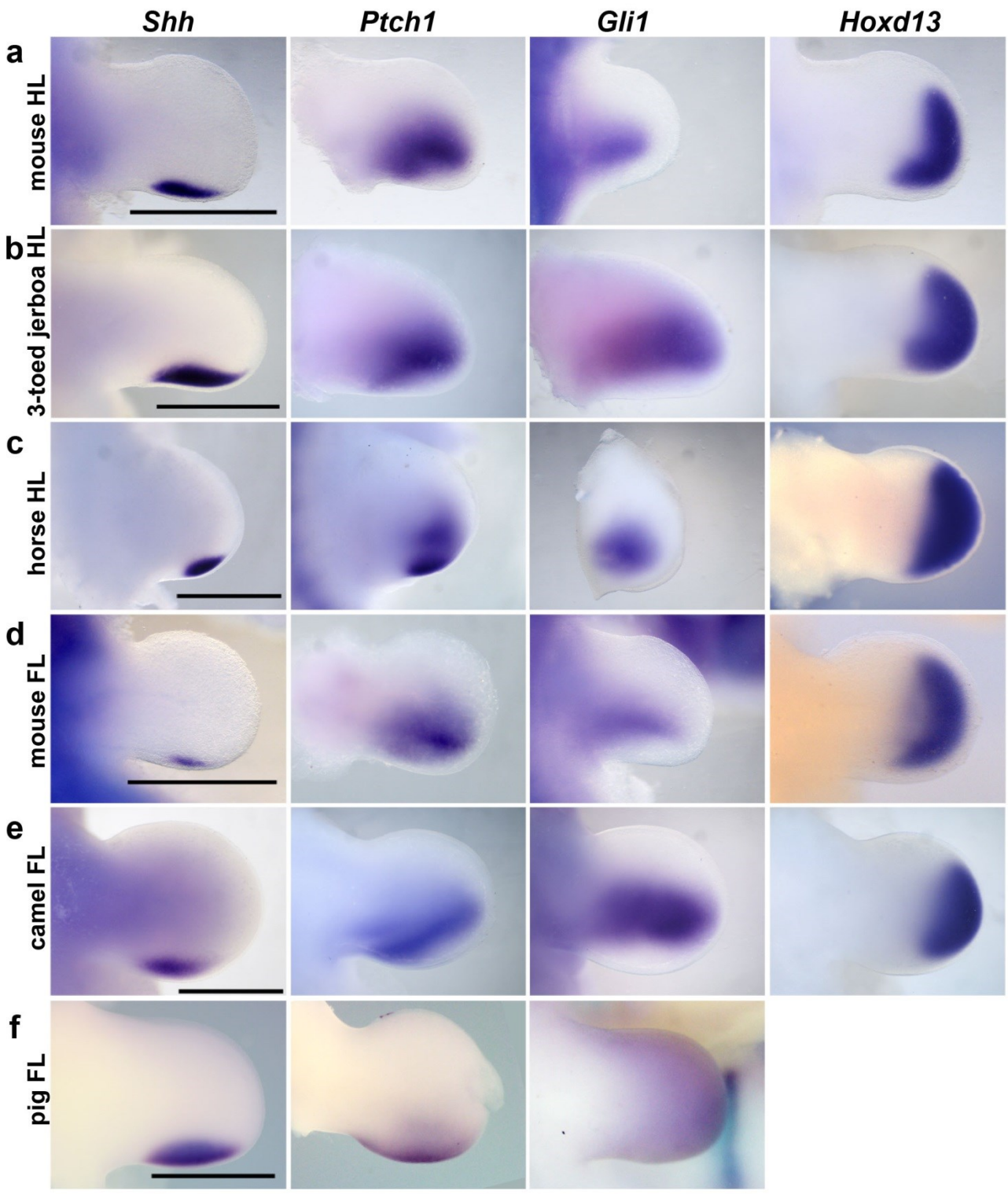

Figure 3.2, continued

We found that *Msx2* is strongly expressed in the *D sagitta* hind limb in tissue surrounding and distal to the truncated first and fifth metatarsals and completely overlaps with domains of TUNEL-positive nuclei (**Figure 3.4a-c**). In different contexts within the limb bud, the secreted protein *Bmp4* can act both upstream and downstream of *Msx2*(Pizette et al. 2001; Ferrari et al. 1998). We observe a transient spatial increase of *Bmp4* expression specific to the *D sagitta* hind limb autopod starting at 12 dpc that resolves at 12.5 dpc into two strong and discrete domains of expression precisely prefiguring the proximal positions of the first and fifth digits (**Supplemental Figure S2.4**). However, *Msx2* is expanded in the *D sagitta* hind limb prior to expanded *Bmp4* expression, as early as 11 dpc (**Supplemental Figure S2.5**). This is when the *D sagitta* hind limb first shows signs of narrowing relative to limbs that will develop five digits (**Supplemental Figure S2.2**), consistent with altered *Msx2* expression potentially being the primary causal mechanism of digit loss in this species.

As the interdigital tissue begins to undergo apoptosis during mouse limb development, *Fgf8* expression is lost in the overlying apical ectodermal ridge (AER), while *Fgf8* expression is maintained above the growing digits (**Figure 3.5a**). *Fgf8* is both necessary and sufficient for digit outgrowth in mouse and chicken embryos(Lewandoski et al. 2000; Mariani et al. 2008; Sun et al. 2002; Sanz-Ezquerro & Tickle 2003). From about 12.75 dpc in the *D sagitta* hind limb, *Fgf8* expression regresses away from the posterior and then anterior AER as well as the interdigital domains, persisting only over the digits that continue to develop to completion (**Figure 3.5a, b; Supplemental Figure S2.6**).

Figure 3.3 Patterns of cell death. DAPI (blue), Sox9 IHC (green), TUNEL (red). **a,** approximately 13.5 dpc three-toed jerboa, *D sagitta,* fore limb; **b,** approximately 13.5 dpc *D sagitta* hind limb (white dashed line indicates truncated metatarsals I and V); **c,** 45 dpc camel fore limb; **d,** approximately 13.5 dpc five-toed jerboa, *A elater,* hind limb **e,** mouse E13.5 with Sox9 and TUNEL; **f,** magnification of boxed region in (e) demonstrating the absence of TUNEL+ nuclei in the nascent mouse digit; **g,** 34 dpc horse fore limb; **h,** magnification of boxed region in (g) highlighting cell death in the Sox9+ condensation at the position of horse digit IV; **i,** 42 dpc camel fore limb; **j,** magnification of boxed region in (i) highlighting cell death in the Sox9+ condensation at the position of camel digit V. Scalebar in (a) = 0.5 mm for a-d, e, g, and i. Scalebar in (f) = 0.1 mm for f, h, and j.

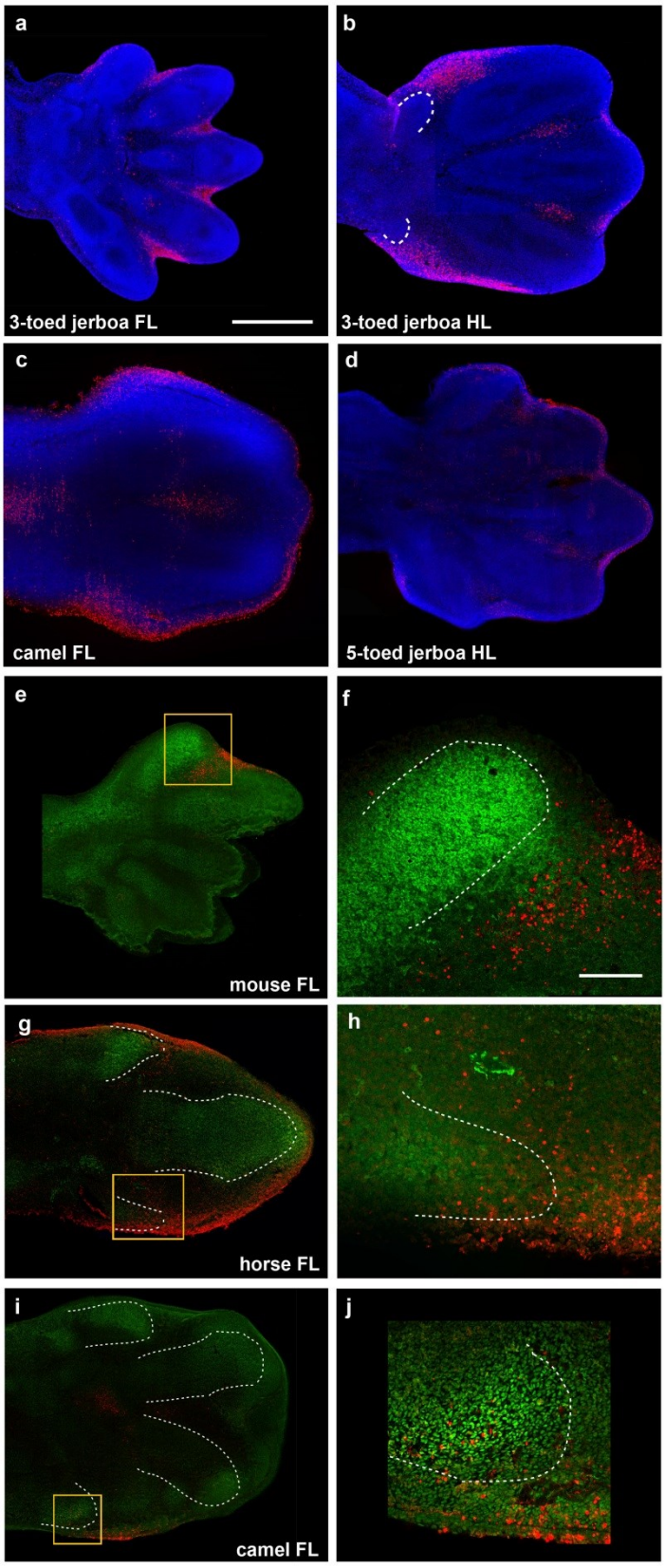

Figure 3.3, continued

The three-toed jerboa hind limb remarkably resembles the limb structure of some of the early ancestral equine species with three toes(Romer 1936). To test possible mechanisms for digit reduction in the horse, we once again started by examining the expression of genes known to be involved in patterning the early limb bud. We observed no obvious differences in expression of *Shh, Ptch1*, *Gli1,* or *HoxD13* relative to those previously described in mice (**Figure 3.2c**). In contrast, we did observe TUNEL-positive nuclei entirely surrounding the central toe and within the distal ends of nascent Sox9+ truncated condensations of metacarpals 2 and 4 (**Figure 3.3g, h**), a condition not observed in mouse (**Figure 3.3 e, f**). Moreover, we found expanded *Msx2* expression in domains correlating with those regions of anterior and posterior cell death (**Figure 3.4d**). We also observed increased posterior expression of *Msx2* earlier in development (**Supplemental Figure S2.5**) and distal expansion of *Bmp4* in both fore and hind limbs (**Supplemental Figure S2.4**) similar to *D sagitta* hind limbs. *Fgf8* expression is also maintained in the horse AER only over the nascent central digit III (**Figure 3.5d**). Thus, in the horse as in the three-toed jerboa, digit reduction appears to have a post-patterning contribution involving expanded domains of lateral apoptosis, possibly in part through similar molecular mechanisms. It is likely that mechanisms yet to be identified eliminate the first and fifth digits while a jerboa-like carving away of digits II and IV occurs by transforming cells from a chondrogenic to an apopototic fate. A more extensive investigation of early patterning may be worthwhile with additional precisely staged early horse embryos.

The even-toed ungulates present yet another opportunity to explore the possible convergence of digit reduction mechanisms in the context of additional skeletal

remodeling. The distal artiodactyl limb has shifted the central axis of symmetry from digit III in the ancestral mesaxonic limb to a derived paraxonic limb where the axis of symmetry runs through the interdigital space between digits III and IV(Prothero & Foss 2007). To explore whether digit loss in these species occurs via patterning and/or post-patterning changes, we obtained embryos from two species of artiodactyls, the pig and camel. While this work was in progress, we learned of similar studies by Lopez-Rios et al(Lopez-Rios et al. n.d.) in a third artiodactyl species with convergent digit loss to two toes, the cow. The accompanying paper identifies a gene regulatory control region for *Ptch1* expression in the limb that is altered in the cow. The resulting expression of *Ptch1* is reduced and more posteriorly restricted than in non-artiodactyl species. One role that *Ptch1* expression serves is to restrict the movement of the morphogen *Shh* across the limb bud(Chen & Struhl 1996; Yina Li et al. 2006). As a consequence of the change in *Ptch1* expression in the cow, *Shh* targets, including *Gli1* and the *Hoxd* genes, are expressed more uniformly across the limb bud(Lopez-Rios et al. n.d.). Mice in which *Ptch1* expression is reduced in the limb display similar changes in downstream genes and a concomitant shift in the central axis of the limb to the space between digits III and IV and loss of the first digit(Butterfield et al. 2009). Importantly, after learning of our results with the three-toed jerboa and horse, Lopez-Rios and colleagues looked closely and saw no evidence of expanded apoptosis in the developing cow limb(Lopez-Rios et al. n.d.). Together these results suggest that, as in *Hemiergis,* the even-toed ungulates might have lost digits through a *Shh*-dependent patterning mechanism, albeit by a different genetic alteration, allowing the digits to be lost in an asymmetrical manner in the artiodactyls.

As would be expected if mutations affecting *Ptch1* regulation play a prominent role in artiodactyl limb evolution, we find *Ptch1* expression in the pig is also posteriorly restricted and down-regulated concomitant with an up-regulation of *Gli1* (**Figure 3.2f**). Further, as in the cow, there is no evidence of increased cell death in developing pig limbs(Karen E Sears et al. 2011). Surprisingly, however, *Ptch1* expression is not down-regulated and restricted in the camel and is instead expressed much like non-artiodactyls (**Figure 3.2e**). Additionally, *Shh*, *Gli1,* and *HoxD13* exhibit ancestral patterns of expression indicating early patterning of the digit field by this subset of molecules is conserved in the camel (**Figure 3.2e**). In contrast, when we examined patterns of cell death in the camel, we found expansive apoptosis throughout outgrowths of tissue flanking digits III and IV at 45 dpc (**Figure 3.3c**) as well as at 42 dpc within small Sox9+ pre-cartilaginous nodules in the positions of missing digits II and V (**Figure 3.3i, j**). As in the three-toed jerboa and horse, this correlates with domains of *Msx2* expression in the anterior and posterior limb bud at the time of digit condensation (**Figure 3.4e**), though earlier expression of *Bmp4* and *Msx2* does not correlate suggesting a distinct initiating mechanism for camel (**Supplemental Figures S2.4, S2.5**).

Regardless of the mechanism by which digit loss occurs, at patterning or post-patterning stages, *Fgf8* expression is lost from the AER anterior and posterior to the digits that continue to develop in the pig, camel (**Figures 3.5c, e**), and cow(Lopez-Rios et al. n.d.) as seen with the three-toed jerboa and horse. Regression of *Fgf8* in the pig and cow, two species that lack expanded domains of cell death, uncouples this

Figure 3.4. Expression of *Msx2* at the start of digit chondrogenesis.

Fore limb and hind limb of **a,** mouse at 13 dpc; **b,** five-toed jerboa, *A elater,* at about 13 dpc; **c,** three-toed jerboa, *D sagitta,* at about 13 dpc; **d,** horse at 34 dpc; **e,** camel at 42 dpc. Scalebar = 1 mm.

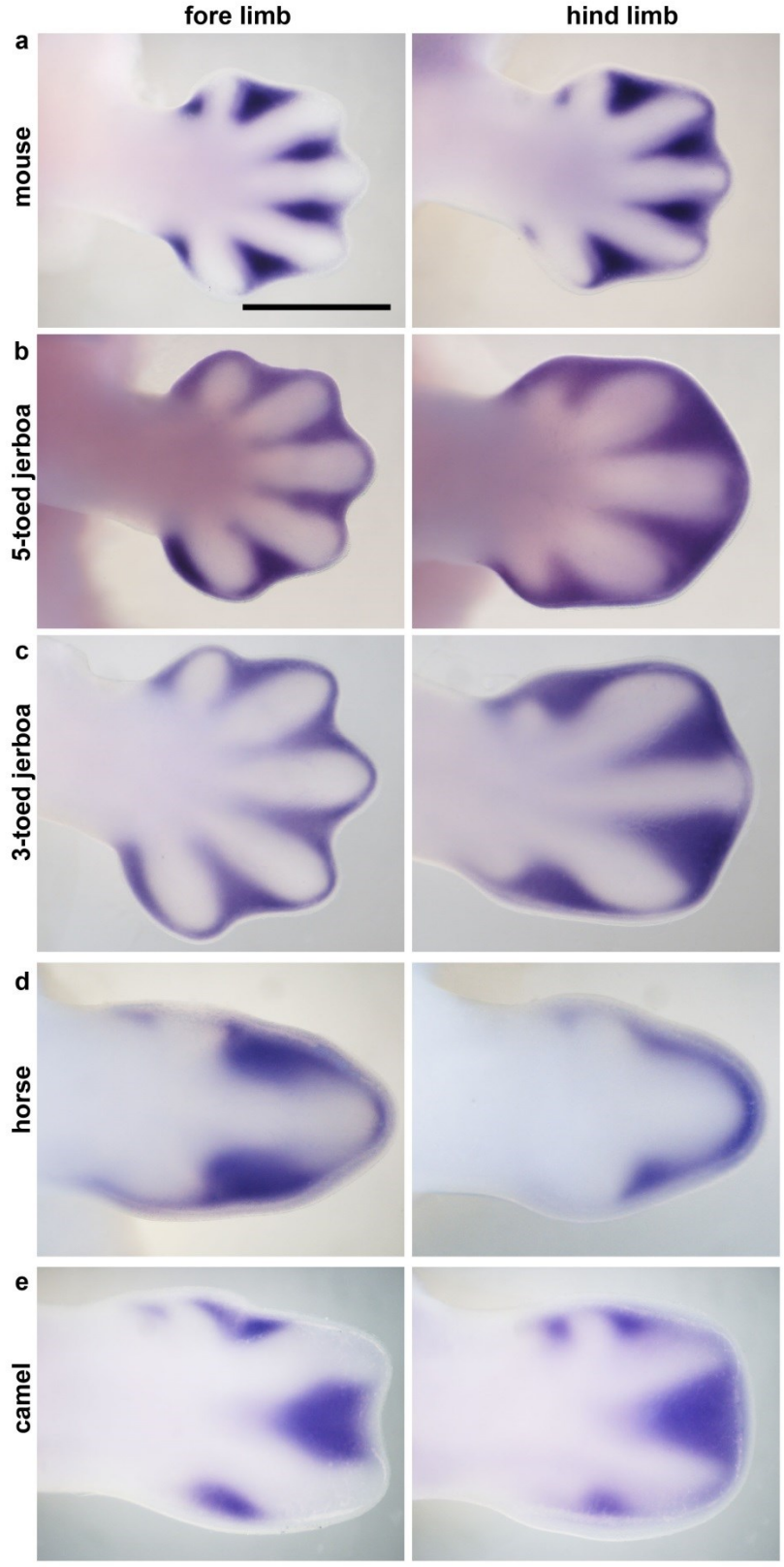

Figure 3.4, continued

expression change from the direct cause of apoptosis and may rather reflect an independent requirement for its elimination to allow for digit termination in all species.

These data indicate that at least two mechanisms of digit reduction are employed in the even-toed ungulates, one (exemplified by the pig and cow) involving changes in early patterning by *Shh* and not involving apoptosis, and a distinct mechanism (seen in camels) involving changes in domains of apoptosis that resculpt the limb after the patterning phase. These data do, however, present a paradox in the context of the well-established artiodactyl phylogeny and fossil record (**Figure 3.1b**). Although the morphology of the cow and pig is remarkably similar to the mouse phenotype when *Ptch1* is lost from the limbs, both in the reduction of digits and shift in the symmetry of toes to the interdigit of III-IV(Lopez-Rios et al. n.d.), it cannot have been responsible for both phenotypes in the artiodactyls as they occurred at different stages evolutionarily. The fact that a change in *Ptch1* regulation is seen in both pigs and cattle indicates that it was likely present in their last common ancestor. As such, it cannot have been solely responsible for the loss of digit 1, as this occurred convergently in these two lineages. Indeed, digit reduction occurred at multiple independent times within the artiodactyl clade (**Figure 3.1b**, orange circles), as the stem group of each major lineage was pentadactyl at least in the forelimb(Clifford 2010). The common ancestor of pigs and cattle would also have been ancestral to the hippos and their Cetacean relatives, the dolphins and whales (**Figure 3.1b**). Like extinct basal artiodactyls, hippos and basal Cetaceans have a relatively small first digit (Lisa Noelle Cooper et al. 2007; Karen E Sears et al. 2011; Prothero & Foss 2007). Thus, a restriction of *Ptch1* in a basal

Figure 3.5. *Fgf8* expression is restricted to the AER overlying nascent digits. Fore limb and hind limb of **a,** mouse at 13 dpc; **b,** three-toed jerboa, *D sagitta,* at about 13 dpc; **c,** pig fore limb at 25 dpc; **d,** horse hind limb at 34 dpc; **e,** camel fore limb at 42 dpc;. Scalebar = 1 mm.

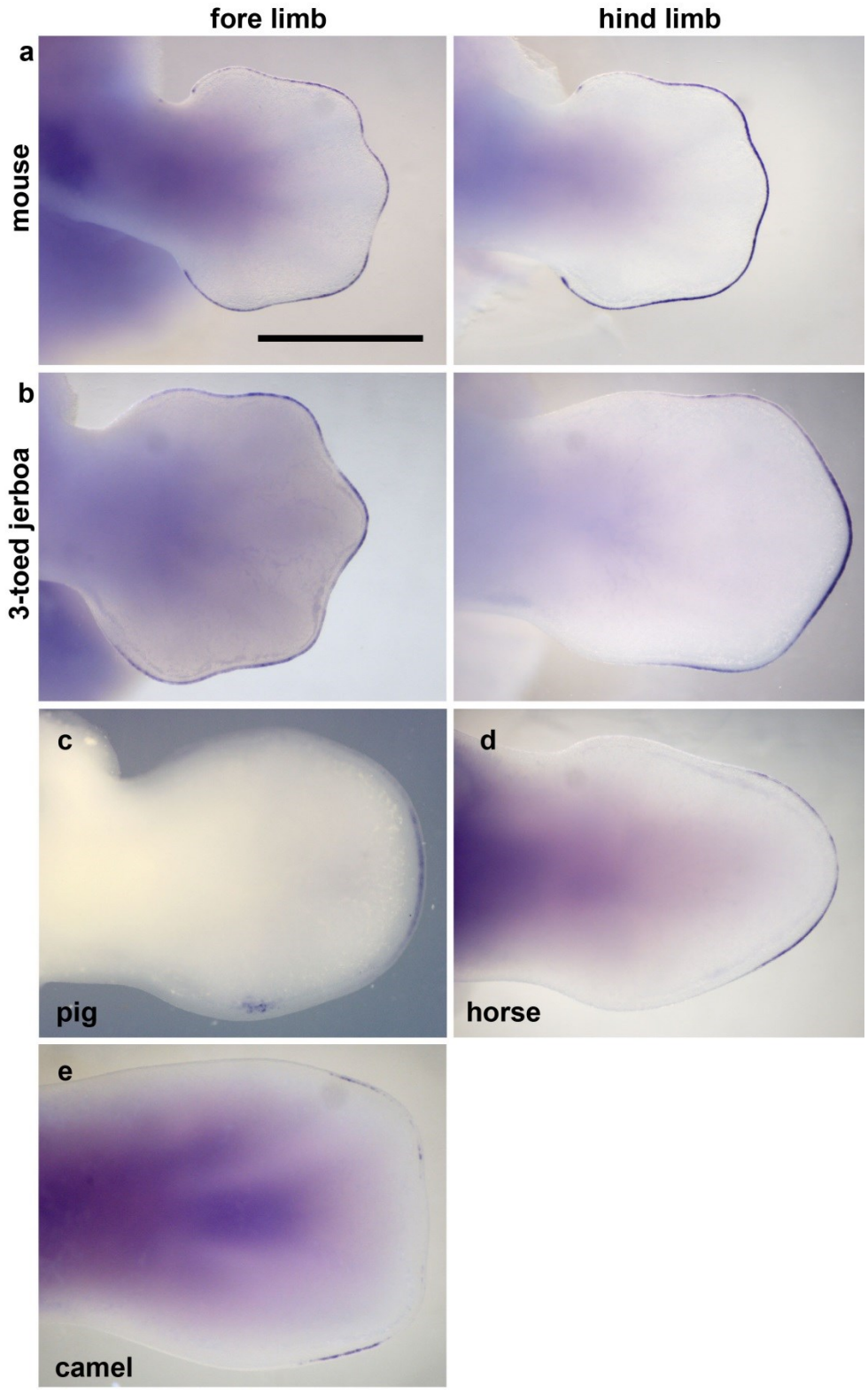

Figure 3.5, continued

member of the group including pigs, hippos, cetaceans, and cattle may have served to reduce the size of the first digit and predispose the limb to further digit loss.

Perhaps even more striking is the absence of altered *Ptch1* regulation in the camel. Without this information, one might have speculated that the *Ptch1* mutation was responsible for the reorientation of the axis of symmetry in artiodactyls similar to the mutant mouse. However, the shift in the position of digits from paraxonic to mesaxonic is believed to be ancestral to the split of modern artiodactyl suborders (and indeed is a defining characteristic trait for this clade(Rose 1982; Rose 1996; Theodor et al. 2007)) (**Figure 3.1b**, purple circle). Given the camel evidence, one has to either conclude that the shift actually arose independently in the ancestors of the camels and those of other artiodactyl lineages, or alternatively, any role *Ptch1* may have in the establishment of digit position in the pig and cow arose secondary to a separate mechanism established prior to the split of camels and their relatives.

The identification of several distinct molecular and cellular mechanisms of digit loss with recurring motifs suggests the developmental program of the tetrapod limb is fairly plastic. This would have provided some flexibility to allow adaptation in different circumstances and ultimately contributed to the diversity of limbs seen today.

Methods Summary

All embryos were collected in accordance with the appropriate Institutional Animal Care and Use Committee guidelines. Alcian blue(Rasweiler et al. 2009a) and alcian blue/alizarin red(Ovchinnikov 2009) skeletal stainings were performed as previously described. Whole mount in situ hybridizations were performed for mouse, three and five-toed jerboa, horse, and camel as in Riddle et al(Riddle et al. 1993).

Whole mount in situ hybridizations were performed in pig embryos as in Rasweiler et al(Rasweiler et al. 2009b). Riboprobes were generated by PCR amplifying from cDNA of the appropriate species, cloning into pGEMT-Easy (Promega), sequence verification, and expression testing first in mouse embryos. Primers used for probe generation are listed in **Supplementary Table S2.1**. Each experiment was performed in at least two limb buds. For TUNEL and IHC, embryos were embedded in paraffin or gelatin and sectioned at 12 or 80 um thickness. TUNEL was performed using the TMRed In Situ Cell Death Detection Kit (Roche) according to the manufacturer's instructions and counterstained with DAPI or Sox9 immunohistochemistry. Sox9 and PH3 IHC were each performed after boiling antigen retrieval in citrate buffer using a 1:500 dilution of rabbit anti-Sox9 (Millipore AB5535) or 1:200 dilution of rabbit anti PH3 (Cell Signal #9701) followed by a Cy2 or Alexa594 conjugated secondary respectively. Fluorescent images were captured by confocal microscopy, and images of sequential sections were overlaid in NIH ImageJ.

References

Alberch, P., & Gale, E. A. (1983). Size dependence during the development of the amphibian foot. Colchicine-induced digital loss and reduction. J Embryol Exp Morphol, 76, 177–197.

Butterfield, N. C., Metzis, V., McGlinn, E., Bruce, S. J., Wainwright, B. J., & Wicking, C. (2009). Patched 1 is a crucial determinant of asymmetry and digit number in the vertebrate limb. Development (Cambridge, England), 136(20), 3515–3524. doi:10.1242/dev.037507

Chen, Y., & Struhl, G. (1996). Dual roles for patched in sequestering and transducing Hedgehog. Cell, 87(3), 553–563. doi:S0092-8674(00)81374-4 [pii]

Clack, J. A. (2009). The Fish–Tetrapod Transition: New Fossils and Interpretations. Evolution: Education and Outreach, 2(2), 213–223. doi:10.1007/s12052-009-0119-2

Clifford, A. B. (2010). The Evolution of the Unguligrade Manus in Artiodactyls. Journal of Vertebrate Paleontology, 30(6), 1827–1839. doi:10.1080/02724634.2010.521216

Cooper, K. L. (2011). The lesser Egyptian jerboa, Jaculus jaculus: a unique rodent model for evolution and development. Cold Spring Harbor Protocols, 2011(12), 1451–1456. doi:10.1101/pdb.emo066704

Cooper, L. N., Berta, A., Dawson, S. D., & Reidenberg, J. S. (2007). Evolution of hyperphalangy and digit reduction in the cetacean manus. The Anatomical Record: Advances in Integrative Anatomy and Evolutionary Biology, 290(6), 654–672. doi:10.1002/ar.20532

Fernández-Terán, M. a., Hinchliffe, J. r., & Ros, M. a. (2006). Birth and death of cells in limb development: A mapping study. Developmental Dynamics, 235(9), 2521–2537. doi:10.1002/dvdy.20916

Ferrari, D., Lichtler, A., Pan, Z., Dealy, C., Upholt, W., & Kosher, R. (1998). Ectopic expression of Msx-2 in posterior limb bud mesoderm impairs limb morphogenesis while inducing BMP-4 expression, inhibiting cell proliferation, and promoting apoptosis. Developmental Biology, 197(1), 12–24.

Harfe, B. D., Scherz, P. J., Nissim, S., Tian, H., McMahon, A. P., & Tabin, C. J. (2004). Evidence for an expansion-based temporal Shh gradient in specifying vertebrate digit identities. Cell, 118(4), 517–528. doi:10.1016/j.cell.2004.07.024 S0092867404007123 [pii]

Lewandoski, M., Sun, X., & Martin, G. R. (2000). Fgf8 signalling from the AER is essential for normal limb development. Nat Genet, 26(4), 460–3.

Li, Y., Zhang, H., Litingtung, Y., & Chiang, C. (2006). Cholesterol modification restricts the spread of Shh gradient in the limb bud. Proceedings of the National Academy of Sciences of the United States of America, 103(17), 6548–6553. doi:10.1073/pnas.0600124103

Lopez-Rios, J., Duchesne, A., Speziale, D., Andrey, G., Peterson, K., German, P., … Zeller, R. (n.d.). Attenuated sensing of SHH by Ptch1 underlies adaptive evolution of bovine limbs. Submitted.

Marazzi, G., Wang, Y., & Sassoon, D. (1997). Msx2 Is a Transcriptional Regulator in the BMP4-Mediated Programmed Cell Death Pathway. Developmental Biology, 186(2), 127–138. doi:10.1006/dbio.1997.8576

Mariani, F. V, Ahn, C. P., & Martin, G. R. (2008). Genetic evidence that FGFs have an instructive role in limb proximal-distal patterning. Nature, 453(7193), 401–405. doi:nature06876 [pii] 10.1038/nature06876

Meredith, R. W., Janečka, J. E., Gatesy, J., Ryder, O. A., Fisher, C. A., Teeling, E. C., … Murphy, W. J. (2011). Impacts of the Cretaceous Terrestrial Revolution and KPg Extinction on Mammal Diversification. Science, 334(6055), 521–524. doi:10.1126/science.1211028

Ovchinnikov, D. (2009). Alcian Blue/Alizarin Red Staining of Cartilage and Bone in Mouse. Cold Spring Harbor Protocols, 2009(3), pdb.prot5170. doi:10.1101/pdb.prot5170

Pizette, S., Abate-Shen, C., & Niswander, L. (2001). BMP controls proximodistal outgrowth, via induction of the apical ectodermal ridge, and dorsoventral patterning in the vertebrate limb. Development (Cambridge, England), 128(22), 4463–4474.

Prothero, D. R., & Foss, S. E. (2007). The Evolution of Artiodactyls. JHU Press.

Rasweiler, J. J., Cretekos, C. J., & Behringer, R. R. (2009a). Alcian Blue Staining of Cartilage of Short-Tailed Fruit Bat (Carollia perspicillata). Cold Spring Harbor Protocols, 2009(3), pdb.prot5165. doi:10.1101/pdb.prot5165

Rasweiler, J. J., Cretekos, C. J., & Behringer, R. R. (2009b). Whole-Mount In Situ Hybridization of Short-Tailed Fruit Bat (Carollia perspicillata) Embryos with RNA Probes. Cold Spring Harb Protoc, 2009(3), pdb.prot5164. doi: 10.1101/pdb.prot5164

Riddle, R. D., Johnson, R. L., Laufer, E., & Tabin, C. (1993). Sonic hedgehog mediates the polarizing activity of the ZPA. Cell, 75(7), 1401–16.

Romer, A. S. (1936). Vertebrate Paleontology. University of Chicago Press.

Rose, K. D. (1982). Skeleton of Diacodexis, Oldest Known Artiodactyl. Science, 216(4546), 621–623. doi:10.1126/science.216.4546.621

Rose, K. D. (1996). On the origin of the order Artiodactyla. Proceedings of the National Academy of Sciences, 93(4), 1705–1709.

Sanz-Ezquerro, J. J., & Tickle, C. (2003). Fgf signaling controls the number of phalanges and tip formation in developing digits. Curr Biol, 13(20), 1830–6.

Sears, K. E., Bormet, A. K., Rockwell, A., Powers, L. E., Noelle Cooper, L., & Wheeler, M. B. (2011). Developmental basis of mammalian digit reduction: a case study in pigs. Evolution & Development, 13(6), 533–541. doi:10.1111/j.1525-142X.2011.00509.x

Shapiro, M. (2002). Developmental morphology of limb reduction inhemiergis (squamata: scincidae): chondrogenesis, osteogenesis, and heterochrony. Journal of Morphology, 254(3), 211–231. doi:10.1002/jmor.10027

Shapiro, M. D., Hanken, J., & Rosenthal, N. (2003). Developmental basis of evolutionary digit loss in the Australian lizard Hemiergis. J Exp Zool B Mol Dev Evol, 297(1), 48–56. Retrieved from http://www.ncbi.nlm.nih.gov/entrez/query.fcgi?cmd=Retrieve&db=PubMed&dopt=Citation&list_uids=12955843

Shenbrot, G. I., Sokolov, V. E., & Heptner, V. G. (2008). Jerboas: Mammals of Russia and Adjacent Regions. Science Publishers.

Skinner, A., Lee, M. S., & Hutchinson, M. N. (2008). Rapid and repeated limb loss in a clade of scincid lizards. BMC Evolutionary Biology, 8(1), 310. doi:10.1186/1471-2148-8-310

Sun, X., Mariani, F. V., & Martin, G. R. (2002). Functions of FGF signalling from the apical ectodermal ridge in limb development. Nature, 418(6897), 501–8.

Theodor, J., Erfurt, J., & Metais, G. (2007). The earliest artiodactyls: Diacodexeidae, Dichobunidae, Homacodontidae, Leptochoeridae and Raoellidae. In The Evolution of Artiodactyls. JHU Press.

Towers, M., Mahood, R., Yin, Y., & Tickle, C. (2008). Integration of growth and specification in chick wing digit-patterning. Nature, 452(7189), 882–886. doi:10.1038/nature06718

Walker, E. P. (1964). Mammals of the world. Baltimore: John Hopkins Press.

Zhu, J., Nakamura, E., Nguyen, M. T., Bao, X., Akiyama, H., & Mackem, S. (2008). Uncoupling Sonic hedgehog control of pattern and expansion of the developing limb bud. Dev Cell, 14(4), 624–32.

Zuzarte-Luis, V., & Hurle, J. M. (2005). Programmed cell death in the embryonic vertebrate limb. Semin Cell Dev Biol, 16(2), 261–9.

Chapter Four

Concluding Discussion

Marty McFly: *Wait a minute, Doc. Ah... Are you telling me that you built a time machine... out of a DeLorean?*

Dr. Emmett Brown: *The way I see it, if you're gonna build a time machine into a car, why not do it with some style?*

This thesis explores morphogenesis in an evolutionary context, focusing on adapting pattern to differential growth and form. The two projects set out to investigate these two variable properties of morphology by using a comparative approach and multiple model and non-model species.

Pertaining to Chapter Two on Scaling Morphogen Mediated Patterns to Variations in Size

The first question I looked into is how morphogen mediated pattern formation is scaled to variations in embryonic size throughout animal kingdom. The three species selected from Class Aves, Zebra Finch, Chick and Emu have different embryonic sizes as well as distinct dynamics of growth and patterning along the neural tube dorso-ventral axis. The smaller bird Zebra Finch, which goes through growth arrest earlier, accelerates its patterning process while the bigger bird Emu, which has a vastly elongated developmental timeline, patterns its neural tube D-V axis more gradually. Through *in vitro* explant assays and *in vivo* chimeric animals, we pinpoint that this difference in timing of patterning is due to a differential response to the morphogen and that this is intrinsic to the cells. Activation of the pathway through Smoothened receptor reveals that it is downstream to the Smo receptor, and we have strong evidence that Gli repressor activity is different, as shown in Finch and Chick both in terms of transcript levels and *in vivo* reporter activity.

Previous studies explore patterning dynamics in the context of how perturbations to size as intra-species variation can be buffered(Hamaratoglu et al. 2011; De Robertis 2009). While alterations in morphogen gradients or interaction of two opposing signals can fine-tune patterning events, we have investigated size variation as a question of evolutionary biology. Importantly, we wanted to explore how much flexibility is inherent

to strictly conserved signaling pathways that orchestrate pattern formation. Avian species have proved to be a perfect system to study this, birds are related close enough that components of patterning events should be highly conserved, but they also exhibit a wide range of egg size variation.

In the three species we investigated, there was not only a difference in size, but also differences in growth dynamics and temporal regulation of growth. However, it appears that differential response to morphogen in the neural tube is independent of the animal's developmental environment, as is shown in the chimeric animals. This suggests that while we assume growth and patterning to be inherently coupled and dependent on the developmental context, cell-autonomous differences among species can alter patterning independent of the growth environment. Interestingly, recent work on quail, duck and emu craniofacial patterning revealed that species-specific and cell autonomous differences in the neural crest mesenchyme dictate differences in timing and patterning of osteogenesis(Hall et al. 2014). It appears that our findings represent a phenomenon not entirely limited to the patterning of the ventral neural tube, but possibly a repeated trend within evolution of pattern. Prior to this work, inter-species variability of morphogen response had not been explored.

While our work was in progress, we exchanged ideas with James Briscoe's group in London, who had data that changes in cell cycle length do not alter morphogen response in the chick neural tube. Moreover, forcing progenitors in the neural tube to keep cycling has been shown to be insufficient to alter cell fate decision(Lobjois et al. 2008). Along with our findings on differences in Gli activity levels, data suggests that changes in cell cycle length or temporal differences in growth dynamics are not drivers

of differential patterning dynamics. Rather, differential response is an intrinsic property of cells and likely due to differences to the intracellular dynamics of Shh signaling. We were able to track this down to differences in Gli activity levels. Since Gli2 levels and notably Ptc1 upregulation seems very similar in Finch and Chick, we focus on the very low Gli3 levels in the Finch tissue. Since Gli3 acts mainly as a repressor, it appears that Finch neural tube tissue inherently has lower Gli repression activity, hence the spontaneous upregulation of Olig2 transcripts in naïve explants. Indeed, when we increase repressor levels in Finch and Chick neural tubes, patterning is decelerated. Therefore, by bringing down the levels of a repressor, the smaller bird, Zebra Finch, can increase its responsiveness to a morphogen gradient. Other possible scenarios for how different species can display differential response to a signal can be through dynamics of the gene regulatory networks or expression and activity of some pan-neural genes like Sox2 (Peterson et al. 2012), but this remains to be explored.

In some systems, such as the Drosophila wing disc, early vertebrate embryo or the Xenopus gastrula, it is reported that the morphogen gradient itself is scaled to size of the tissue, thereby scaling the tissue pattern to size(Hamaratoglu et al. 2011; Gregor et al. 2005; Cheung et al. 2014; Inomata et al. 2013; Ben-Zvi et al. 2008). While scaling models that rely on scaling of the morphogen gradient itself may be valid for a range of biological systems, it appears that in the neural tube, neither the morphogen gradient nor the Gli activity gradient scale to perturbations in size. Rather, a complex dynamical gene regulatory network, differentiation rate and anisotropic growth of the neural tube seem to explain how pattern adapts to size variability within individuals (Kicheva, A., Bollenbach, T., Ribeiro, A., Perez Valle, H., Lovell-Badge, R., Episkopou, V., Briscoe

n.d.). Therefore, along with work from the Briscoe group, our scaling models for inter-species and intra-species size variation in the neural tube propose an alternative to models that focus on scaling of the gradient. However, how the gradient shape and amplitude differ in Finch, Chick and Emu is also an interesting question that we aim to address in the near future. We have been able to visualize the Shh morphogen gradient in all species, and hope to quantify the amplitude of the gradient at different stages of development.

Another noteworthy difference within the neural tubes of the three species was the circumferential growth, or in other words, thickness of the neural tube tissue along the apico-basal direction. As neurons proliferate, differentiate and migrate basally, the pseudostratified progenitor layer changes in thickness (Saade et al. 2013). Even though cell size is comparable between species, we noticed that especially in earlier stages, ventral midline apico-basal thickness of the neural tube is smallest in the Finch, and greatest in the Emu. While this is correlated with proliferation and differentiation dynamics, it is important to investigate how it contributes to shape of the morphogen gradient or reception of the morphogen protein by the cells. Size and shape of the progenitor domains, as expected, can also be altered with differences in the depth of the tissue.

Follow up questions on patterning and anisotropic growth in the neural tube brings us to the issue of whether dynamics of growth, cell cycle length and differentiation are also inherently different in the three species. The early arrest of growth cycle in the Finch neural tube compared to chick, and the extended duration of growth in the Emu suggest entirely different growth dynamics for the three species,

which is intuitive considering the overall difference in size at the end of development. Some candidate pathways to study include Notch signaling, Hippo pathway, and certain pan neural genes that may regulate differentiation. In the future, it would be interesting to tackle the mechanisms of differences in growth.

Pertaining to Chapter Three on Digit Reduction in Vertebrate Limb Evolution

The second part of this thesis, evolutionary mechanisms of digit reduction, is the flip side of the medallion compared to the work in the first part. With this project, we addressed how a conserved pattern is modified, as opposed to how it is maintained throughout evolution as was explored in the scaling project. A recurrent adaptive modification to the vertebrate limb is digit reduction, observed in a wide range of animals from different taxa of tetrapods. In collaboration with Dr. Kim Cooper, we explored whether the developmental mechanisms underlying this convergent adaptation is shared between animals. Our findings show that lateral cell death is a post-patterning mechanism to sculpt the autopod, and employed as a modification mechanism by the odd-toed jerboa, horse and the even toed camel. On the other hand, the pig and the cow have achieved a convergent phenotype through down-regulation of Ptch1 expression with a conserved change in Ptch1 enhancer region *(as is shown in Lopez-Rios et al)*. Together, these data demonstrate that there is a remarkable plasticity in how patterns can be modified to achieve a convergent phenotype. Reduction to digit number can be achieved either through changes during the patterning process, or subsequent to it.

Previous research on tetrapod digit reduction is limited, but Shapiro et al. have explored digit reduction in closely related populations of Australian skinks from the

genus *Hemiergis*, inhabiting 4 different isolated areas in Western Australia. The skink populations are unique in that each isolated habitat is home to a species with a unique number of digits, ranging from 2 to 5. Shapiro et al.'s work reveals early termination of Shh expression in species with reduced digit number, with 2-digit embryo having the shortest period of Shh expression. This is thought to be what drives reduction in digit number, especially because the digits are reduced in the reverse order that they develop. Notably, functional studies on *Ambystoma mexicanum* salamanders where Shh signaling was blocked with drug cyclopamine also result in digit loss in a pattern that mimicks the reverse order of digit formation(Stopper GF 2007).

Yet, what we observe with the odd-toed jerboa and odd-toed horse is symmetrical digit loss, where lateral digits are the first ones to be reduced. Identities of the outgrowing digits are homologous to the central digits. Then, an entirely different strategy for digit reduction, one that is post- patterning, can explain how the digit number is reduced in these animals. The expansive cell death we identified in lateral limb mesenchyme of jerboa and horse autopoda is preceded by extended BMP4 and Msx2 expression in the earlier stages, suggesting that pathways that are known to regulate cell death in the limb mesenchyme are involved with the lateral apoptotic cascade that prevents digit outgrowth. Functional studies in model organisms can complement these results. Importantly, a work that is to be followed up by Kim Cooper involves identification of regulatory differences and test expression with reporter BACs, using jerboa-specific sequences. Finally, functional tests will be performed with specific knock-in mice at these regulatory sites, to recapitulate phenotype.

In parallel, work from Lopez-Rios et al. reports an alternative strategy through which digit number is regulated. In bovine limbs, they identified an evolutionary alteration to a *Ptch1 cis*-regulatory module, as a consequence of which Ptch1 upregulation is disrupted and Gli1 expression is uniform along the limb bud. Interestingly, we have observed the same phenomenon within the pig limb buds. As Bovidae (includes cows) and Suidae (includes pigs) have both diverged early during artiodactyl evolution, modification to the *Ptch1 cis*-regulatory module may have emerged before this diversion, as a shared characteristic of even-toed ungulates with reduced digit number and shifted axis.

However, the camel, which is another even-toed ungulate that has diverged early during the artiodactyl evolution, does not follow this trend. Instead, *Ptch1* upregulation is not disrupted, and the embryos have expanded cell death on the lateral sides of the autopod. Curiously, this expanded apoptosis is not preceded by distal expansion of BMP4 that we observe for three toed jerboa and horse, leaving the camel with an entirely unique strategy for digit reduction. Moreover, with these finding, we cannot assume *Ptch1* rotation to be responsible for the shift in axis of symmetry. The axis shift either arose independently in even-toed ungulates, or, Ptch1's role in digit reduction was secondary to a separate mechanism that caused axis shift prior to split of camels from this cluster.

Distal restriction of AER-Fgf8 expression is a convergent phenotype for all species we studied. Interestingly, Lopez-Rios et al. have observed a similar distal restriction of Fgf8 expression in bovine limb buds. This makes it likely that regression of Fgf8 expression is a consequence of signaling events subsequent to mechanisms that

inhibit outgrowth of lateral digits, such as elevated Bmp signaling or Grem1 levels. In this case, Fgf8 restriction is correlated, not causative, during digit reduction, even though its elimination would likely contribute to failure of chondrogenesis for lateral digits.

Fossil record shows that primitive artiodactyls, just like most rodents, are indeed pentadactylous. The fact that animals from different taxa have converged on mechanism of post-patterning sculpting suggests that extreme developmental modifications to the earliest stages of limb formation may be selected against. The initial formation of the limb bud and the set of pentadactyl pattern is constrained to some degree, making it more likely that evolutionary modification to later stages of limb formation is what generates diverse adult morphologies and digit number variation(Galis F Metz JAJ 2001; Sears 2011). It is also noteworthy to mention that the earliest phase of limb bud outgrowth and onset of pentadactyl pattern have been reported to be maintained the pig embryonic development, as well as in other artiodactyls that have a similar functional loss in lateral digits, such as cows(K E Sears et al. 2011).

Among the species we investigated, digit identities are roughly conserved between taxa, and each digit is distinct in terms of its morphology and position along the antero-posterior axis. What appear to be different in digit development between different taxa is slight differences in timing of digital condensation and growth, as well as notable differences in size of the digits. This was particularly impressive with the horse limbs, where the middle toe, while retaining its identity, was remarkable larger in size. When looked into at early stages with the lateral condensations, it was also evident that not just the digit, but the non-digit spacing is also quite large. In the future, it could be

interesting to explore what could be causing differences in digit and non-digit sizes in different species.

It is important to note that while we investigated patterns of digit reduction extensively and have seen repeated examples of it in nature, we hardly ever see gain of digit, even though polydactyly is a common anomaly. One reason may be that common mutations of polydactyly in animals have pleiotropic effects that prevent it from being selected. Moreover, polydactyly does not provide a new digit identity, but duplicates an existing one. Therefore, duplication of an existing form is not likely to reveal a new function for the animal(Tabin 1992). Instead, what we observe in nature is exaptation (modification of existing structures into new form and function). The panda bear, mole and elephant all have modified a sesamoid bone so it appears as an extra digit with a unique form and function, while retaining the functionality of their pentadactyl digital palette(Mitgutsch et al. 2012; Gould 1978; Hutchinson et al. 2011) .

In summary, it appears that morphogen mediated patterning in animal development provides a robust, species specific morphology with great precision for proper form and function. Yet, we also observe a remarkable plasticity to this process in evolution, whereby patterns can be scaled to the overall size of the animal or modified to fit form to function.

Taken together, I hope this dissertation can expand our understanding of how conserved pathways of morphogen mediated patterning can be adapted to modify morphogenesis and generate new forms and functions throughout evolution.

References

Ben-Zvi, D., Shilo, B.-Z., Fainsod, A., & Barkai, N. (2008). Scaling of the BMP activation gradient in Xenopus embryos. *Nature*, *453*(7199), 1205–11.

Cheung, D., Miles, C., Kreitman, M., & Ma, J. (2014). Adaptation of the length scale and amplitude of the Bicoid gradient profile to achieve robust patterning in abnormally large Drosophila melanogaster embryos. *Development (Cambridge, England)*, *141*(1), 124–35.

De Robertis, E. M. (2009). Spemann's organizer and the self-regulation of embryonic fields. *Mechanisms of Development*, *126*(11-12), 925–41. doi:10.1016/j.mod.2009.08.004

Galis F Metz JAJ, van A. J. J. M. (2001). Why five fingers? Evolutionary constraints on digit numbers. *TREE*, (16), 637–646.

Gould, S. J. (1978). The Panda's Peculiar Thumb. *Incorporating Nature Magazine*, *Vol. LXXXV*(No.9).

Gregor, T., Bialek, W., de Ruyter van Steveninck, R. R., Tank, D. W., & Wieschaus, E. F. (2005). Diffusion and scaling during early embryonic pattern formation. *Proceedings of the National Academy of Sciences of the United States of America*, *102*(51), 18403–7.

Hall, J., Jheon, A. H., Ealba, E. L., Eames, B. F., Butcher, K. D., Mak, S.-S., … Schneider, R. a. (2014). Evolution of a developmental mechanism: Species-specific regulation of the cell cycle and the timing of events during craniofacial osteogenesis. *Developmental Biology*, *385*(2), 380–95.

Hamaratoglu, F., de Lachapelle, A. M., Pyrowolakis, G., Bergmann, S., & Affolter, M. (2011). Dpp signaling activity requires Pentagone to scale with tissue size in the growing Drosophila wing imaginal disc. *PLoS Biology*, *9*(10), e1001182.

Hutchinson, J. R., Delmer, C., Miller, C. E., Hildebrandt, T., Pitsillides, A. A., & Boyde, A. (2011). From flat foot to fat foot: structure, ontogeny, function, and evolution of elephant "sixth toes." *Science*, *334*(6063), 1699–1703.

Inomata, H., Shibata, T., Haraguchi, T., & Sasai, Y. (2013). Scaling of dorsal-ventral patterning by embryo size-dependent degradation of Spemann's organizer signals. *Cell*, *153*(6), 1296–311.

Kicheva, A., Bollenbach, T., Ribeiro, A., Perez Valle, H., Lovell-Badge, R., Episkopou, V., Briscoe, J. (n.d.). Sequential control of spinal cord progenitor proportions by morphogen signaling and anisotropic growth. *Unpublished*.

Lobjois, V., Bel-Vialar, S., Trousse, F., & Pituello, F. (2008). Forcing neural progenitor cells to cycle is insufficient to alter cell-fate decision and timing of neuronal differentiation in the spinal cord. *Neural Development*, *3*(February), 4.

Mitgutsch, C., Richardson, M. K., Jimenez, R., Martin, J. E., Kondrashov, P., de Bakker, M. A., & Sanchez-Villagra, M. R. (2012). Circumventing the polydactyly “constraint”: the mole’s “thumb.” *Biol Lett*, *8*(1), 74–77.

Peterson, K. a, Nishi, Y., Ma, W., Vedenko, A., Shokri, L., Zhang, X., … McMahon, A. P. (2012). Neural-specific Sox2 input and differential Gli-binding affinity provide context and positional information in Shh-directed neural patterning. *Genes & Development*, *26*(24), 2802–16.

Saade, M., Gutiérrez-Vallejo, I., Le Dréau, G., Rabadán, M. A., Miguez, D. G., Buceta, J., & Martí, E. (2013). Sonic hedgehog signaling switches the mode of division in the developing nervous system. *Cell Reports*, *4*(3), 492–503.

Sears, K. E. (2011). Novel insights into the regulation of limb development from natural mammalian mutants. *Bioessays*, *33*, 327–331.

Sears, K. E., Bormet, A. K., Rockwell, A., Powers, L. E., Noelle Cooper, L., & Wheeler, M. B. (2011). Developmental basis of mammalian digit reduction: a case study in pigs. *Evol Dev*, *13*(6), 533–541.

Stopper GF, W. G. P. (2007). Inhibition of Sonic hedgehog Signaling Leads to Posterior Digit Loss in Ambystoma mexicanum: Parallels to Natural Digit Reduction in Urodeles. *Developmental Dynamics*, *236*, 321–333.

Tabin, C. J. (1992). Why we have (only) five fingers per hand: hox genes and the evolution of paired limbs. *Development*, *116*(2), 289–296.

Appendix

Supplementary Figures for Chapters Two and Three

Appendix

Part I: Supplementary Figures for Chapter Two

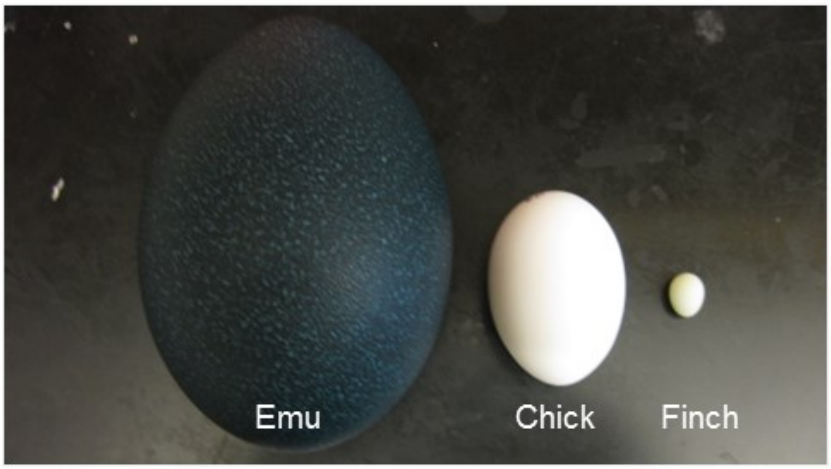

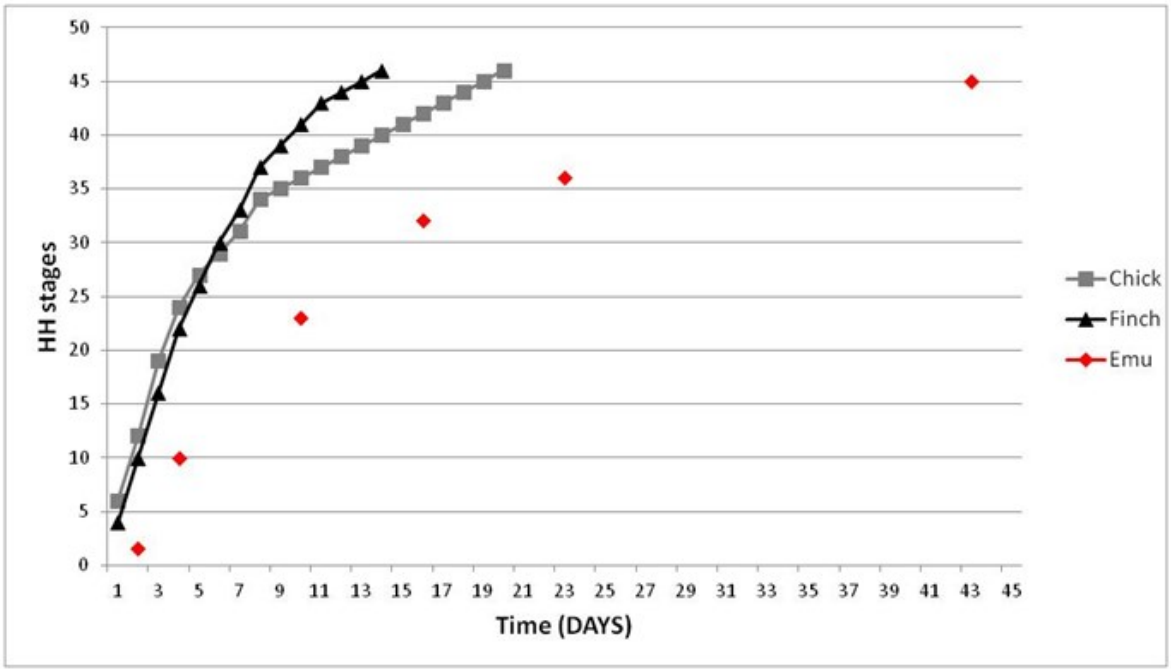

Figure S1.1 Finch, Chick, Emu eggs and development. Eggs of the three bird species used for this study. They cover a range of embryonic sizes from an early time point in development. While developmental timing is more similar between Finch and Chick, Emu is more delayed.

Figure S1.2: Chick versus Finch development across stages: Developmental series of Chick versus Finch embryos, compared at equivalent stages starting from stage HH8 through HH28. Difference in size is noticeable from stage 8 (day 1) through hatching (not shown).

Figure S1.2, continued

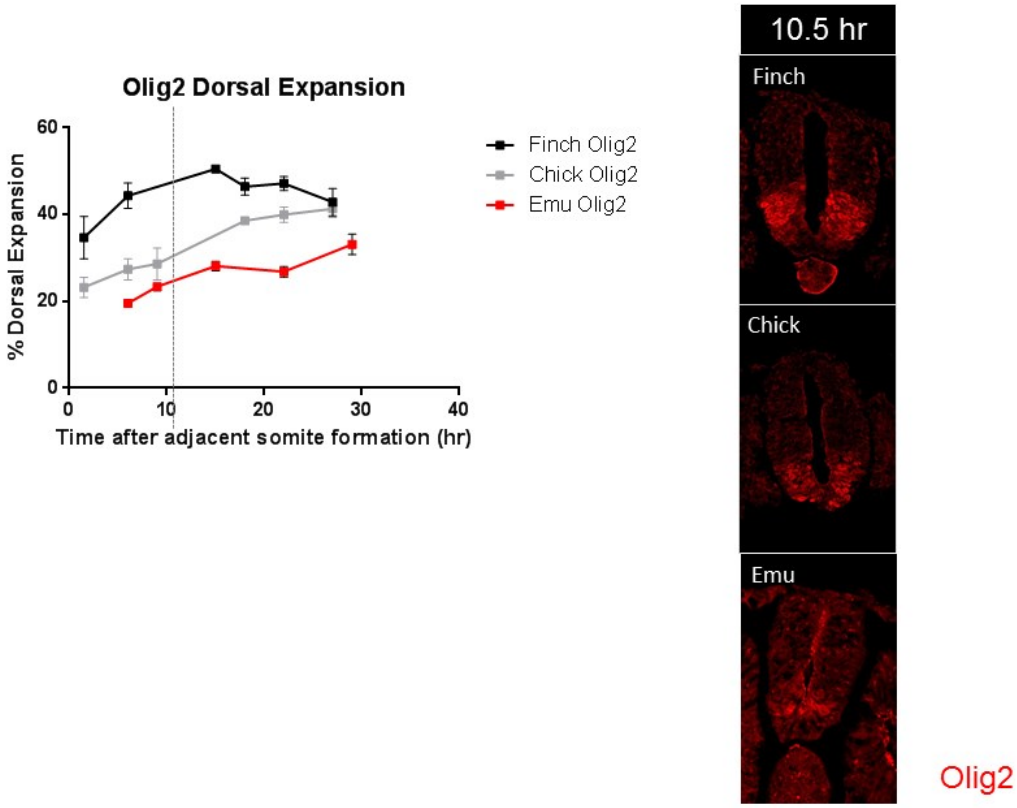

Figure S1.3: OLIG2 dorsal expansion across time. Dorsal expansion of pattern, as shown for OLIG2 at 10.5 hours post formation of somite 15.

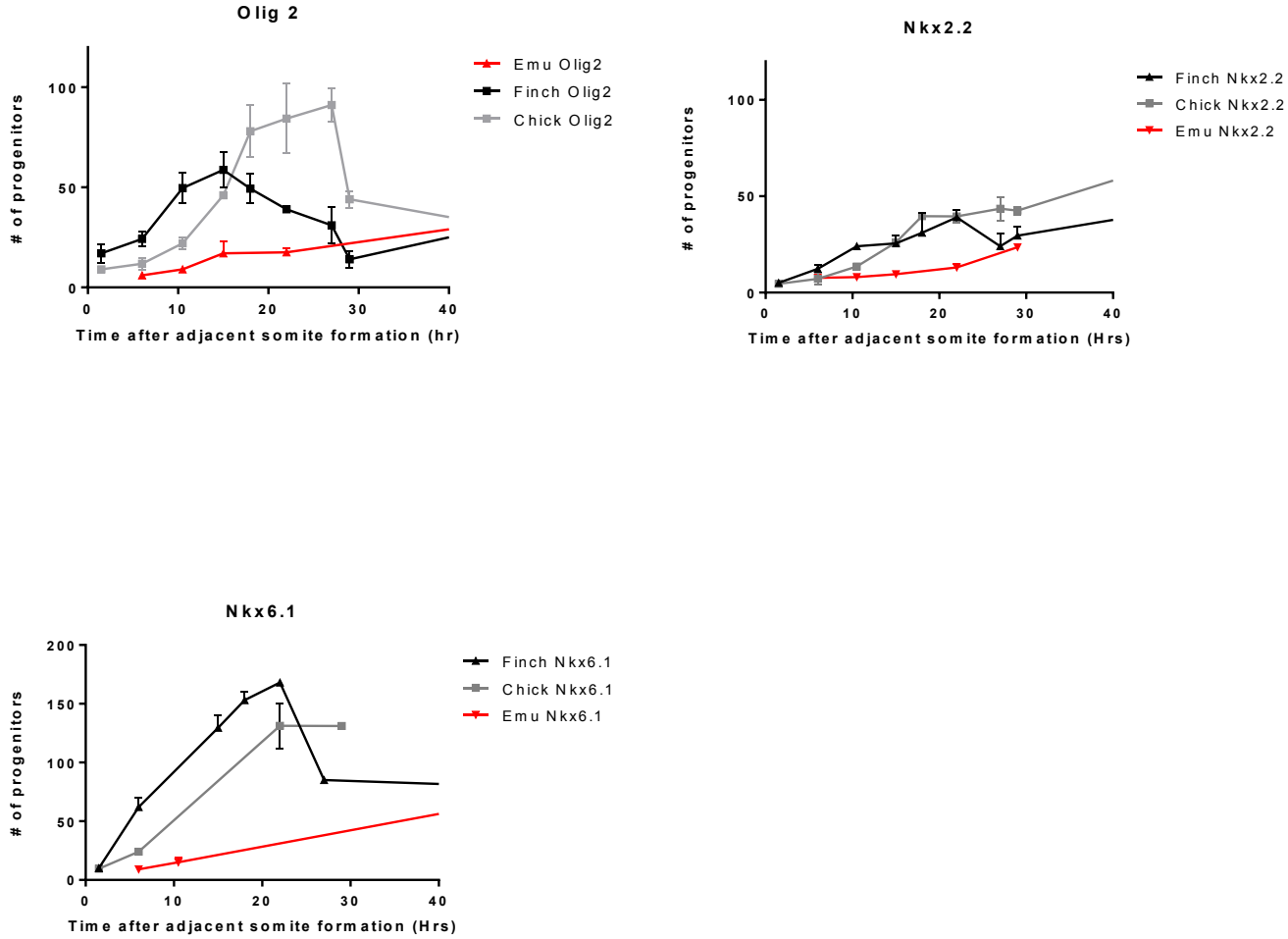

Figure S1.4: Pattern progression in the three species plotted as number of progenitors: Instead of % dorsal expansion of the transcription factor expression domains, this graph plots the number of progenitors expressing the specific TF, plotted against time.

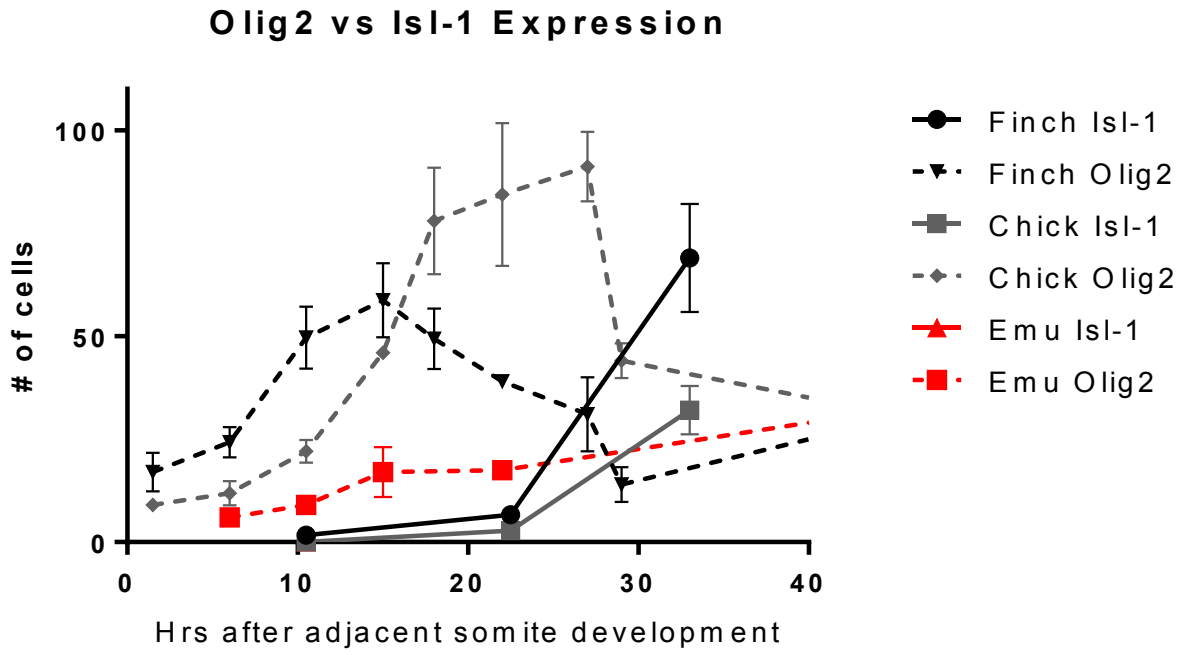

Figure S1.5: Isl-1 expression starts earlier in Finch: Expression of the motor neuron differentiation marker Isl-1 starts earlier in Finch, with a few cells already expression Isl-1 at stage HH14. For all earlier stages we quantified, Isl-1 in Finch tissue is more advanced than Chick and Emu (Emu tissue does not start Isl-1 expression for a long time). While an inherent different in differentiation rates is possible, this trend could also stem from earlier peak of Olig2 expression in the Finch, and latest in the Emu. More advanced patterning in the Finch at same time point may mean a naturally earlier initiation for differentiation phase.

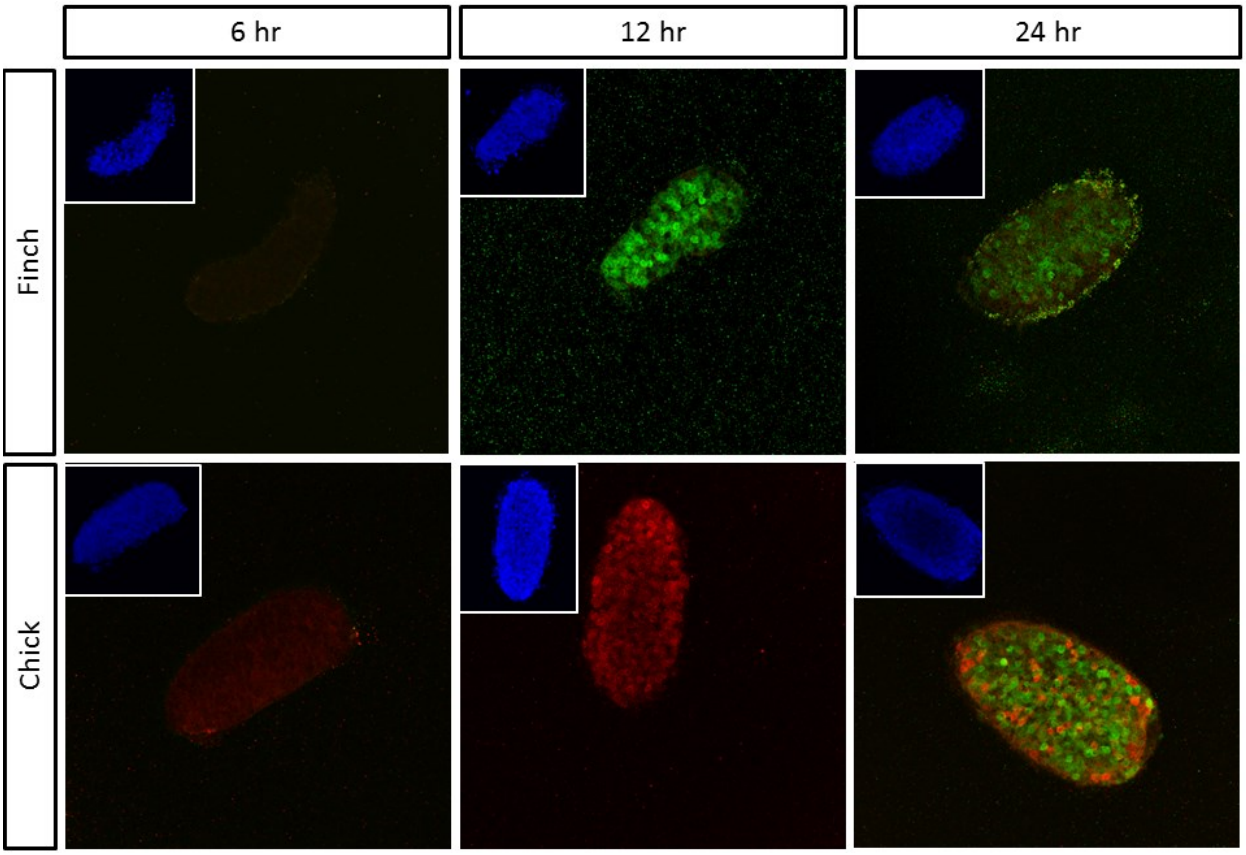

Extended Figure S1.6: Finch and Chick naïve explants grown *in vitro* with a fixed concentration of Shh, for different durations. Duration of morphogen exposure has been shown to be critical to morphogen response as much as morphogen concentration, as discussed in text. When naïve explants from Finch and Chick are incubated at a fixed concentration that elicits differential response at 24 hours (Finch explants saturated for NKX2.2 response and Chick explants expressing both NKX2.2 and OLIG2), we find that this altered response can be observed as early as 12 hours. At 6 hours, tissue from both species did not stain for either of the markers. At 12 hrs, Finch is saturated with NKX2.2 response, while Chick is saturated with OLIG2 response. We later did a qRT-PCR series for these genes and saw a similar trend (See Figure 2.7*).*

n > 5 for all panels. Results are representative.

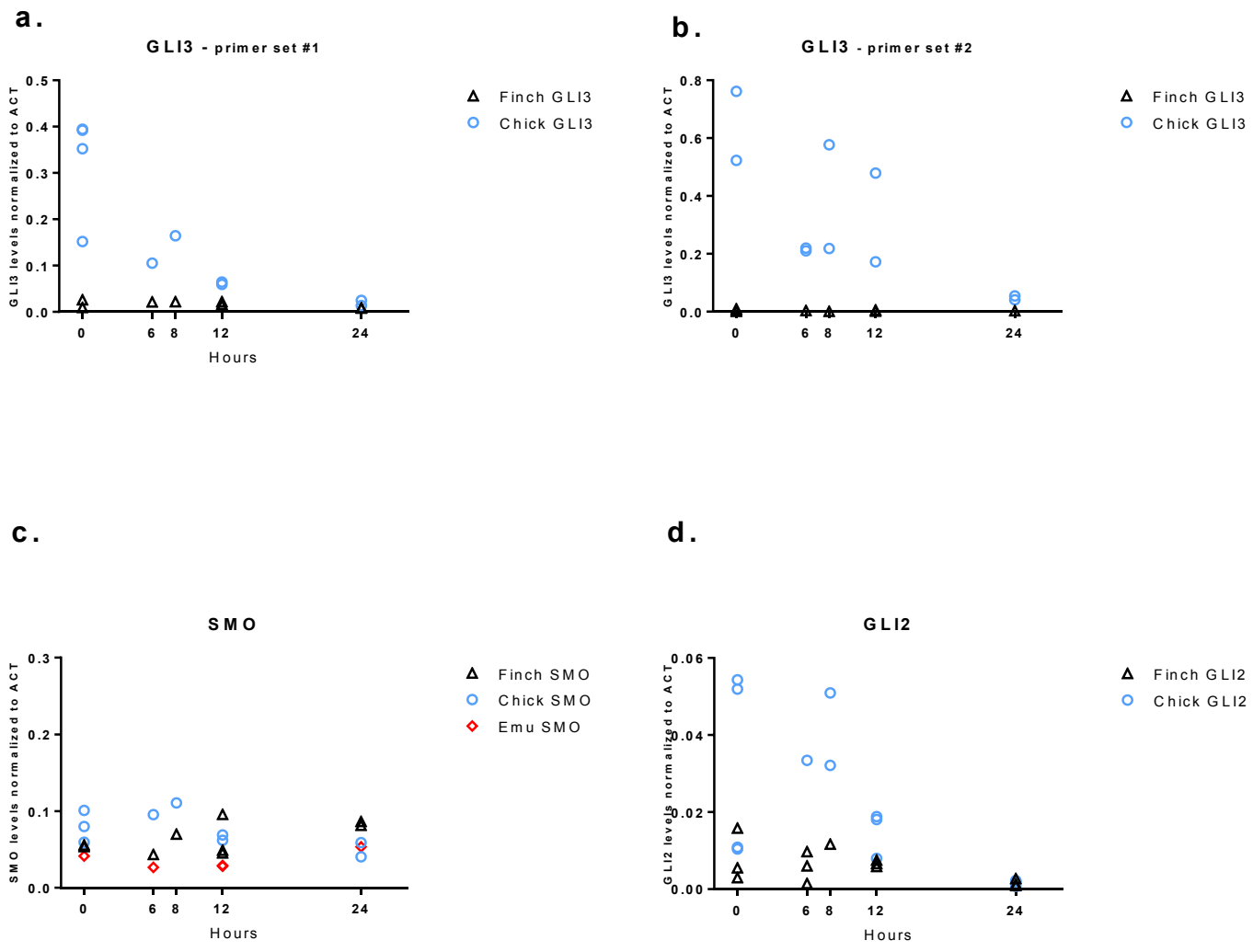

Extended Figure S1.7: Expression of different SHH pathway components

Expression of several SHH pathway components in Finch versus Chick as assayed by qRT-PCR**. a-b.** GLI3 levels are drastically different in the two species, when assayed by two different sets of species specific primers **c.** Smoothened levels are comparable, and **d.** GLI2 levels do not appear to be significantly different. Each data point represents 15-25 explants pooled together.

Table S1.1 Primers used for qRT-PCR assays

Gene	Species	FW primer	REV primer
Actin	Finch	GCGCGAGATCGTGCGCGACA	TCTTCTCCAGCGAGGAGGAG
	Chick	GAGGGAGATCGTCCGTGATA	TTTTCTCCAGGGAGGAGGAT
	Emu	AAGGGAGATTGTCCGTGACA	TCTTCTCAAGGGAGGAGGAA
GAPDH	Finch	CACACAGAAGACAGTGGATG	CGGAAAGCCATTCCAGTAAG
	Chick	CACACAGAAGACGGTGGATG	CGGAAAGCCATTCCAGTAAG
	Emu	CACCCAGAAGACAGTGGATG	CGGAAAGCCATTCCAGTAAG
Ptch1	Finch	AAGCGAACAGGAGCAAGTGT	TGCTGCTTGGAGTGAAAATG
	Chick	AAGCGAACAGGAGCAAGTGT	TGCTGCTTGGAGTGAAAATG
	Emu	TTGCCTTTTCTTGCTCTTGG	AGCACAGGGAAAATCAGCAGAA
Smo	Finch	TTTGTCATGCTCACCTATGC	ACCAGGTGATGAGGTGGAAG
	Chick	TTTGTCATGCTGACCTACGC	ACCAGGTGATGAGGTGGAAG
	Emu	TTCGTCATGCTCACCTACGC	ACCAGGTGATGAGGTGGAAG
Gli2	Finch	GCAACTAAGGAAACACATGA	CCCATGAGCAGGAATCCTTA
	Chick		
	Emu	GCAGTCTAATGAAACACATGA	
Gli3 set#1	Finch	ATTTCCCCGCACCGAAAT C	AATGTATGGGTGAGGGGTGC
	Chick	TCCCCACACAGAGCCTTATC	AATGTACGGGTGAGGAGTGC
Olig2	Finch	GGATGCACGACCTCAACC	CTTCATCTCCTCCAGGGAGT
	Chick	GGATGCACGACCTCAACA	CTTCATCTCCTCCAGCGAGT
Nkx2.2	Finch	ACGCAGGTGAAGATCTGGTT	TTGTACTGCATGTGCTGCTG
	Chick	ACCTTCCAGACGGGCATC	TGTAATGGGCGTTGTATTGC
Gli3 set#2	Finch	ACAGGAGGGACAGCAATACT	CTGCAACGCTCACATCTTGT
		ACAGGAGGGACAGCAATACG	CTGCAACGCTCACATTTTGT

Appendix

Part II: Supplementary Figures for Chapter Three

Extended Data Figure S2.1. The proximal remnants of truncated skeletal elements in *D sagitta* are correctly patterned. Alcian blue and alizarin red stained skeletons of postnatal day 0 mouse (left) and three-toed jerboa, *D sagitta* (right) with proximal (ankle) at the top. **c,** Anterior view highlights the first metatarsal (arrow head). **d,** Posterior view highlights the fifth metatarsal (arrow). **e,** Dissected first tarsal-metatarsal elements demonstrate the morphology of the truncated first metatarsal of *D sagitta* (right, arrow head) compared to mouse (left). Joint interzone indicated by white dashed line.

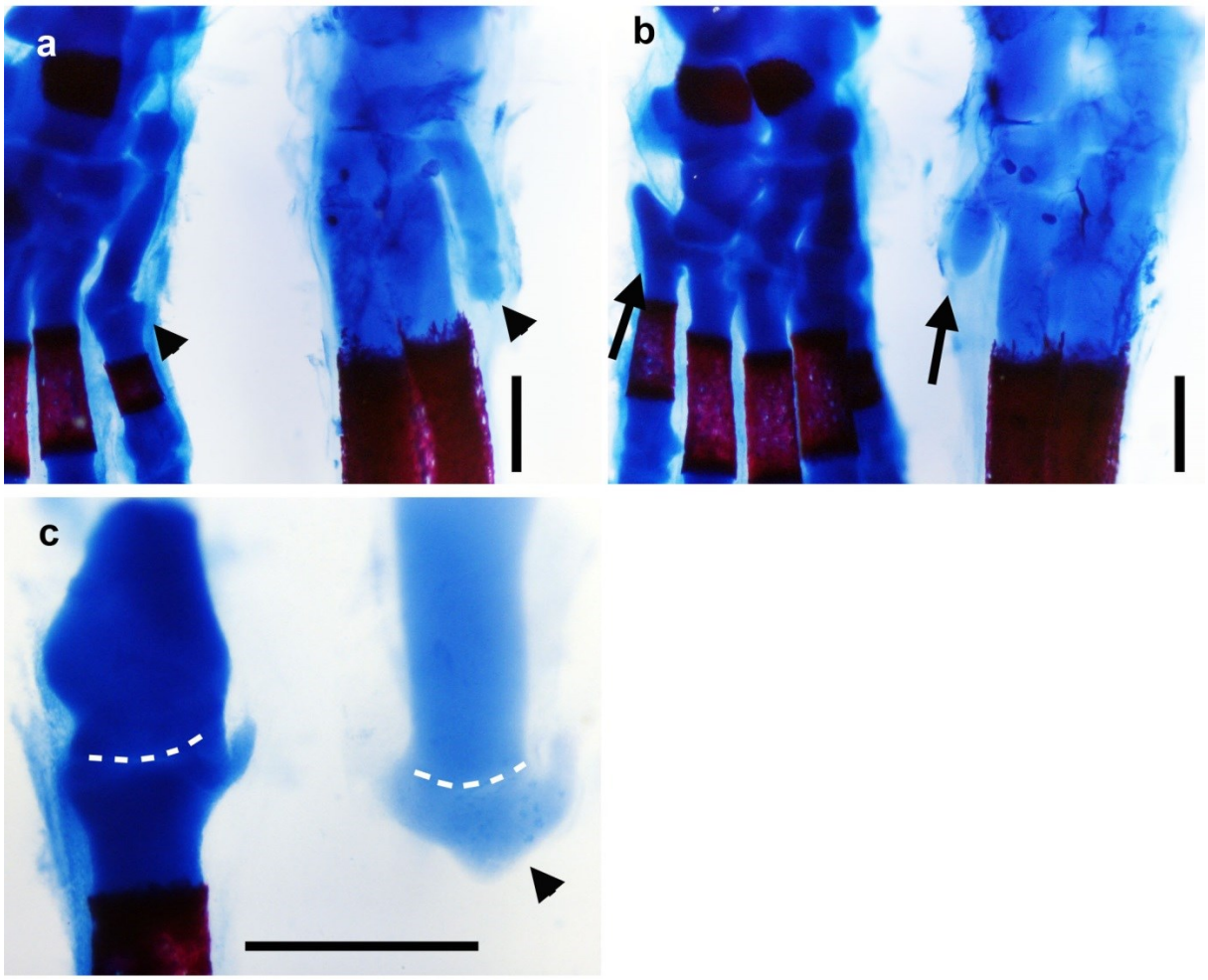

Extended Data Figure S2.1, continued

Extended Data Figure 2.2. The shape of the three-toed jerboa hind limb differs from the mouse as early as 11.5 dpc Trace outlines of limb buds of the mouse (black) and three-toed jerboa, *D sagitta* (green) over a developmental time series.

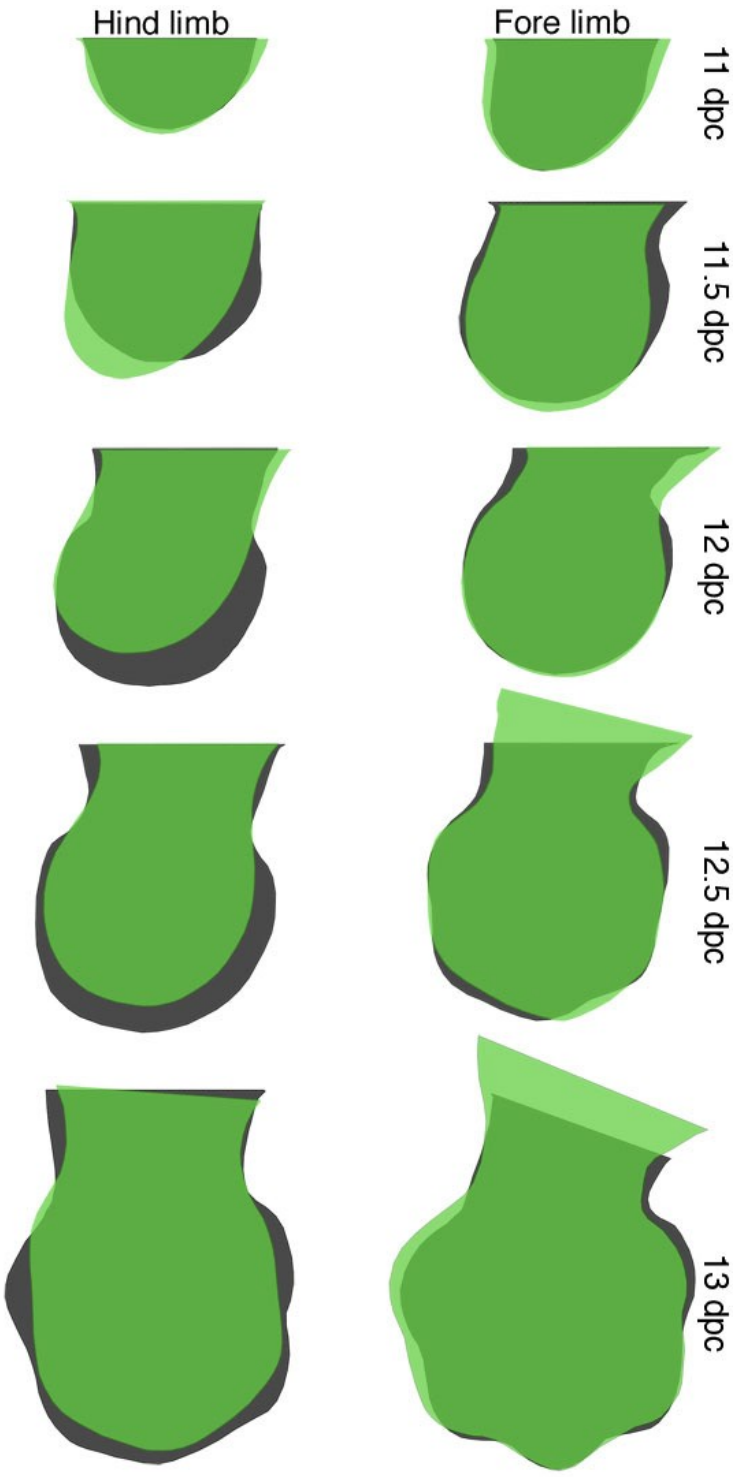

Supplementary Figure S2.2, continued

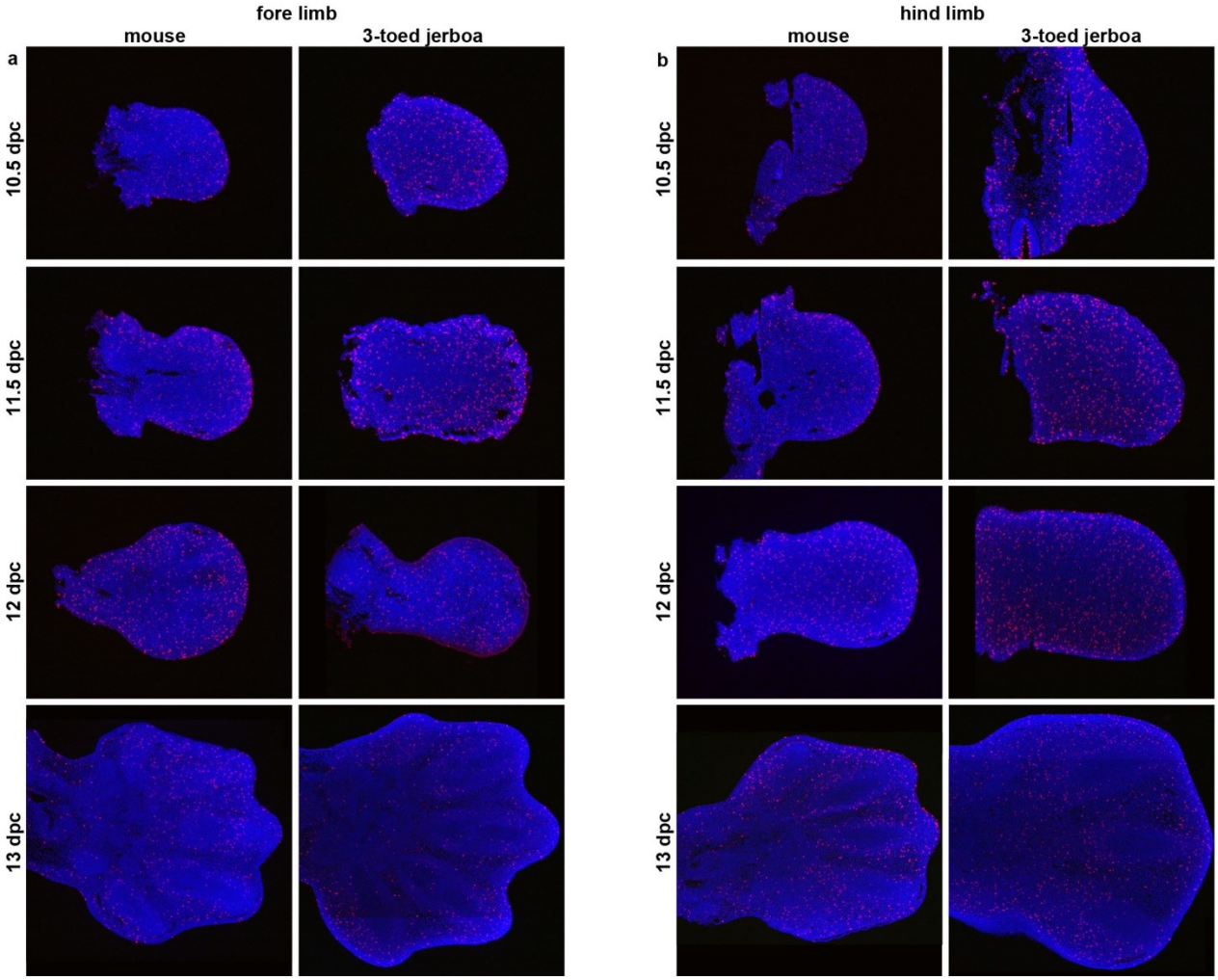

Extended Data Figure 2.3. Cell proliferation is unchanged in the *D sagitta* hind limb bud. Phospho-histone H3 detection in sections of mouse and three-toed jerboa, *D sagitta,* limb buds. **a,** fore limbs; **b,** hind limbs.

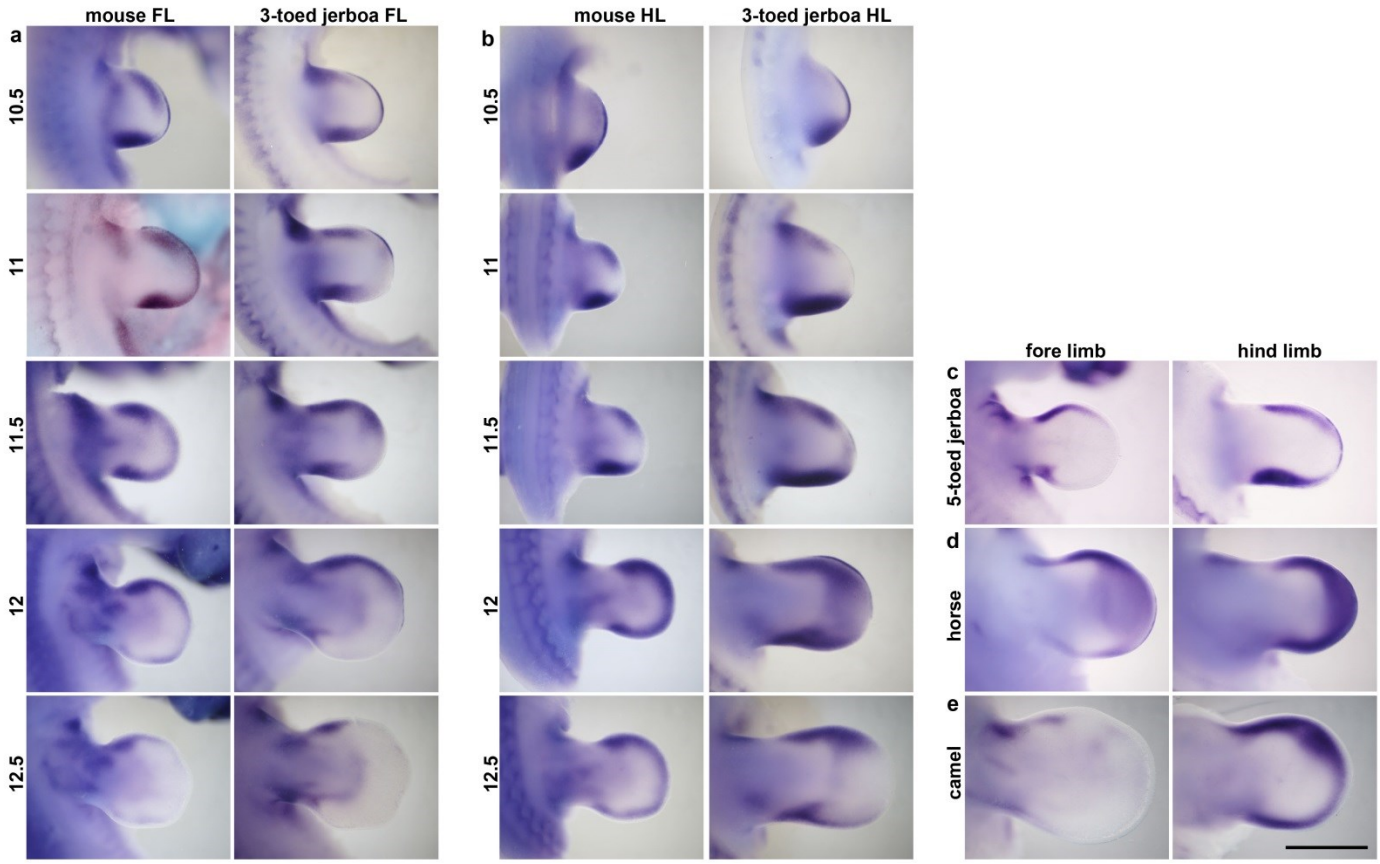

Extended Data Figure 2.4. Developmental time course and species comparisons of *Bmp4* expression. a, Fore limb buds (FL) and **b,** hind limb buds (HL) of mouse and the three-toed jerboa, *Dipus sagitta*, at 10.5, 11, 11.5, 12, and 12.5 dpc. **c,** Fore limb and hind limb of the five-toed jerboa, *A elater,* at approximately 12.25 dpc. **d,** Fore limb and hind limb of the horse at 30 dpc (approximately equivalent to mouse 12 dpc). **e,** Fore limb and hind limb of the camel at 38 dpc (approximately equivalent to mouse 12.5 dpc). Scalebar = 1 mm.

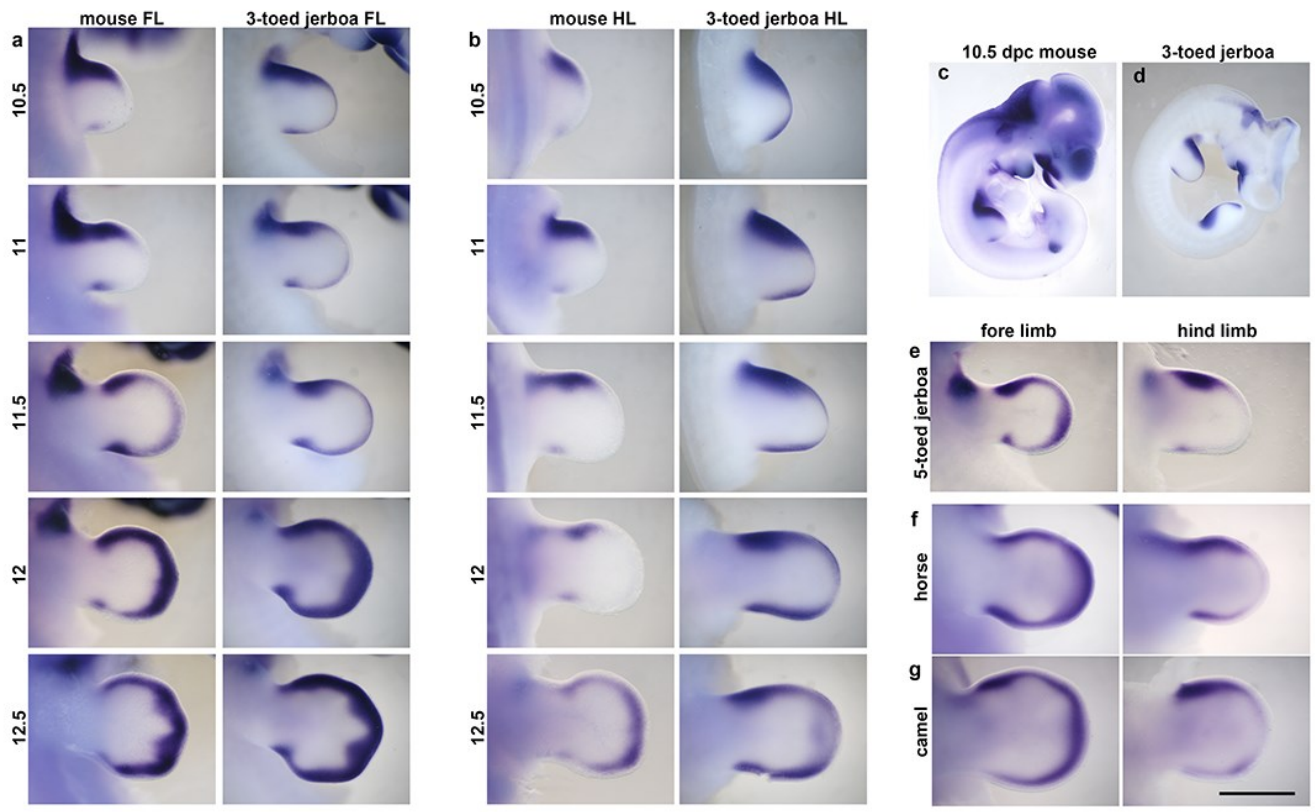

Extended Data Figure 2.5. Developmental time course and species comparisons of *Msx2* expression. a, Fore limb buds (FL) and **b,** hind limb buds (HL) of mouse and the three-toed jerboa, *Dipus sagitta*, at 10.5, 11, 11.5, 12, and 12.5 dpc. **c, d,** *Msx2* expression in the (c) mouse and (d) *D sagitta* embryo at 10.5 dpc. **e,** Fore limb and hind limb of the five-toed jerboa, *A elater,* at approximately 12.25 dpc. **f,** Fore limb and hind limb of the horse at 30 dpc (approximately equivalent to mouse 12 dpc). **g,** Fore limb and hind limb of the camel at 38 dpc (approximately equivalent to mouse 12.5 dpc). Scalebar = 1 mm for *D sagitta, A elater,* horse, and camel and 0.8 mm for mouse limbs.

Extended Data Figure 2.6. Time series of *Fgf8* expression a. in the mouse and three-toed jerboa, *D sagitta,* hind limb. **b,** *Fgf8* expression in the pig (25 dpc) and camel (42 dpc) hind limbs of embryos in Figure 7. TUNEL labeling of cell death in the 12.5 dpc *D sagitta* hind limb. Limbs in (b) are aligned with the closest stage matched embryos in (a).

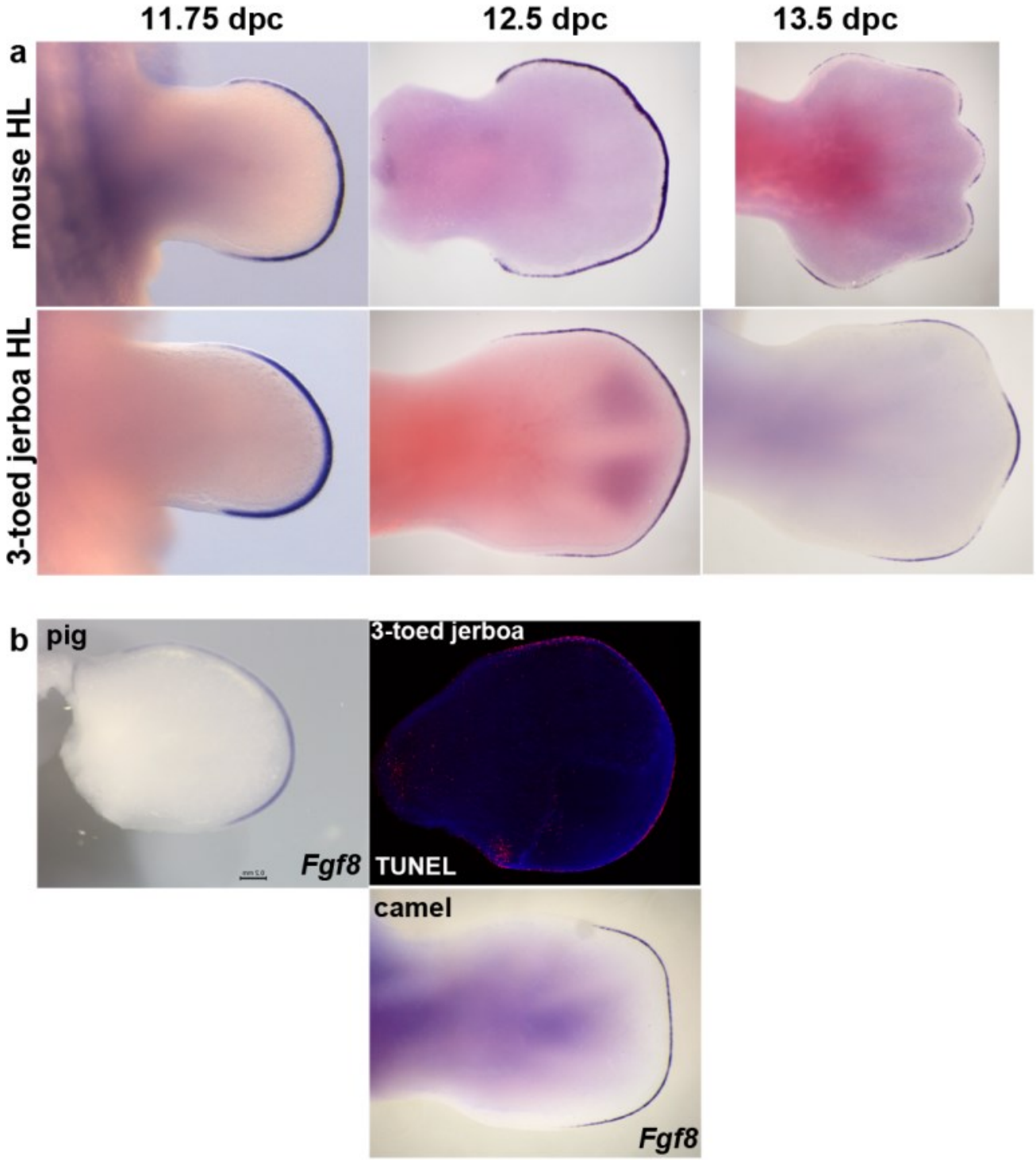

Extended Data Figure 2.6, continued

Table S2.1 Primers used to generate species specific probes

Shh	Forward	Reverse
mouse	GACCCCTTTAGCCTACAAGCAGTTT	GCGTCTCGATCACGTAGAAGACCT
jerboa	GACCCCTTTAGCCTACAAGCAGTTT	GCGTCTCGATCACGTAGAAGACCT
horse	CTGGTGGTTCTGGTCTCCTC	CCCTCGTCCGATCACGTA
camel	used horse probe	
pig	CCGGCTGATGACTCAGAGAT	GCAGGTCCTTCACCAGCTT
Ptch1		
mouse	CTTCGCTCTGGAGCAGATTT	GCATGGTTAAACAGGCATAGG
jerboa	CTTCGCTCTGGAGCAGATTT	GCATGGTTAAACAGGCATAGG
horse	CGCCAGAAGATTGGAGAAGA	CCTGAGTTGTTGCAGCGTTA
camel	CGCCAGAAGATTGGAGAAGA	CCTGAGTTGTTGCAGCGTTA
pig	GGAGCAGATTTCCAAGGGGA	CGGAGAGCTTCTGTGGTCAG
Gli1		
mouse	TACATGCTGGTGGTGCACAT	GGCTGTGGCGAATAGACAGA
jerboa	TACATGCTGGTGGTGCACAT	GGCTGTGGCGAATAGACAGA
horse	GTGACCACTCCCCAGCAG	GATTCAGACCACTGCCCATC
camel	TACATGCTGGTGGTGCACAT	GGCGGTCAAGAGAAACTGG
Hoxd13		
mouse	CTATGGCTACCATTTCGGCAAC	ACTGGTAGCCCTCCATGGAAAT
jerboa	CTATGGCTACCATTTCGGCAAC	ACTGGTAGCCCTCCATGGAAAT
horse	TTCCCGGTGGAGAAGTACA	TTGAGCTTGGAGACGATTTTC
camel	TTCCCGGTGGAGAAGTACA	TTGAGCTTGGAGACGATTTTC
Msx2		
mouse	CTCTCGTCAAGCCCTTCGAGAC	AGCCATTTTCAGCTTTTCCAGTT
jerboa	CTCTCGTCAAGCCCTTCGAGAC	AGCCATTTTCAGCTTTTCCAGTT
horse	TCGCTTAGGGTGGTGTAAGC	TTGCTAATTCACCCCTCTCTG
camel	used horse probe	
Bmp4		
mouse	AGTGAGAGCTCTGCTTTTCGTTTC	GGCAGTAGAAGGCCTGGTAGCC
jerboa	AGTGAGAGCTCTGCTTTTCGTTTC	GGCAGTAGAAGGCCTGGTAGCC
horse	CCAGCGAAAACTCTGCTTTT	GATCAATATGGTCAAAACATTTGC
camel	CCAGCGAAAACTCTGCTTTT	GATCAATATGGTCAAAACATTTGC
Fgf8		
mouse	TGCTGTGCCTGCAGGCNCARGARGG	CAGCTTGCCCTTCTTGTTCATRCADAT
jerboa	TGCTGTGCCTGCAGGCNCARGARGG	CAGCTTGCCCTTCTTGTTCATRCADAT
horse	CCTAATTTTACACAGCATGTGAGG	GGCGGGTAGTTGAGGAACTC
camel	CCTAATTTTACACAGCATGTGAGG	GGCGGGTAGTTGAGGAACTC
pig	CAGGGTGTTTCCCAACAGGT	GGCAATCAGCTTCCCCTTCT